SuperKEKB LUMINOSITY QUEST[*]

Y. Ohnishi[†], KEK, Tsukuba, Japan
on behalf of the SuperKEKB and Belle II commissioning groups

Abstract

SuperKEKB is a positron-electron collider with a nano-beam scheme and continues to achieve the world's highest luminosity for the production of B meson pairs. The luminosity performance has been improved by the full-scale adoption of the crab-waist scheme. The nano-beam scheme allows the vertical beta function at the interaction point (IP) to be much smaller than the bunch length. The vertical beta function and the beam size at the collision point are the smallest in the world among colliders. As the result, the peak luminosity of 4.65×10^{34} cm^{-2}s^{-1} has been achieved with the Belle II detector in 2022. Recent progress will be presented, and then the problems and issues to be overcome from the beam physics point of view will be discussed for further improvement of luminosity performance in the future.

INTRODUCTION

The SuperKEKB accelerator [1, 2] is a positron-electron collider whose main purpose is B meson pair production. The target integrated luminosity is 50 ab^{-1}. The accelerator will be stopped for the first long-term shutdown (LS1) after about 3 years and half of the operation from March 2019, when Phase 3 began, to June 2022. The LS1 will cover upgrades to the Belle II detector [3] and minor modifications to the accelerator. This paper reports on the accelerator performance achieved until 2022. The run from February to the end of March is denoted as a, the run from April to July as b, and the run from October to December as c, with each denoted at the end of the calendar year. The run preceding LS1, the most recent operating period, is represented as 2022b.

The SuperKEKB accelerator consists of an electron ring (HER) with the beam energy of 7 GeV and a positron ring (LER) with the beam energy of 4 GeV, an electron-positron injector [4] with a positron damping ring [5], and beam transport lines connecting them. In the main ring, which has a circumference of about 3 km, the Belle II detector is placed at a collision point.

In order to achieve collisions with asymmetric energies, a double ring is required. It makes to accumulate many bunches while maintaining a single collision point. In addition, a large horizontal crossing angle at the collision point realizes a nano-beam scheme [6, 7]. A final focusing system (QCS) [8] consists of superconducting magnets is placed in the interaction region (IR) to strongly squeeze the beam.

In the LER, ARES RF accelerating cavities [9], which are normal-conducting cavities, are installed, and ARES cavities and superconducting RF accelerating cavities (SCC) [10, 11] are installed in the HER. The linac injector provides beams of the same energy as the main ring with a top-up injection. The energy lost by emitting synchrotron radiation is compensated by the RF cavities. The arc section employs non-interleaved chromaticity correction similar to that of the KEKB accelerator [12], and the emittance can be adjusted in combination with wiggler magnets in the straight sections (OHO and NIKKO). This enables the low emittance required by the nano-beam scheme.

Local chromaticity correction is placed in the straight section (TSUKUBA) where the IR is located, and the chromatic aberration generated in the drift space from the final focus quadrupole magnets to the collision point is efficiently corrected. The sextupole magnets for the local chromaticity correction are also used to perform the crab-waist scheme [13, 14].

The optical functions are calculated by using *SAD* [15] for the model lattice to compare with the measured optical functions and correct them [16]. Typical residual errors after optics corrections are 5 % for the beta functions (rms of $\Delta\beta_{x,y}/\beta_{x,y}$), 5 mm for dispersions (rms of $\Delta\eta_y$). The X-Y couplings as the leakage orbit in the vertical direction from the horizontal single-kick orbit (ratio of rms of Δy to rms of Δx) are obtained to be 0.012–0.016.

LUMINOSITY PERFORMANCE

The highest luminosity achieved through June 2022 is 4.65×10^{34} cm^{-2}s^{-1}. The unofficial record without data acquisition by the Belle II detector is 4.71×10^{34} cm^{-2}s^{-1}. These records are more than twice the highest luminosity achieved with the KEKB accelerator. The integrated luminosity provided by the accelerator is 491 fb^{-1}, of which 428 fb^{-1} (4 fb^{-1} is data not used in the analysis) was recorded at the Belle II detector. Table 1 shows the best integrated luminosity records per 8 hours(per shift), per day, and per 7 days.

Table 1: Integrated Luminosity Records

	Recorded	Delivered	Unit
Shift (8 hours)	958	1036	pb^{-1}
1 day	2.5	2.9	fb^{-1}
7 days	15.0	16.6	fb^{-1}

The maximum beam current is 1.46 A for the LER and 1.14 A for the HER. The maximum number of bunches achieved is 2346 which corresponds to about 4 nsec for a 2-bucket spacing. The vertical beta function at the IP is

FCC-ee FEASIBILITY STUDY PROGRESS*

Michael Benedikt, Frank Zimmermann[†], CERN, Geneva, Switzerland

Abstract

The Future Circular Collider (FCC) "integrated programme" consists of a proposed high-luminosity e+e- collider, FCC-ee, serving as Higgs and electroweak factory, which would, in a second stage, be succeeded by a 100 TeV hadron collider, FCC-hh. FCC-ee and FCC-hh share the same 91 km tunnel and technical infrastructure. In summer 2021 a detailed FCC Feasibility Study (FCC FC), focused on siting, tunnel construction, environmental impact, financing, operational organisation, etc., was launched by the CERN Council. This FCC Feasibility Study (FCC FS) should provide the necessary input to the next European Strategy Update expected in 2026/27. In this paper we briefly review the FCC key design features, status and plans.

This paper is an updated, slightly modified version of an article submitted to the proceedings of NA-PAC'22 [1] (published under the Creative Commons Attribution 3.0 license). Sections on two planned accelerator mock-ups and on regional activities were taken from an article in the ECFA Newsletter [2].

INTRODUCTION

This paper is an updated, slightly modified version of an article submitted to the proceedings of NA-PAC'22 [1] (published under the Creative Commons Attribution 3.0 license). Sections on two planned accelerator mock-ups and on regional activities were taken from an article in the ECFA Newsletter [2].

The Future Circular electron-positron Collider, FCC-ee, is a proposed new storage ring of 91 km circumference, designed to carry out a precision study of Z, W, H, and tt̄ with an extremely high luminosity, ranging from 2×10^{36} cm^{-2}s^{-1} per interaction point (IP), on the Z pole (91 GeV c.m.), 7×10^{34} cm^{-2}s^{-1} per IP at the ZH production peak and 1.3×10^{34} cm^{-2}s^{-1} per IP at the tt̄. In the case of four experiments, the total luminosity on the Z pole will be close to 10^{37} cm^{-2}s^{-1}. FCC-ee will also offer unprecedented energy resolution, both on the Z pole and at the WW threshold.

The FCC-ee represents a low-risk technical solution for an electroweak and Higgs factory, which is based on 60 years of worldwide experience with e⁺e⁻ circular colliders and particle detectors. R&D is being carried out on components for improved performance, but there is no need for "demonstration" facilities, as LEP2, VEPP-4M, PEP-II, KEKB, DAΦNE, or SuperKEKB already demonstrated many of the key ingredients in routine operation.

The FCC shall be located in the Lake Geneva basin and be linked to the existing CERN facilities. The FCC utility requirements are similar to those in actual use at CERN.

The FCC "integrated programme" consists of the FCC-ee Higgs and electroweak factory as a first stage, succeeded by a 100 TeV hadron collider, FCC-hh, as the ultimate goal. This sequence of FCC-ee and FCC-hh is inspired by the successful past Large Electron Positron collider (LEP) and Large Hadron Collider (LHC) projects at CERN. A similar two-stage project is under study in China, under the name CEPC/SPPC [3].

The FCC technical schedule foresees the start of tunnel construction around the year 2030, the first e⁺e⁻ collisions at the FCC-ee in the mid or late 2040s, and the first FCC-hh hadron collisions by 2065–70.

DESIGN OUTLINE

The FCC-ee is conceived as a double ring e⁺e⁻ collider. It shares a common footprint with the 100 TeV hadron collider, FCC-hh, that would be the second stage of the FCC integrated programme.

The FCC-ee design features a novel asymmetric interaction-region (IR) layout and optics to limit the synchrotron radiation emitted towards the detector (a lesson from LEP [4]), and to generate the large crossing angle of 30 mrad, required for the crab-waist collision scheme [5].

The latest FCC layout features a superperiodicity of four, and can accommodate either two or four experiments, in four 1.40 km long straight sections, which are alternating with 2.03 km straight sections hosting technical systems, in particular radiofrequency (RF) cavities. Each of the 8 separating arc sections has a length of 9.6 km. Figure 1 sketches the layout and possible straight-section functions for the FCC-ee.
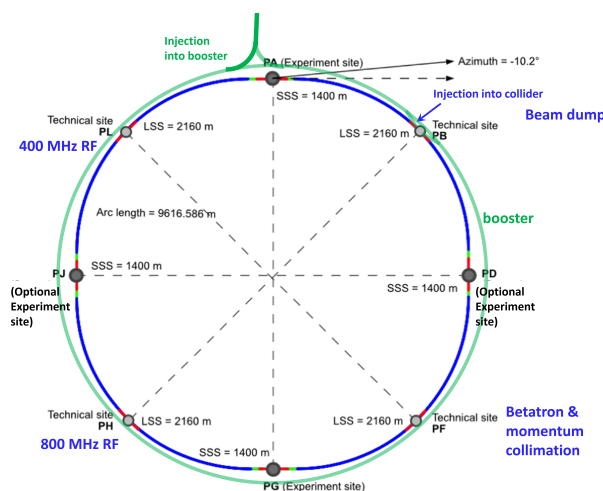

Figure 1: Schematic layout of the FCC-ee collider with a circumference of 91.1 km and four-fold superperiodicity. The full-energy booster and part of its injection transfer line are also indicated.

CEPC ACCELERATOR TDR STATUS OVERVIEW

Yuhui Li

Institute of High Energy Physics, Beijing, China

Abstract

The Circular Electron-Positron Collider (CEPC) was proposed in the year of 2012, shortly after the observation of Higgs boson. After years of pre-studies, the CEPC study group has completed the Conceptual Design Report (CDR) in 2018. Since then a series of key technology R&D was carried out, and the accelerator design has been kept optimizing as well. The accelerator design can meet the scientific objectives by allowing the operation in different energies for W/Z, Higgs and ttbar with high luminosities. Key technologies required for the mass production have been developed, such as the superconducting accelerating cavities, high efficiency RF power source, magnets and vacuum systems etc. The accelerator Technical Design Report (TDR) is scheduled to be finished in the cross period of 2022-2023. All of the key technology R&D accomplishments will presented and the optimized accelerator parameters will be updated in it.

INTRODUCTION

The Higgs boson was discovered in July 2012. It plays an important role as the unique "elementary particle" in the SM. Chinese scientists proposed the Circular Electron-Positron Collider (CEPC) in September 2012. CEPC is an electron-positron Higgs factory which can produce 4 million Higgs bosons in a clean background, hence it will boost the precision of the Higgs by about 1 order of magnitude compare to HL-LHC. Except for Higgs, CEPC is expected to generate hundreds of millions W bosons, and 4 trillions of Z bosons with 4-5 orders of magnitude higher than that of the latest generation of the Large Electron Positron Collider. Moreover, CEPC can be upgraded in its center of mass energy to 360 GeV, and produces roughly 1 million top or anti-top quarks. Beyond the electron-positron collision, since the cross size of the CEPC tunnel is wide enough it can accommodate an independent proton-proton collider in the long term plan.

Since 2013, the CEPC has carried out design and key technology R&D. It has received total funding of roughly 260 million CNY from the MOST, the NSFC, the CAS, and some local governments. The Conceptual Design Report (CDR) was published in 2018 [1], followed by significant key technology achievements among the systems that require a high budget ratio in the accelerator construction. What's more, in the years after the CDR was released the design of CEPC was kept being optimized and its luminosity is competitive among the suggested Higgs factories in the world, as shown in Fig. 1.

CEPC aims at getting approved and then commencing the accelerator construction in the years between 2025-2030, thereby the machine operation and data collection can start in the decade of 2030's. Based on the achievements since the publication of CDR, the Technical Design

Report (TDR) is planned to be finished in early 2023, in which the optimized accelerator design and the key technology R&D status will be presented in detail.
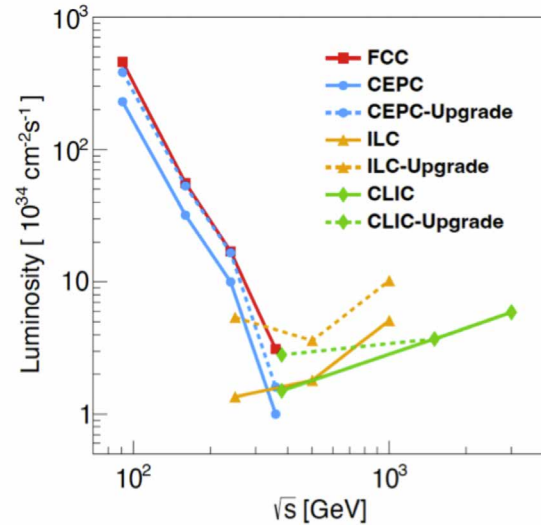

Figure 1: Comparison of the design luminosity of the CEPC and those of other electron-positron Higgs factories.

CEPC DESIGN

The majority CEPC accelerator complex consists of the 100 km collider and booster rings and the Linac including a positron damping ring as the injector. Table 1 lists the major parameters of CEPC at the power of 30 MW [2, 3].

Table 1: Margin Specifications

	Higgs	**W**	**Z**	**top**
Number of IPs	2	2	2	2
Circumference [km]	100	100	100	100
Energy [GeV]	120	80	45	180
Bunch number	249	1297	11951	35
Beam current [mA]	16.7	84.1	803.5	3.3
$\beta x/\beta y$ at IP [m/mm]	0.33 /1	0.21 /1	0.13 /0.9	1.04 /2.7
Bunch length (SR/total) [mm]	2.3 /3.9	2.5 /4.9	2.5 /8.7	2.2 /2.9
Beam-beam parameters ($\xi x/\xi y$)	0.015 /0.11	0.012 /0.113	0.004 /0.127	0.071 /0.1
RF frequency [MHz]	650	650	650	650
Luminosity per IP [10^{34}/cm^2/s]	5.0	16	115	0.5

CEPC adopts a compatible design with the partial or full double-rings collider for electrons and positrons. A special

REALIZATION, TIMELINE, CHALLENGES AND ULTIMATE LIMITS OF FUTURE COLLIDERS

V. Shiltsev[1,*], Fermilab, Batavia, IL 60510, USA

Abstract

This paper consists of two parts: in first, we briefly summarize the US particle physics community planning exercise "Snowmass'21" that was organized to provide a forum for discussions among the entire particle physics community to develop a scientific vision for the future of particle physics in the U.S. and its international partners. The Snowmass'21 Accelerator Frontier activities include discussions on high-energy hadron and lepton colliders, high-intensity beams for neutrino research and for "Physics Beyond Colliders", accelerator technologies, science, education and outreach as well as the progress of core accelerator technologies, including RF, magnets, targets and sources. We also discuss main outcomes of the Snowmass'21 Implementation Task Force which was changed to carry our comparative evaluation of future HEP accelerator facilities, their realization strategies, timelines, and challenges.

In the second part, we present an attempt to evaluate limits on energy, luminosity and social affordability of the ultimate future colliders - linear and circular, proton, electron positron and muon, based on traditional as well as on advanced accelerator technologies.

SNOWMASS'21

Snowmass is a particle physics community study that takes place in the US every 7-9 years (the last one was in 2013). The Snowmass'21 study (the name is historical, originally held in Snowmass, Colorado) took place in 2020-22, it was organized by the the American Physical Society divisions (DPF, DPB, DNP, DAP, DGRAV) and strived to define the most important questions for the field and to identify promising opportunities to address them, to identify and document a scientific vision for the future of particle physics in the U.S. and its international partners - see [1]. The P5, Particle Physics Project Prioritization Panel, chaired by H.Murayama (UC Berkeley), has taken the scientific input from Snowmass'21 to develop (by the Spring of 2023) a strategic plan for U.S. particle physics that can be executed over a 10 year timescale in the context of a 20-year global vision for the field.

Snowmass'21 activities are managed along the lines of ten "Frontiers": Energy Frontier (EF), Neutrino Physics Frontier (NF), etc, with the Accelerator Frontier (AF) among them. More than three thousand scientists have taken part in the Snowmass'21 discussions and about 1500 people participated in the final Community Summer Study workshop (Seattle, July'22) in person and remotely. In general, the international community was very well represented and many scientists from Europe and Asia have been either organizers

_____
* shiltsev@fnal.gov

of sessions and events, or conveners of topical groups, or submitted numerous Letters of Interest (short communications) or White Papers (extended input documents).

More than 300 Letters of Interest and 120 White Papers have been submitted to the Snowmass'21 AF topical groups. There were more than 30 topical workshops, 8 cross-Frontier *Agoras* (5 on various types of colliders: $e + e - /\gamma\gamma$, linear/circular, $\mu\mu$, pp, advanced ones and three on experiments and accelerators for rare processes physics), and several special cross-Frontier groups were organized such as *the eeCollider Forum, the Muon Collider Forum, the Implementation Task Force* (see below), the 2.4MW proton power upgrade design group at FNAL, etc.

Most important outcomes of the Snowmass AF deliberations are presented in the topical groups' reports and summarized in the Accelerator Frontier report (all available in [2]):

Facilities for Neutrino Frontier: The needs of neutrino physics call for the next generation, higher-power, megawatt and multi-MW-class superbeams facilities. There is a broad array of accelerator and detector technologies and expertise to design and construct a 2.4 MW beam power upgrade of the Fermilab accelerator complex for the LBNF/DUNE Phase II, a world leading neutrino experiment, expand the volume of Liquid Argon detectors by 20 ktons, and build a new neutrino near-detector on the Fermilab site.
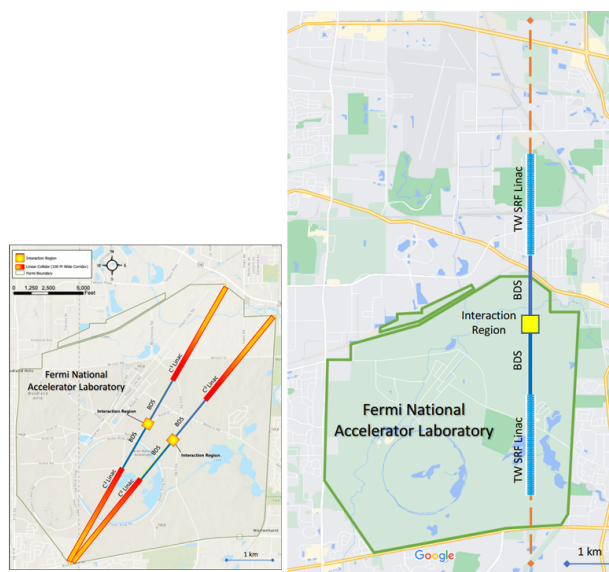

Figure 1: Possible placements of future linear e^+e^- Higgs/EW factory colliders C^3 and HELEN on the Fermilab site map - both about the same length: (left) 250 GeV c.m.e. options with a 7-km footprint, and (right) higher c.m. energy options (12 km dashed line) (from the AF report [2]).

FUTURE PROJECTS FOR THE NEXT GENERATION TAU-CHARM FACTORIES IN CHINA AND RUSSIA*

Q. Luo, School of Nuclear Science and Technology and National Synchrotron Radiation Laboratory, University of Science and Technology of China, Hefei, China

Abstract

Based on the key scientific questions in the frontier of particle physics field, the current status and future development trend globally and domestically of accelerator-based particle physics experiments, new generation electron-positron colliders in tau-charm energy region (around 4 GeV center-of-mass) are proposed both in China and Russia. This paper discussed the general collision scheme and the key issues of accelerator physics and technologies. Also, the accelerator research and the progress of the projects in Russia and China are presented.

INTRODUCTIONS

As we know, there's two frontiers for accelerator-based particle physics. One is high energy frontier, in which scientists search for new physics beyond the standard model with very high beam energy. Meanwhile, a super particle factory usually refers to a collider which operates in the high luminosity frontier of particle physics with relatively lower energy. With a center-of-mass energy of around 4 GeV (tau-charm region), the super particle factory collider will operate in the quantum chromodynamics (QCD) perturbative and non-perturbative transition region and have unique features, such as rich resonance structures, threshold production, quantum correlation, etc, and will provide unique opportunities to study the internal structure of hadrons and explore the nature of non-perturbative QCD, to measure charge-parity (CP) violations and test the electroweak models precisely, and search for the new physics beyond-standard-model [1]. As the most successful tau charm factory of the world, the Beijing Electron Positron Collider II (BEPCII) will finish its historical mission in the next decade and certainly need a successor. Therefore, a new super tau charm factory which will have abundant physics program and great potential for scientific discoveries in high energy physics fields is required. It is expected to achieve major breakthroughs in tau-charm and hadron physics fields in future.

Both Chinese and Russian scientists have made their efforts in conceptual design study of the next generation tau charm factory and applied for funds to develop key technologies and construct test facilities since 2010s. Scientists from other countries also played an important part in related discussion. There're annual international joint workshops since the year 2018, first held in Paris, then Moscow and Hefei.

As a next generation facility, a super tau charm factory will be a dual-ring electron-positron collider with high current symmetric and flat beams, which have very small transversal size at interaction point (IP) so as to reach 50-100 times as BEPCII's luminosity. Compared to head-on collision and large emittance beams for BEPCII, the new super tau charm factory will utilize a fundamentally new scheme called Crab Waist and large Piwinski angle [2, 3]. Although this scheme has been successfully applied in low luminosity situation by the Φ-factory DAΦNE (INFN LNF, Frascati) [4], there're still a lot of work to do if we want to achieve much higher current and luminosity in tau-charm region, especially based on SuperKEKB experience [5]. This paper discusses the key issues of accelerator physics and technologies and presented the progress of the accelerator research and the situation of the projects in China and Russia.

MAJOR CHALLENGES FOR SUPER TAU CHARM ACCELERATORS

The new approach of large Piwinski angle and Crab Waist (CW) scheme allows raising the luminosity by one or two orders of magnitude without significant increase in the intensity of the beams or the dimensions of the installation or decrease in the bunch length. The idea was first offered by P. Raimondi, M. Zobov and D. Shatilov [6], see Fig. 1.
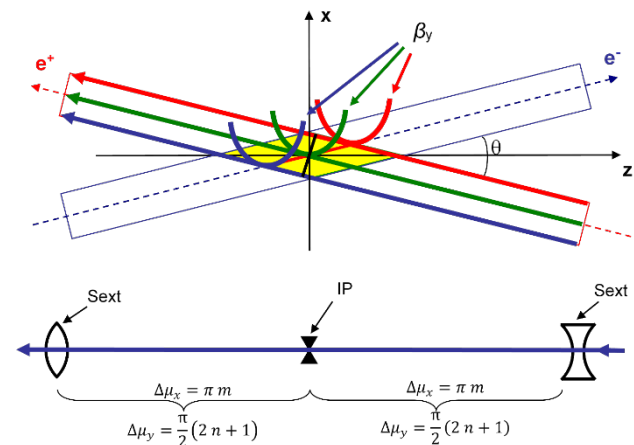

Figure 1: Large Piwinski angle and Crab Waist.

The theoretical luminosity satisfies $L = \frac{\gamma}{2er_e} \cdot \frac{I_{tot}\xi_y}{\beta_y^*} R_H$.

With a Piwinski angle $\phi = \sigma_z/\sigma_x \tan(\theta/2)$ large enough, the hourglass effect will be suppressed and the bunch length doesn't have to be decreased. Crab waist sextupoles suppress the betatron and synchro-betatron resonances so the luminosity is increased [7].

LATEST RESULTS ON KAON PHYSICS AT KLOE-2

A. Di Domenico*, Sapienza University of Rome and INFN Sez. Roma, Rome, Italy
on behalf of KLOE-2 Collaboration

Abstract

The most recent results obtained by the KLOE-2 collaboration with entangled neutral kaons produced at DAΦNE are briefly reviewed: (i) an improved search for decoherence and $\mathscr{CPT}$ violation effects in the process $\phi \to K_S K_L \to \pi^+\pi^-\pi^+\pi^-$, constraining with the utmost precision several phenomenological models; (ii) the first direct test of the $\mathscr{T}$ and $\mathscr{CPT}$ symmetries in neutral kaon transitions between flavor and $\mathscr{CP}$ eigenstates, by studying the processes $\phi \to K_S K_L \to \pi^+\pi^- \pi e\nu$, $\phi \to K_S K_L \to \pi e\nu \, 3\pi^0$; (iii) a new measurement of the $K_S \to \pi e\nu$ branching fraction, that in combination with the previous KLOE result improves the total precision by almost a factor of two, and allows a new derivation of $f_+(0)|V_{us}|$.

KLOE AND DAΦNE

DAΦNE, the Frascati ϕ-factory [1], is an e^+e^- collider working at a center of mass energy of $\sqrt{s} \sim 1020$ MeV, corresponding to the peak of the ϕ resonance. The ϕ production cross section is ~3 μb, and the $\phi \to K^0\bar{K}^0$ decay has a branching fraction of 34%. The neutral kaon pair is produced into a fully anti-symmetric entangled state with quantum numbers $J^{\mathscr{PC}} = 1^{--}$:

$$|i\rangle = \frac{1}{\sqrt{2}}\{|K^0\rangle|\bar{K}^0\rangle - |\bar{K}^0\rangle|K^0\rangle\}$$
$$= \frac{\mathscr{N}}{\sqrt{2}}\{|K_S\rangle|K_L\rangle - |K_L\rangle|K_S\rangle\} \quad (1)$$

with $\mathscr{N} = \sqrt{(1+|\epsilon_S|^2)(1+|\epsilon_L|^2)}/(1-\epsilon_S\epsilon_L) \simeq 1$ a normalization factor, and $\epsilon_{S,L}$ the small $\mathscr{CP}$ impurities in the mixing of the physical states $K_{S,L}$ with definite widths $\Gamma_{S,L}$ and masses $m_{S,L}$.

The double differential decay rate of the state $|i\rangle$ into decay products f_1 and f_2 at proper times t_1 and t_2, respectively, is an observable quantity at a ϕ-factory. After integration on $(t_1 + t_2)$ at fixed time difference $\Delta t = t_2 - t_1 \geq 0$, the decay intensity can be written as follows [2]:

$$I(f_1, f_2; \Delta t) = C_{12}\{|\eta_2|^2 e^{-\Gamma_L \Delta t} + |\eta_1|^2 e^{-\Gamma_S \Delta t}$$
$$-2|\eta_1||\eta_2|e^{-\frac{(\Gamma_S + \Gamma_L)}{2}\Delta t}\cos[\Delta m \Delta t + \phi_1 - \phi_2]\} . \quad (2)$$

with $\Delta m = m_L - m_S$, $\eta_i \equiv |\eta_i|e^{i\phi_i} = \frac{\langle f_i|T|K_L\rangle}{\langle f_i|T|K_S\rangle}$, and $C_{12} = \frac{|\mathscr{N}|^2}{2(\Gamma_S + \Gamma_L)}|\langle f_1|T|K_S\rangle\langle f_2|T|K_S\rangle|^2$.

The detection of a kaon at large times t_2 satisfying the condition $e^{-(\Gamma_S - \Gamma_L)\Delta t}/|\eta_2| \ll 1$ post-tags a K_S state in the opposite direction. This is a unique feature at a ϕ-factory,

---

* antonio.didomenico@roma1.infn.it

not possible at fixed target experiments, that can be exploited to select very pure K_S beams [3].

The KLOE experiment operated at DAΦNE with a detector mainly consisting of a large volume drift chamber [4] surrounded by an electromagnetic calorimeter [5], both immersed in a 0.52 T uniform magnetic field provided by a superconducting coil. KLOE completed its data taking campaign in 2006 collecting an integrated luminosity of 2.5 fb^{-1}. A second data taking campaign was carried out in years 2014-2018 by the KLOE-2 experiment [6], the successor of KLOE, at an upgraded DAΦNE collider [7, 8], collecting an integrated luminosity of 5.5 fb^{-1}. In total KLOE and KLOE-2 collected 8 fb^{-1} of data, corresponding to ~ 2.4×10^{10} ϕ-mesons and ~ 8×10^9 $K_S K_L$ pairs produced. All the results presented in this paper have been obtained using the KLOE data sample.

SEARCH FOR DECOHERENCE AND $\mathscr{CPT}$ VIOLATION EFFECTS

The quantum interference between the decays of the entangled kaons in state (1) is studied in the $\mathscr{CP}$-violating process $\phi \to K_S K_L \to \pi^+\pi^-\pi^+\pi^-$, which exhibits the characteristic Einstein–Podolsky–Rosen correlations that prevent both kaons to decay into $\pi^+\pi^-$ at the same time. The measured Δt distribution can be fitted with the distribution:

$$I(\pi^+\pi^-, \pi^+\pi^-; \Delta t) \propto e^{-\Gamma_L \Delta t} + e^{-\Gamma_S \Delta t}$$
$$-2(1-\zeta_{SL})e^{-\frac{(\Gamma_S + \Gamma_L)}{2}|\Delta t|}\cos(\Delta m \Delta t) , \quad (3)$$

where the quantum mechanical expression (2) in the $\{K_S, K_L\}$ basis has been modified with the introduction of a decoherence parameter ζ_{SL}, and a factor $(1 - \zeta_{SL})$ multiplying the interference term. Analogously, a $\zeta_{0\bar{0}}$ parameter can be defined in the $\{K^0, \bar{K}^0\}$ basis [9]. Δt resolution and detection efficiency effects, as well as background contributions due to K_S-regeneration on the beam pipe wall, and the non-resonant $e^+e^- \to \pi^+\pi^-\pi^+\pi^-$ process, are all taken into account in the fit. Figure 1 shows as an example the result in the case of the ζ_{SL} decoherence model. The analysis of a data sample corresponding to L ~ 1.7 fb^{-1} yields the following results [10]:

$$\zeta_{SL} = (0.1 \pm 1.6_{stat} \pm 0.7_{syst}) \times 10^{-2}$$
$$\zeta_{0\bar{0}} = (-0.5 \pm 8.0_{stat} \pm 3.7_{syst}) \times 10^{-7} , \quad (4)$$

compatible with the prediction of quantum mechanics, i.e. $\zeta_{SL} = \zeta_{0\bar{0}} = 0$, and no decoherence effect. In particular the result on $\zeta_{0\bar{0}}$ has a high precision, $\mathcal{O}(10^{-6})$, due to the $\mathscr{CP}$ suppression present in the specific decay channel; it is an improvement of five orders of magnitude over the limit obtained by a re-analysis of CPLEAR data [9, 11]. This

SuperKEKB OPTICS TUNING AND ISSUES

H. Sugimoto*, Y. Ohnishi, A. Morita, H. Koiso

High Energy Accelerator Research Organization, Tsukuba, Japan

Abstract

SuperKEKB is an electron-positron double-ring asymmetric-energy collider at the High Energy Accelerator Research Organization (KEK) in Japan. It adopts a novel collision method named nano-beam scheme to avoid the so-called hourglass effect. In the nano-beam scheme, two beams are squeezed to extremely small sizes at the interaction point and are collided with a large crossing angle between them. Since starting the collision operation in April 2018, numerous machine tunings and beam studies have been performed to improve the machine performance. The highest peak luminosity so far is 4.65×10^{34} cm^{-2}s^{-1} reached in June 8th, 2022. This record is the world's highest instantaneous luminosity and is more than two times higher than that of the previous KEKB collider This paper presents some important topics related to beam optics tuning in the SuperKEKB operation. Major issues to be resolved to boost the machine performance are also addressed.

INTRODUCTION

SuperKEKB [1] is a 7 GeV electron (HER) and 4 GeV positron (LER) double ring collider. Beam commissioning without final focusing system (QCS) was carried out from February 2016 to June 2016 [2]. Beam commissioning with QCS was started March 2018 [3]. SuperKEKB adopts a novel collision scheme named nano-beam scheme to open up new luminosity frontier. In the nano beam scheme, two beams collide with a large horizontal crossing angle with extremely small beam sizes. The nano beam scheme realizes small betatron function at the interaction point (IP) while avoids so-called hourglass effect which limits the luminosity performance.

Luminosity L is written by beam current I, vertical beam-beam parameter ξ_y, vertical betatron function at IP β_y^* and a reduction factor R as,

$$L = \frac{\gamma_\pm}{2er_e} \frac{I_\pm \xi_{y\pm}}{\beta_y^*} R, \qquad (1)$$

where e, r_e, and $\gamma_\pm$ are elementary charge, classical electron radius and the Lorentz gamma factor, respectively. Since the beam-beam parameter ξ_y is proportional to $\sqrt{\beta_y^*/\varepsilon_y}$, the vertical emittance ε_y should be also very small as well as β_y^* to realize the nano-beam collision. Therefore the low emittance tuning is one of the important machine parameters in the SuperKEKB machine tuning.

The nominal β_y^* in the present operation is $\beta_y^* = 1$ mm while the final target of β_y^* is $\beta_y^* = 0.3$ mm. The operation with $\beta_y^* = 0.8$ mm was carried out for short-term trial. The achievable bunch currents is smaller than of $\beta_y^* = 1$ mm

_____
* hiroshi.sugimoto@kek.jp

case due to poor injection efficiency. Improvement of the injection efficiency is a major issue in both squeezing β_y^* and increasing stored beam current.

Crab waist scheme (CW) [4, 5] is incorporated to both LER and HER in 2020 to mitigate a sort of hourglass effect in the transverse direction. CW is realized by applying different filed strength to sextupole magnets (SLY) used in the vertical local chromaticity correction (Y-LCC) as shown in Fig. 1. The vertical betatron function at SLY and field strength of SLY are quite large owing to the extremely small β_y^* and the resultant large chromaticity. Therefore beam optics is easily distorted by a tiny amount of lattice or orbit errors. Optics tuning and the machine operation should be performed with careful attention to the Y-LCC section as well as the interaction region (IR).

OPTICS TUNING

Beam Position Monitor and Corrector

Beam Position Monitor (BPM) is attached to each of quadrupole magnets for precise orbit and optics control. The BPM system is successfully used in the beam tuning with an averaging mode of 0.25 Hz. In addition to closed orbit measurement, more than 100 BPMs per ring can be used as gated turn-by-turn BPMs. The gated turn-by-turn BPMs are very helpful in the beam injection tuning. Optics measurement with turn-by-turn beam position is performed only for dedicated beam study. Usual optics tuning is based on closed orbit measurement.
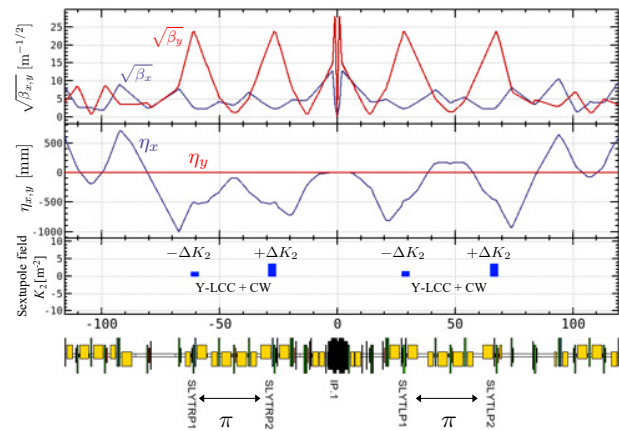

Figure 1: Betatron and dispersion functions at the Y-LCC section in LER. Two sextupoles pairs installed in both left and right sides of the interaction region. The sextupole pairs are utilized for Y-LCC and CW. Betatron phase advance between the two sextupoles is π.

TUXAT0103

BEAM PHYSICS FRONTIER PROBLEMS*

Frank Zimmermann[†], CERN, Geneva, Switzerland

Abstract

The main challenges for far-future higher-energy particle colliders are discussed along with possible technological paths to overcome them.

COLLIDER LANDSCAPE

This workshop paper is mostly an abbreviated version of an article published in the "Frontiers in Physics" journal [1] (open access under the Creative Commons Attribution 4.0 International licence). The topic of electric power generation using accelerators has been added.

High-energy physics calls for particle colliders with much higher energy and/or luminosity than any past or existing machine. Various types of future particle colliders are being proposed and under development.

Technically closest to construction are the International Linear Collider (ILC) in Japan, the Future Circular electron-positron Collider (FCC-ee) in Europe, and the Circular Electron Positron Collider (CEPC) in China. The ILC design is grounded in more than 30 years of dedicated and successful R&D efforts. Another type of linear collider, CLIC, is based on higher-gradient normalconducting RF cavities, and powered with a novel two-beam acceleration scheme. The two circular collider designs, FCC-ee and CEPC, build on 60 years of experience with operating colliding beam storage rings, and in particular, they include ingredients of the former LEP collider at CERN, and of the KEKB, PEP-II and SuperKEKB B factories. Combining successful concepts and introducing a few new ones allows for an enormous jump in performance. For example, FCC-ee, when running on the Z pole is expected to deliver more than 100,000 times the luminosity of the former LEP collider. The circular lepton colliders FCC-ee and CEPC would be succeeded by energy frontier hadron colliders, FCC-hh and SPPC, respectively, providing proton collisions at a centre-of-mass energy of about 100 TeV or higher.

Several colliders based on energy-recovery linacs (ERLs) also are under discussion. A Large Hadron electron Collider (LHeC), with an electron beam from a dedicated ERL, could extend the physics programme at the LHC [2, 3]. A similar collider option, called FCC-eh [4], is considered for the FCC-hh. Recently, high-energy, high-luminosity ERL-based versions of the FCC-ee [5] and of the ILC [6, 7] have been proposed.

The above proposals are complemented by still others, presumably in the farther future, such as photon colliders, muon colliders, or colliders based on plasma acceleration.

Technical feasibility, affordability, and sustainability are among the questions which the collider designers may need to address.

ACCELERATOR CHALLENGES

Five major challenges are driving the design and, ultimately, the feasibility of future high-energy colliders. These are: (1) synchrotron radiation, (2) the bending magnetic field, (3) the accelerating gradient, (4) the production of rare or unstable particles (positrons or muons), and (5) cost and sustainability.

A charged particle deflected transversely to its velocity vector emits electromagnetic radiation which, if emitted due to the influence of an external magnetic field, is called synchrotron radiation. Denoting the charge of the particle by e, its relativistic Lorentz factor by γ, and considering a particle that follows a circular orbit of bending radius ρ, the energy loss per turn is given by

$$U_0 = \frac{e^2}{3\epsilon_0} \frac{\gamma^4}{\rho} . \qquad (1)$$

If there is not a single particle but a beam with current I_{beam}, the power of the emitted synchrotron radiation becomes

$$P_{\text{SR}} = \frac{I_{\text{beam}}}{e} U_0 . \qquad (2)$$

To provide some examples, the maximum synchrotron radiation power at the former Large Electron Positron collider (LEP) was about 23 MW, while for the proposed future circular electron-positron collider FCC-ee a total constant value of 100 MW has been adopted as a design constraint.

For the same particle energy, the Lorentz factor of protons is much (about 2000 times) lower than for electrons. Consequently, until now, synchrotron radiation power for proton beams has been much less significant, even if not fully negligible. For the Large Hadron Collider (LHC), it amounts to about 10 kW. However, this value increases to a noticeable 5 MW for the proposed future circular hadron collider FCC-hh. Removal of this heat from inside the cold magnets of the collider arcs, requires more than 100 MW of electric cryoplant power. These numbers reveal that for both future electron-positron and hadron circular colliders, synchrotron radiation alone implies more than 100 MW of electric power needs.

Possible mitigation measures to limit or suppress the synchrotron radiation include:

- increasing the bending radius ρ, which translates into a large(r) circular collider, and is a key part of the FCC concept;
- the construction of a linear collider, which features only minor arcs, but still faces the issues of radiation in the

---

FCC-ee LATTICE DESIGN

J. Keintzel*, A. Abramov, M. Benedikt, M. Hofer, K. Oide,
R. Tomás, F. Zimmermann, CERN, Geneva, Switzerland
P. Hunchak, University of Saskatchewan, Saskatoon, Canada
T. O. Raubenheimer, SLAC National Accelerator Laboratory, USA

Abstract

Within the framework of the Future Circular Collider Feasibility and Design Study, the design of the electron-positron collider FCC-ee is being optimised, as a possible future double collider ring, currently foreseen to start operation during the 2040s. FCC-ee is designed to operate at four different energy stages, allowing for precision measurements: from the Z-pole up to above the t̄t-threshold. This synchrotron with almost 100 km circumference is designed including advanced accelerator concepts, such as the crab-waist collision scheme or one combined off-momentum and betatron collimation insertion. Furthermore, numerous optics tuning and measurement studies are being performed to drive the collider design at an early stage and guarantee its feasibility and efficient operation.

INTRODUCTION

The Future Circular electron positron Collider [1], FCC-ee, is the first part of the so-called integrated FCC program [2], which foresees, first, the construction of an almost 100 km long tunnel infrastructure and the integration and commissioning of the FCC-ee. After completion of its physics program, it is then envisaged to decommission the FCC-ee, followed by integration of the hadron FCC [3], FCC-hh, into the same tunnel infrastructure. First collisions are presently foreseen in the mid-2040s for the FCC-ee and around 2065 for the FCC-hh [4].

A flexible high energy electron-positron collider such as the FCC-ee, offers the potential for high precision physics experiments at various particle physics resonances [5, 6]. In case of the FCC-ee beam energies from 45.6 GeV, corresponding to the Z-pole, and up to above the top-pair-threshold with 182.5 GeV are foreseen. To limit the synchrotron radiation (SR) power to 50 MV per turn the beam current decreases with increasing energy. Each energy stage leads, therefore, to unique beam dynamics challenges, and solutions need to be found in accordance with the general layout.

Within the framework of the FCC feasibility study, launched in 2021, it is aimed to provide a self-consistent design of the required technical infrastructure and the accelerator complex for the FCC-ee by end of 2025 with a mid-term review in mid-2023 [7, 8].

REVISED PLACEMENT

The tunnel infrastructure required to host the FCC in the Geneva basin is assumed to be constructed approximately 100 m below ground, similar to the tunnel which presently hosts the Large Hadron Collider, LHC [9]. Tunnel construction is one of the main cost drivers, and depends on the tunnel dimensions, depth and composition of the ground material. Additionally, shafts and surface sites around the circumference are required to host various infrastructures, demanding dedicated civil engineering solutions. Geographic constraints to integrate a circular collider into the Franco-Swiss-Basin are the various mountain ranges surrounding it, including the Jura-mountains in the north-west and the Plateau des Bornes in the south-east in addition to the Geneva lake in the north-east. Furthermore, a possible circular tunnel should surround the Salève-mountain and, hence, these constraints already limit the circumference to about 80 km to 100 km.

Considering all described constraints it has been found that a 90 km tunnel with a four-fold symmetry together with 8 surface sites and straight sections is the most suitable layout. Figure 1 shows the FCC and the LHC placement schematically. The FCC-hh and the FCC-ee lattices have, therefore, been adapted to follow this new tunnel infrastructure and the latter is described in the following.
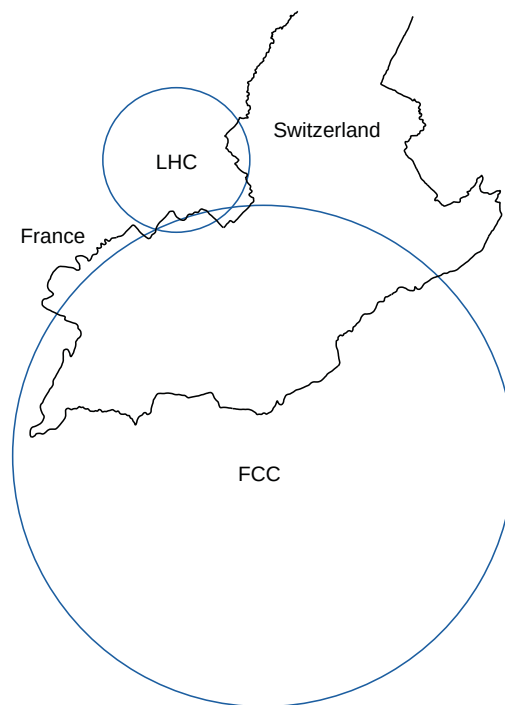

Figure 1: Comparison between the LHC, the FCC and the Franco-Swiss border.

---

* jacqueline.keintzel@cern.ch

CEPC BOOSTER LATTICE DESIGN *

D. Wang[†], D. H. Ji, Y. M. Peng, C. H. Yu[1], Y. D. Liu, Y. Zhang[1], X. H. Cui, J. Y. Zhai, M. Li[1],
C. Meng, J. Gao[1], Institute of High Energy Physics, Beijing, China
[1]also at University of Chinese Academy of Sciences, Beijing, China

Abstract

The CEPC booster provides electron and positron beams to the collider at different energies. The newest booster design is consistent with the TDR higher luminosity goals for four energy modes. The emittance of booster is reduced significantly in order to match the lower emittance of collider in TDR. Both FODO structure and TME structure was studied for booster design. A lot of efforts are made to overcome the difficulty of error sensitivity for the booster and hence the dynamic aperture with errors can fulfil the requirements at all energy modes. Also, the combined magnets scheme (B+S) are proposed to minimize the cost for magnets and power supplies. The design status of CEPC booster in TDR including parameters, optics and dynamic aperture is discussed in this paper.

INTRODUCTION

CEPC booster needs to provide electron and positron beams to the collider at different energy with required injection efficiency. The injection system consists of a 30 GeV Linac, followed by a full-energy booster ring. Electron and positron beams are generated and accelerated to 30 GeV in the Linac. The beams are then accelerated to full-energy in the booster, and injected into the collider. For different beam energies of tt, Higgs, W, and Z experiments, there will be different particle bunch structures in the collider [1]. To maximize the integrated luminosity, the injection system will operate mostly in top-up mode, and also has the ability to fill the collider from empty to full charge in a reasonable length of time [2]. The lowest field of dipole magnets in booster is 90 Gauss and the tolerance for field error at 30 GeV can be realized by the ion based magnets.

After CDR, we have reduced the emittance of collider ring and beta function at the interaction point in order to get higher luminosity for Higgs energy mode [3]. With the booster design in CDR [2, 4], it is difficult to realize the injection from booster to collider for Higgs mode even with on-axis injection scheme. For TDR design, the dynamic aperture requirement of collider ring in horizontal direction due to injection process is shown in Fig. 1. From Fig. 1, we know that the booster emittance at 120 GeV should be lower than 1.7 nm, while it is 3.6 nm in CDR.

Actually, we have made a long effort to develop a lower emittance booster since the CEPC CDR was published. After careful study and comparison among different designs, the optics based on modified-TME structure is adopted as the best candidate. The progress of booster design based on

TME structure has been published in 2021 [5]. After that, we found this design is so sensitive to errors that the dynamic aperture of booster cannot fulfil the requirement when we consider the real error effects. So the booster design with TME structure is updated to make a balance between error sensitivity and emittance. We also made an alternative booster design with FODO structure. After the comparison between FODO and TME lattice including error effects, we chose the modified-TME lattice as our baseline for TDR because only the TME can fulfil the dynamic aperture requirement at all energy modes.
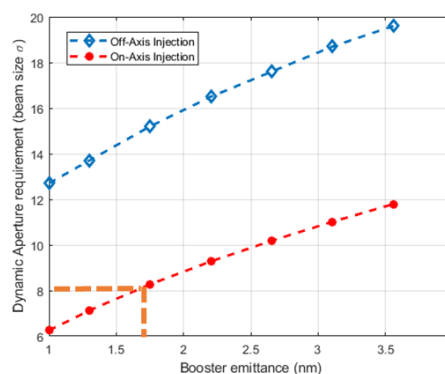

Figure 1: The dynamic aperture requirement of collider ring in horizontal direction due to injection process vs. booster emittance at 120 GeV. The horizontal emittance in collider ring at 120 GeV is 0.64 nm. The horizontal beta function at the injection point is 1800 m.

OPTICS DESIGN FOR LOWER EMITTANCE BOOSTER

New Lattice Design Based on TME

The arc is made of modified-TME cells. Figure 2 shows the optics design for the arc cell. The length of TME cell in the arc is 78 m.
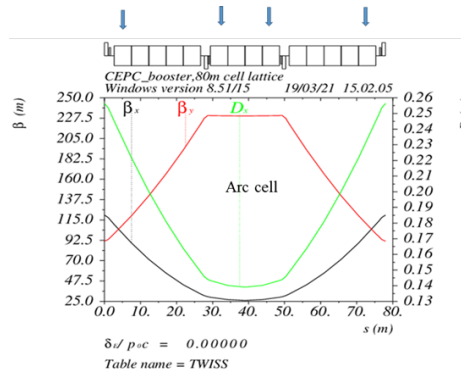

Figure 2: The Twiss functions of the TME cell in the arc region.

IR DESIGN ISSUES FOR HIGH LUMINOSITY
AND LOW BACKGROUNDS*

M. K. Sullivan†, SLAC National Accelerator Laboratory, Menlo Park, CA, USA

Abstract

New e^+e^- collider designs use high beam currents (>1 A) to help obtain a high luminosity value. This leads to several issues that affect detector background levels. I will discuss several of these issues and indicate some of the backgrounds the detectors at these new colliders will encounter. The experience of the first two B-factories (PEP-II and KEKB) and also of the currently operating SuperKEKB accelerator will be used and the discussion will also include the new Electron-Ion Collider to be built at Brookhaven National Laboratory.

INTRODUCTION

The first e^+e^- collider was the storage ring AdA built by Bruno Touschek at the INFN laboratory at Frascati in the early 1960s. This was the first of many matter anti-matter colliders. The late 1960s and early 1970s saw the construction and commissioning of several new e^+e^- colliders. SPEAR at SLAC, Menlo Park, ADONE at INFN Frascati, DORIS at DESY, Hamburg. VEPP-2 and VEPP-2M at BINP, Novosibirsk followed in the late 1970s. The early 1980s had PEP at SLAC and PETRA at DESY. These accelerators were at the e^+e^- energy frontier for new particle searches at that time. It was thought that the PEP and PETRA storage rings with E_{cm} energies of 29 GeV for PEP and 32-48 GeV for PETRA would discover the top quark which had an expected mass at the time of about 15 GeV. Cornell University started up CESR in 1979 as a new e^+e^- collider with an E_{cm} energy range of 3.5 to 12 GeV. This machine was the first of several more accelerators to specialize in producing B mesons.

A new e^+e^- collider called TRISTAN started up in 1987 at KEK in Tsukuba, Japan with an initial beam energy of 25 GeV (50 GeV E_{cm}). In only a few years it was upgraded to a beam energy of 32 GeV. No top quark was seen but the experiments at TRISTAN confirmed the gluon first seen by PETRA experimental detectors and also measured the vacuum polarization effect of the electron. The accelerator also was a pioneer in the use of super-conducting cavities for electron storage rings along with CESR and PETRA. Shortly after TRISTAN turned on, two other e^+e^- colliders, the SLC at SLAC and LEP at CERN, Geneva, specializing in the production of the Z resonance (91.2 GeV E_{cm}) and further studies of the WW threshold (160 GeV E_{cm}) by LEP.

The 1990s saw the construction and commissioning of two new e^+e^- colliders concentrating on generating high luminosity at the Upsilon (4S) resonance (10.56 GeV) in order to produce very large samples of B mesons. The design luminosity values were 5-30 times higher than anything that had been achieved to that point.

In order to achieve these high design luminosities, both asymmetric-energy B-factory designs (PEP-II and KEKB) used a separate storage ring for each beam and then filled each ring with as many bunches as possible. This led to the first high-current (greater than 1A) collider storage rings. It should be stated that, at this time, INFN in Frascati also built and commissioned a high-current double ring collider (DAΦNE) designed for specialized studies of the φ resonance (1.02 GeV) [1-2].

HIGH-CURRENT BEAMS

The asymmetric-energy B-factories (PEP-II and KEKB) achieved and collided multi-ampere beams. The PEP-II B-factory at SLAC reached beam currents of 1.9 A for the 9 GeV electrons and 2.9 A for the 3.1 GeV positrons and the KEKB machine achieved 1.1 A in the 8 GeV electron ring and 2.6 A in the 3.5 GeV positron ring.

The B-factories encountered and solved many issues related to these high-current beams. To name a few: High-Order Mode (HOM) heating, high synchrotron power in the arcs and subsequent beam pipe outgassing, coupled bunch instabilities, synchrotron radiation backgrounds in the detector, and general beam-related backgrounds in the detector as well as the onset of backgrounds related to the collision.

The success of the B-factories has led to the design of future accelerators that implement the use of high-current storage rings as a way of achieving high luminosity design values.

NEW COLLIDER DESIGNS

Here, I touch upon some of the new collider designs that employ high-current storage rings of either electrons and/or positrons. All of the machines mentioned below are described in greater detail in presentations at this workshop. I have selected a few of the design parameters for this discussion. The first machine is an already running accelerator, SuperKEKB.

SuperKEKB

This accelerator is an upgrade of the previous B-factory machine KEKB. KEKB achieved a luminosity of $2.11 \times 10^{34} \text{cm}^{-2}\text{s}^{-1}$ the world record at that time [3]. SuperKEKB is aiming to achieve a peak luminosity of $5\text{-}6 \times 10^{35} \text{cm}^{-2}\text{s}^{-1}$, 30 times higher than KEKB. SuperKEKB uses a new idea called the "nanobeam" colliding scheme [4] in which the crossing angle is large, and

BEAM-INDUCED BACKGROUND SIMULATION AND MEASUREMENTS IN Belle II AT SuperKEKB*

A. Natochii†, University of Hawaii, Honolulu, Hawaii 96822, USA
on behalf of the Belle II Beam Background and Machine Detector Interface (MDI) groups

Abstract

Seeking New Physics beyond the Standard Model, the Belle II experiment at the SuperKEKB electron-positron collider has already reached a peak luminosity of about 4.7×10^{34} cm^{-2} s^{-1}. Its unprecedented target luminosity of 6.3×10^{35} cm^{-2} s^{-1} requires stable machine operation and proper control of beam-induced backgrounds for safe detector operation at high beam currents. The leading background components originating from stored and colliding beams can now be predicted with reasonable accuracy. Dedicated simulations based on the particle tracking software Strategic Accelerator Design (SAD) and Geant4 are used to predict beam-induced backgrounds. These simulations are important for studying realistic collimation scenarios, estimating associated background levels at future machine optics, and making informed choices between possible machine and detector protection upgrades.

This paper reports on the Belle II beam-induced background status in 2021–2022. It overviews background simulation and measurement methodology, and discusses the expected background evolution and mitigation strategies at higher luminosity.

INTRODUCTION

The Belle II/SuperKEKB [1–3] experiment is an upgrade of Belle/KEKB [4, 5] ran between 1999 and 2010. These two projects share same goals of i) studying CP-symmetry violation in a B-meson system, and ii) searching for New Physics beyond the Standard Model. This implies a certain set of requirements for the experiments such as: i) high collision luminosity to produce a large number of $B\bar{B}$-pairs; ii) asymmetric-energy colliding beams of particles to facilitate B-meson decay time difference measurements; and iii) a high quality general-purpose spectrometer (detector) around the interaction point (IP) of two beams for precise measurements of the $B\bar{B}$-mixing rate.

Inspired by Belle/KEKB achievements, which along with BaBar/PEP-II observed large time-dependent CP-asymmetries and contributed to the 2008 Physics Nobel Prize [6], Belle II/SuperKEKB aims to collect 50 times larger data set by the 2030s. To reach this goal, an extremely high collision luminosity above 1×10^{35} cm^{-2} s^{-1} is required. Therefore, the experiment upgraded almost all detector and collider sub-systems, and implemented so-called *nano-beam*

and *crab waist* collision schemes to squeeze beam sizes at the IP and improve luminosity performance [7].

Since 2019, when the detector was rolled in for comprehensive data taking, SuperKEKB has reached the world highest peak luminosity of about 4.7×10^{34} cm^{-2} s^{-1} in June 2022, while Belle II has successfully accumulated more than 0.4 ab^{-1} of data, which is about as large as BaBar's data set collected in almost nine years of PEP-II operation [8].

The SuperKEKB is a 3 km-long circular collider of 4 GeV positrons and 7 GeV electrons accumulated in low-energy ring (LER) and high-energy ring (HER), respectively. Its design has 40 times higher collision luminosity ($\mathcal{L} \sim I_\pm / \beta_y^*$) than KEKB with two times higher beam currents ($I_\pm$) and 20 times smaller vertical beta functions at the IP (β_y^*). This causes higher beam-induced backgrounds in the Belle II detector and leads to i) a high rate of particles leaving the beam, requiring a more frequent top-up beam injection, ii) damage of sensitive detector and collider components, reducing their longevity, and iii) a high rate of beam losses in the interaction region (IR), where the Belle II locates, increasing detector hit occupancy and physics analysis noise. To reach the target luminosity of 6.3×10^{35} cm^{-2} s^{-1}, a comprehensive understanding of beam-induced backgrounds and their countermeasures is essential.

In this paper, we describe main beam loss sources and their countermeasures, report on dedicated background measurements and simulation software, and discuss background estimation towards higher luminosity with a brief overview of our plans in order to facilitate stable and safe detector and machine operation.

BEAM-INDUCED BACKGROUND SOURCES

At SuperKEKB, stray particles which do not follow the nominal trajectory and hit the inner walls of the beam pipe or any other machine element are defined as lost. These particles interact with machine and detector materials producing electromagnetic (EM) showers and neutrons which may hit the detector. These losses we call a beam-induced background (BG).

Below, we define the main types of beam-induced backgrounds which contribute the most to the machine and detector performance degradation and longevity.

Touschek BG is due to a single Coulomb scattering of two particles in the same beam bunch leading to their energy change. It is one of the major backgrounds in Belle II, mainly from the LER.

Beam-gas BG is caused by Bremsstrahlung and Coulomb scatterings of a beam particle by beam pipe residual gas

MDI DESIGN FOR CEPC

S. Bai, H.Y. Shi, H.J. Wang, Y.W. Wang, J. Gao
Institute of High Energy Physics, Beijing, China

Abstract

The Circular Electron Positron Collider (CEPC) is a proposed Higgs factory with center of mass energy of 240 GeV to measure the properties of Higgs boson and test the standard model accurately. Machine Detector Interface (MDI) is the key research area in electron-positron colliders, especially in CEPC, it is one of the criteria to measure the accelerator and detector design performance. In this paper, we will introduce the CEPC MDI layout and (Interaction Region) IR design, IR beam pipe design, thermal analysis and injection background etc on, which are the most critical physics problem.

INTRODUCTION

With the discovery of a Higgs boson at about 125 GeV, the world high-energy physics community is investigating the feasibility of a Higgs Factory, a complement to the LHC for studying the Higgs [1]. There are two ideas now in the world to design a future Higgs factory, a linear 125×125 GeV e⁺e⁻ collider and a circular 125 GeV e⁺e⁻ collider. From the accelerator point of view, the circular 125 GeV e⁺e⁻ collider, due to its low budget and mature technology, is becoming the preferred choice to the accelerator group in China. Machine Detector Interface (MDI) is one of the most challenging field in Circular Electron Positron Collider (CEPC) design, it almost covered all the common problems in accelerator and detector.

In this paper, we will introduce the critical issues of CEPC MDI, including the IR beam pipe design, thermal analysis and injection background etc on.

MDI LAYOUT AND IR DESIGN

The machine-detector interface is about ±7 m in length in the IR as can be seen in Fig. 1, where many elements need to be installed, including the detector solenoid, luminosity calorimeter, interaction region beam pipe, beryllium pipe, cryostat and bellows. The cryostat includes the final doublet superconducting magnets and anti-solenoid. The CEPC detector consists of a cylindrical drift chamber surrounded by an electromagnetic calorimeter, which is immersed in a 3 T (2 T in Z) superconducting solenoid of length 7.3 m. The accelerator components inside the detector should not interfere with the devices of the detector. The smaller the conical space occupied by accelerator components, the better will be the geometrical acceptance of the detector. From the requirement of detector, the conical space with an opening angle should not larger than 8.11 degrees. After optimization, the accelerator components inside the detector without shielding are within a conical space with an opening angle of 6.78 degrees. The crossing angle between electron and

positron beams is 33 mrad in horizontal plane. The final focusing quadrupole is 1.9 m from the IP [2].
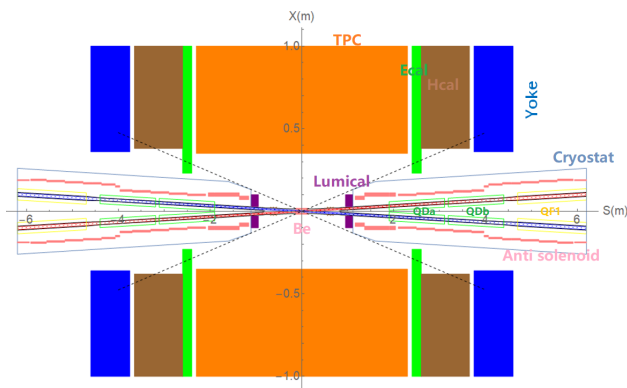

Figure 1: CPEC IR layout.

BEAM PIPE

To reduce the detector background and radiation dose from beam loss, the vacuum chamber has to accommodate the large beam stay clear region. In order to keep precise shaping, all these chambers will be manufactured with computer controlled machining and carefully welded to avoid deformation.

In the present design (Table 1 and Fig. 2), the inner diameter of the beryllium pipe was decided to be 20mm by considering both the mechanical assembly and beam background issues. The length of beryllium pipe is 85mm in longitudinal. Due to bremsstrahlung incoherent pairs, the shape of the beam pipe between 180~655 mm is selected as conic. There is a bellows for the requirements of installation in the crotch region which is located about 0.7 m away from the IP. The crotch point is at 805 mm away from the IP with slope. A race-track shape beam pipe is adopted between 805~855 mm from IP with the inner diameter 39 mm (single pipe) ~20 mm (double pipes), which is considered to control the heating problem of HOM. For the beam pipe within the final doublet quadrupoles, a room temperature beam pipe has been adopted.

Table 1: CEPC IR Central Beam Pipe Design

From IP(mm)	Shape	Inner diameter(mm)	Material	Marker
0-85	Circular	20	Be	
85~180	Circular	20	Al	
180~655	Cone	20~35	Al	Taper: 1:70
655~700	Circular	35	Al	
700~780	Circular	35	Cu	
780~805	Cone	35~39	Cu	
805~855	Race-track	39~20 double pipe	Cu	

FCC-ee MDI: TRAPPED MODES AND OTHER POWER LOSSES*

A. Novokhatski†, SLAC National Accelerator Laboratory, Menlo Park, CA, USA

Abstract

We discuss the beam power loss related to the heating of the vacuum beam pipe walls of the FCC-ee interaction region (IR). We analyse the excitation of trapped modes, which can accumulate electromagnetic energy and determine the locations of these modes. We study the unavoidable resistive-wall wake field, which is responsible for the direct beam pipe walls heating. We present the distribution of the heat load along the central part of IR. The results are very important for knowledge of the temperature distribution and the following cooling system design.

INTRODUCTION

It is planned that a future e+e− collider (FCC-ee) will have a very high energy, up to 375 in the center of mass and unprecedented luminosities [1]. To achieve high luminosity, currents of the electron and positron beams must be more than 1.2 A. High current beams will produce an additional heating of the beam pipe in both rings and in the interaction region. The heating of the beam pipe happens when a beam excites electromagnetic fields due to diffraction of the beam self-field from the inhomogeneous beam pipe. In a time, the diffracted fields are absorbed in the metal walls somewhere in the beam pipe. The beam loses its kinetic energy to restore its self-field when it is deaccelerated by the diffracted fields. The diffracted fields are usually called as wake fields. The FCC IR consists of an intersection of four beam pipes and present a very complicated inhomogeneity geometry. Both beams generate electromagnetic fields in IR. Depends upon the bunch spacing frequency, this may lead to a resonant excitation of a trapped mode located in some special places. There can be several trapped higher order modes (HOMs).

Another heating effect is an excitation and diffusion of the image current inside the metal beam pipe walls. This leads to a direct heating of the beam pipe. Naturally, the beam also loses energy as it is decelerated by the longitudinal electric component of the field generated by the image current. These fields are usually called as resistive-wall wake fields.

Previously, we optimized the geometry of the FCC IR beam pipe for a minimum geometrical impedance [2-4]. We use a numerical code CST [5] for 3D electromagnetic calculations. In these calculations we assume that the beam pipe materials have infinite electrical conductivity. Now the engineering design of the IR suggests what kind of materials will be used. So now, we include the additional beam losses due to interaction of the beam electromagnetic field with conductive materials of the beam pipe. Using the correspondent conductivity of the materials we calculate the heat load distribution along IR beam pipe.

In the first section of this paper, we discuss what kind of electromagnetic fields are excited in IR. Then we present our concept of a low impedance IR beam pipe and show the last CAD model. Next we present results for geometrical wake potentials and an estimate beam energy loss. Then we discuss how we calculate the heat load distribution from the circulating beams and present results for wake potentials and trapped modes. Finally, we present the heat load distribution in IR. In the conclusion section we discuss the importance of the results for a colling system and future steps.

ELECTROMAGNETIC FIELDS IN IR

We can distinguish three types of the fields excited in the FCC IR by circulating beams. The first type is the electromagnetic field, which is exciting in IR in the form of propagating waves that can leave IR and then be absorbed somewhere in the rings. During the PEP-II SLAC B-Factory operation we watch these traveling waves propagating the distance more than 100 m long [6]. The second type is the field that is excited in some trapped locations of IR and be absorbed there. These fields are usually called higher order modes HOMs. There is one mode located near the pipe connection is an unavoidable mode [2]. Under resonant conditions the amplitude of the trapped mode field can be strongly magnified. The third type is an unavoidable resistive-wall wake field, which is responsible for directly heating of the metal walls. Excitation and absorption of these fields in IR may lead to additional detector background because heating effects and high frequency waves interference.

Important parameters, which characterize the excited field are a loss factor and an impedance. The loss factor tells how much energy a bunch of particle losses passing by some beam pipe element. This is equivalent to the total amount of energy of the excited fields. The loss factor is strongly depending upon the bunch length. Smaller bunches lose more energy. The impedance is a Fourier spectrum of a wake potential. The wake potential is an integral of the longitudinal electrical component of the excited fields along the bunch trajectory. The impedance shows possible trapped modes as resonate spikes in the frequency spectrum.

CONCEPT OF A LOW IMPEDANCE IR BEAM PIPE AND CAD MODEL

The main idea to decrease the wake field radiation or minimize the impedance of the chamber is naturally to use a very smooth transition from one pipe to a conjunction of two pipes. One of possibilities how to make it, is demonstrated in Fig. 1. Starting with a round pipe we make a smooth transition to a pipe with a cross section of a half of ellipse. Then we combine two half-ellipses in one full ellipse making one pipe from two pipes. It is important the

MACHINE INDUCED BACKGROUNDS IN THE FCC-ee MDI REGION AND BEAMSTRAHLUNG RADIATION

A. Ciarma*, E. Perez, G. Ganis, CERN, Geneve, Switzerland
M. Boscolo, INFN-LNF, Frascati, Italy

Abstract

The design of the Machine Detector Interface area (MDI) for the Future Circular Collider (FCC) is particularly challenging. Initial studies published in 2018 in the FCC Concept Design Report (CDR) are now being enhanced in the context of the ongoing FCC Feasibility Study. With respect to the CDR, a new design for the beam-pipe central chamber of the e+e- collider (FCC-ee), featuring a smaller radius and shorter length, is being considered. The new design allows for an inner layer of the Vertex Detector Barrel to be placed closer to the interaction point. The effect of the background induced occupancy due to Incoherent Pairs Creation (IPC), beam losses in the MDI area and Synchrotron Radiation have been investigated for the CLD detector, one of the detector concepts considered for FCC-ee. The characterisation of the intense Beamstrahlung radiation produced at FCC-ee is also presented.

INTRODUCTION

Machine induced background studies were performed for the FCC-ee Conceptual Design Report (CDR) [1], including the beam losses in the Interaction Region (IR), pairs production and the development of Synchrotron Radiation (SR) masks and shieldings. After the CDR, the design of the beam pipe central chamber has changed to a reduced radius of R=10 mm and length of L=18 cm (originally R=15 mm and length of L=25 cm), allowing to have the inner layer of the Vertex Detector Barrel closer to the Interacion Point (IP).

The Vertex Detector (VXD) geometry description of the CLIC-Like Detector concept (CLD) [3] has been modified in order to fit the new FCC-ee MDI region and to study the effects of several beam induced backgrounds. In particular, the first and the second layers of the barrel have been reduced both in radius to keep the same distance from the beam pipe, and in length in order to to preserve the angular acceptance of the original design. Also, the number of sectors in the innermost layer has been reduced from 16 to 12 because the staves' width is constrained by the manufacturing process. A sketch of the new version of the CLD VXD barrel is shown in Fig. 1. To the same purpose, a re-design of the IDEA [4] Vertex Detector is currently work in progress.

In addition to the design of the 10 mm radius central part of the beam pipe and consequent modifications to the detectors, also the design of the lattice has progressed since the CDR. The current instance of the collider has 4 IPs and different beam parameters. The parameters considered for the studies presented in this work are reported in Table 1.

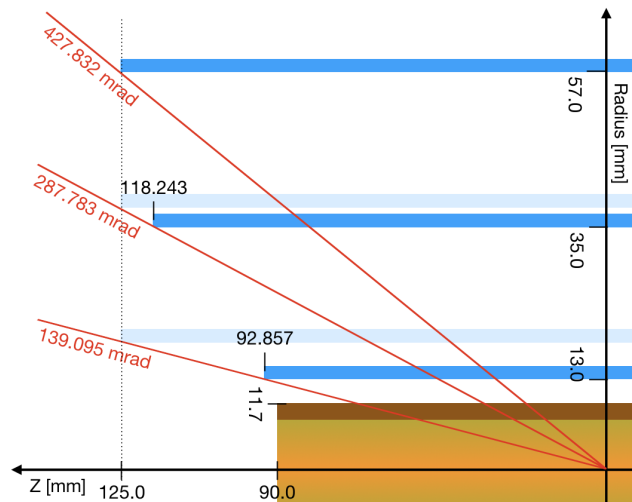* Corresponding Author, andrea.ciarma@cern.ch

Figure 1: Sketch of the new design of the CLD VXD barrel. The blue shapes represent the dimensions of the layers in the new version, the light blue shapes refer to the CDR version. The gold shape is the beam pipe central chamber.

These modifications, together with the migration to the turnkey software Key4HEP [2], make it is necessary to repeat and extend the studies performed for the CDR. In this manuscript I present the status of the studies on the beam induced backgrounds due to the Incoherent Pairs Creation (IPC), beam losses due to failure scenarios, and synchrotron radiation on the CLD vertex detector and tracker. I also give the characterization of the beamstrahlung radiation produced at the IP at the four working points of FCC-ee.

INCOHERENT PAIRS CREATION

Secondary e^+e^- pairs can be produced via the interaction of the beamstrahlung photons with real or virtual photons

Table 1: FCC-ee beam parameters for the 4 IPs lattice

		Z	WW	ZH	tt̄
GeV	E	45.6	80.0	120.0	182.5
nm rad	ϵ_x	71	2.16	64	1.49
pm rad	ϵ_y	1.42	4.32	1.29	2.98
mm	β_x/β_y	100/0.8	200/1	300/1	1000/1.6
μm	σ_x	8.426	20.78	13.86	38.60
nm	σ_y	33.70	65.73	35.92	69.05
mm	σ_z	15.4	8.01	6.0	2.8
10^{11}	N_e	2.43	2.91	2.04	2.37
1	N_{bunch}	10000	880	248	40

FAST LUMINOSITY MONITOR FOR FCC-ee
BASED ON THE LEP EXPERIENCE

A. Di Domenico*, Sapienza University and INFN Rome, Rome, Italy

Abstract

The measurement of luminosity and beam divergence performed by the LEP-5 experiment at CERN based on the detection of photons from the single breamsstrahlung process $e^+e^- \rightarrow e^+e^-\gamma$ at the LEP interaction point 1 is briefly reviewed. A possible implementation of the same methodology for a very fast luminosity monitor at FCC-ee is preliminarily discussed.

INTRODUCTION

The measurement of luminosity at colliders is essential in view of two different objectives: (i) for cross section measurements, where an accurate knowledge of the integrated luminosity is required, and (ii) for machine performance optimization and operation, where a quick feedback from a fast luminosity monitor is desirable.

The luminosity at electron-positron colliders is commonly measured and monitored by detecting the QED Bhabha scattering (BS) process $e^+e^- \rightarrow e^+e^-$. An intense R&D program is on-going for the FCC-ee collider project to reach the ambitious goal of a precision of 10^{-4} on the absolute luminosity measurement around the Z pole by detecting BS events at very small angles [1]. It is worth reminding that at the Large Electron Positron collider (LEP), the second-generation of Bhabha luminosity monitor achieved on the absolute luminosity an experimental precision of 3.4×10^{-4} [2].

Before LEP, the idea to measure the luminosity using the QED process $e^+e^- \rightarrow e^+e^-\gamma$, i.e. the single bremsstrahlung (SB), also called radiative Bhabha scattering, was first exploited at ADONE in Frascati in the '70 [3], and then at VEPP in Novosibirsk [4]. The main feature of this process is that its cross-section slightly increases with energy, $\sigma_{SB} \sim \ln s$, unlike for the BS, whose cross-section decreases as $1/s$. Moreover the BS cross-section depends on the $e^\pm$ scattering angle θ as θ^{-4}, while almost all SB photons are extremely collimated with an angular distribution in a narrow cone in the forward direction $\theta_\gamma \simeq m_e/E$. This makes SB especially convenient at high energy machines as a faster *monitor process* than BS for the easily reachable high rates, as for instance at LEP and in all four beam energy configurations foreseen at FCC-ee, namely Z, WW, HZ and $t\bar{t}$, as shown in Table 1 (for the complete set of parameters used for the present study see Refs. [5, 6]).

In the following, the measurement of luminosity and beam divergence performed by the LEP-5 experiment at the LEP interaction point 1 is briefly reviewed [7, 8]. Finally, a possible implementation of this methodology for a fast luminosity monitor at FCC-ee is considered and its feasibility briefly discussed.

---

* antonio.didomenico@roma1.infn.it

Table 1: Expected BS rate (for $10 < \theta < 20$ mrad) and SB rate (for $E_\gamma > 0.5$ GeV) in the four beam energy configurations of FCC-ee

	Beam energy (GeV)	BS rate (Hz)	SB rate (Hz)
Z	45	$2 \cdot 10^6$	$6 \cdot 10^{11}$
WW	80	$5 \cdot 10^4$	$6 \cdot 10^{10}$
HZ	120	$8 \cdot 10^3$	$2 \cdot 10^{10}$
$t\bar{t}$	182.5	$6 \cdot 10^2$	$9 \cdot 10^9$

THE LEP-5 EXPERIMENT

At LEP with a luminosity $L \simeq 10^{31}$ cm^{-2} s^{-1} the expected SB photon rate is of the order of 3 MHz, which means about 100 Single Bremsstrahlung photons per bunch-crossing, 5-6 orders of magnitude greater than the Bhabha Scattering rate at small angles. Another important feature is the extremely collimated angular distribution of SB photons, the typical emission angle being $\theta_\gamma \simeq \frac{m_e}{E} \simeq 10$ μrad at LEP. In Fig. 1 a sketch of the LEP straight section 1 is shown: the photons travelling with the beams escape the beam-pipe at the beginning of the arc, reaching a detector placed at the end of the straight section, about 350 m far apart from the Interaction Point (IP).

The high SB photon rate implies to work in a multi-photon regime, in which the luminosity is obtained from a measurement of the integrated energy on the detector in a certain time interval, rather than from photon counting:

$$E_{meas} - E_{bckg} = AL \int_0^{E_{beam}} \epsilon(k)k\frac{d\sigma_{SB}}{dk}dk \qquad (1)$$

where k is the photon energy, L the integrated luminosity, E_{meas} the total measured energy in the time interval, E_{bckg} the background measured energy, E_{beam} the beam energy, A the acceptance, $\epsilon(k)$ the energy detection efficiency and threshold function, and $\frac{d\sigma_{SB}}{dk}$ the differential SB cross section. E_{meas} is the measured amount of energy deposited in the detector. E_{bckg} represents the background energy to be subtracted, and which is measured under the condition of no beam crossing in IP-1, with dominant contributions from the beam-gas bremsstrahlung and Compton scattered thermal photons. In Fig. 2 the expected spatial distribution of the deposited energy on the detector is shown, compared with the angular distribution of the SB. From a two dimensional fit of this distribution, the acceptance A is evaluated, obtaining in this way a measurement of the beam position in the transverse plane, and of the beam divergence at the IP.

The SB differential cross section $d\sigma_{SB}/dk$ in eq.(1) has to be evaluated taking into account the finite transverse sizes

LONGITUDINALLY POLARIZED COLLIDING BEAMS AT THE CEPC*

Z. Duan†, T. Chen[1], W. H. Xia[1], J. Gao[1], D. H. Ji, X. P. Li, D. Wang, Y. W. Wang, J. Q. Wang[1]

Key Laboratory of Particle Acceleration Physics and Technology,

Institute of High Energy Physics, Chinese Academy of Sciences, Beijing, China

[1]also at University of Chinese Academy of Sciences, Beijing, China

Abstract

This paper reports the recent progress in the design studies of longitudinally polarized colliding beams for the Circular Electron Positron Collider (CEPC). The overall design concept is outlined, followed by more detailed descriptions of the polarized beam generation, polarization maintenance in the booster, and spin rotators in the collider rings.

INTRODUCTION

The Circular Electron Positron Collider (CEPC) [1, 2] is a next generation electron-positron circular collider, working at center-of-mass energies of 91 GeV (Z-factory), 160 GeV (W- factory), 240 GeV (Higgs-factory), upgradable to 360 GeV (ttbar energy), and aiming at ultra-high precision measurements and probe into new physics beyond Standard Model. The resonant depolarization technique (RD) [3] is essential for precision measurements of the mass of Z and W bosons, this requires transversely polarized e⁺ and e⁻ beams with at least 5% to 10% beam polarization. Meanwhile, probing the spin dimension with longitudinally polarized colliding beams can be very beneficial to enhance particular channels, reduce background and facilitate searches for beyond Standard Model chiral new physics. This application requires 50% or more longitudinal polarization (for e- beam alone, or for both beams) at the Interaction Points (IPs) as well as a high luminosity. These applications demand a careful study of the polarized beam generation and maintenance as well as spin manipulation in the collider rings.

Top-up injection will be adopted in the CEPC collider rings, to maximize the integrated luminosity. In this operation mode, the time-averaged beam polarization P_{avg} of the colliding beams contains two different contributions, one is from the Sokolov-Ternov effect [4] in the storage ring, characterized by the equilibrium beam polarization P_{DK}, the other is from the injected beam polarization P_{inj},

$$P_{avg} = \frac{P_{DK}}{1 + \tau_{DK}/\tau_b} + \frac{P_{inj}}{1 + \tau_b/\tau_{DK}} \qquad (1)$$

where τ_b is the beam lifetime, which is mainly limited by the radiative Bhabha effect and is correlated to the luminosity. τ_{DK} is the polarization build-up time, $\tau_{DK}^{-1} = \tau_{BSK}^{-1} + \tau_{dep}^{-1}$, where τ_{BSK} and τ_{dep} are the time constants characterizing

the Sokolov-Ternov effect and the radiative depolarization effect [5], respectively. The equilibrium beam polarization P_{DK} [6] can be approximated by

$$P_{DK} \approx \frac{P_\infty}{1 + \frac{\tau_{BKS}}{\tau_{DK}}} \qquad (2)$$

where P_∞ is the equilibrium beam polarization taking into the orbital imperfections, but disregarding the radiative depolarization effect, $P_\infty = 92.4\%$ in an ideal planar ring, and is generally lower in an imperfect ring.

If a highly polarized beam is injected into the collider ring, and in the case of $\tau_b \ll \tau_{DK}$, the time-averaged beam polarization of the colliding beams can be evaluated by

$$P_{avg} \approx \frac{P_{inj}}{1 + \frac{\tau_b}{\tau_{BKS}} \frac{P_\infty}{P_{DK}}} \qquad (3)$$

this indicates that a very low level of P_{DK} would reduce P_{avg}. In Table 1, we assume $P_{inj} = 80\%$, and calculate the required minimum P_{DK} to reach $P_{avg} \geq 50\%$. Given the relative ratio between τ_b and τ_{BKS}, a larger P_{DK} is required at a higher beam energy, which poses a greater challenge in the mitigation of the radiative depolarization effect in the collider rings. Nevertheless, injection of highly polarized beams into the collider rings, has the potential of reaching a high level of P_{avg} besides a high luminosity, and is essential to realize longitudinally polarized colliding beams.

Table 1: CEPC Beam Parameters Related to P_{avg}

Beam energy	45.6 GeV Z	80 GeV W	120 GeV Higgs
τ_b(hour)	2.5	1.4	0.43
τ_{BKS}(hour)	256	15.2	2.0
$P_{DK,min}$	0.6%	5%	11%

In addition, pilot non-colliding bunches might be necessary for RD measurements, since the beamstruhlung of colliding bunches substantially increases the rms beam energy spread and could limit the achievable accuracy of RD measurements. These pilot bunches operate in the decay mode, and the Sokolov-Ternov effect [4] can be used to generate the required polarization for RD measurements, where asymmetric wigglers [7] are required to boost the self-polarization process at Z-pole [8]. Nevertheless, injection of highly polarized beams into these pilot bunches could be a viable alternative approach for RD measurements as well.

Figure 1 shows the envisaged modification of the CEPC accelerator complex to implement polarized beams. Electron beam with over 80% polarization can be generated from

SPIN POLARIZATION SIMULATIONS FOR THE FUTURE CIRCULAR COLLIDER e+e- USING BMAD*

Y. Wu[1,†], F. Carlier[2], L. Van Riesen-Haupt[1], T. Pieloni[1]

[1]École Polytechnique Fédérale de Lausanne (EPFL), Lausanne, Switzerland

[2]European Organization for Nuclear Research (CERN), Geneva, Switzerland

Abstract

Measurements of particle properties with unprecedented accuracy in the Future Circular Collider e+e- (FCC-ee) are reliant on the high precision center-of-mass energy calibration, which could be realized via resonant depolarization measurements. The obtainable equilibrium spin polarization levels under the influence of lattice imperfections should be estimated via spin polarization simulations. An early-stage exploration of spin simulations in the FCC-ee has been conducted using Bmad. An effective model has been used to generate residual errors for the simulation of realistic orbits after lattice corrections. The influences of depolarization effects near the first-order spin-orbit resonances are displayed in linear polarization simulations, highlighting the demand for good closed orbit control. Furthermore, the first attempts at performing nonlinear spin tracking simulations in the FCC-ee reveals the full impact of lattice perturbations.

INTRODUCTION

The Future Circular Collider (FCC) was proposed to push both the energy and intensity frontiers of particle physics [1]. The FCC-ee, which is an electron-positron collider, as the first step of the FCC project, is designed to operate on multiple center-of-mass collision energies $\sqrt{s}$ between 88 GeV and 365 GeV for the production of Z^0 bosons ($\sqrt{s} \sim 91$ GeV), WW pairs ($\sqrt{s} \sim 160$ GeV), Higgs bosons ($\sqrt{s} \sim 240$ GeV) and top quark pairs ($\sqrt{s} \sim 350 - 365$ GeV) [1, 2].

The current precision requirements at Z mass and W mass are 4 keV and 250 keV respectively [3]. Resonant depolarization is a high precision energy calibration method that has been used in previous lepton machines such as the Large Electron–Positron Collider (LEP) [4], and is the proposed method in the FCC-ee to reach the unprecedented precision target at the Z and W pair threshold [2]. Spin polarization simulations are required to validate this energy calibration method in the FCC-ee by investigating the effects of lattice perturbations on spins. A minimum of 10% transverse polarization level at equilibrium should be guaranteed under various possible lattice conditions in order to ensure accurate energy calibration measurements [5].

Basics of Spin Dynamics

The spin precession motion in electromagnetic fields can be described by the Thomas-Bargmann-Michel-Telegdi (T-BMT) equation [6, 7],

---

$$\frac{d\vec{S}}{dt} = \vec{\Omega}_{BMT} \times \vec{S}, \tag{1}$$

where $\vec{S}$ is the spin expectation and the precession vector $\vec{\Omega}_{BMT}$ is in the form of [8]

$$\vec{\Omega}_{BMT} = -\frac{e}{m}\left[\left(a + \frac{1}{\gamma}\right)\vec{B} - \frac{a\gamma}{\gamma+1}\vec{\beta}(\vec{\beta}\cdot\vec{B}) - \left(a + \frac{1}{\gamma+1}\right)\vec{\beta}\times\vec{E}\right], \tag{2}$$

where e and m are the particle charge and mass respectively, $\vec{\beta}$ and γ are the relativistic factors, $\vec{B}$ and $\vec{E}$ are the magnetic and electric fields, and the gyromagnetic anomaly a is approximately 0.0011597 for electrons and positrons. The precession vector can be decomposed into the periodic closed orbit term $\vec{\Omega}^{c.o}(s)$ and the other term brought by synchro-betatron motions $\vec{\omega}^{s.b}(\vec{u}; s)$

$$\vec{\Omega}_{BMT}(\vec{u}; s) = \vec{\Omega}^{c.o}(s) + \vec{\omega}^{s.b}(\vec{u}; s), \tag{3}$$

where s is the azimuthal position and vector $\vec{u} \equiv (x, x', y, y', z, \delta)$ denotes the phase space position of a particle with δ being the relative energy deviation $\delta = \Delta E/E_0$ [8]. The unit length one-turn periodic solution of the T-BMT equation on the closed orbit is denoted as $\hat{n}_0$, which is the stable spin direction on the closed orbit [9, 10]. In a perfectly aligned flat machine, arbitrary spins on the closed orbit will perform $a\gamma$ precessions around $\hat{n}_0$ during one orbital revolution, which is the closed orbit spin tune ν_0. Nevertheless, ν_0 will experience a slight deviation from $a\gamma$ when there are errors and misalignments in the machine [10].

The emission of synchrotron radiation when electrons and positrons are moving in the ring can enable spin flip which switches the spin direction between spin up and down, through the Sokolov-Ternov effect [11]. The slight difference in the transition rates between two spin states allows an accumulation of polarization along the opposite direction of the magnetic field for electrons. An equilibrium polarization level of $P_{ST} \simeq 92.38\%$ can be reached in uniform magnetic fields, while in arbitrary fields it can be estimated with the following equation [12, 13]

$$\vec{P}_{bks} = -\frac{8}{5\sqrt{3}}\hat{n}_0\frac{\oint ds\frac{\hat{n}_0(s)\cdot\hat{b}(s)}{|\rho(s)|^3}}{\oint ds\frac{[1-\frac{2}{9}(\hat{n}_0\cdot\hat{s})^2]}{|\rho(s)|^3}}, \tag{4}$$

where ρ represents the instantaneous bending radius, $\hat{b} = (\hat{s}\times\dot{\hat{s}})/|\dot{\hat{s}}|$ is the magnetic field direction, and $\hat{s}$ is the unit

PROGRESS IN EIC POLARIZATION STUDIES FOR THE INJECTORS AND STORAGE RING

V. H. Ranjbar*, Brookhaven National Laboratory, Upton NY, USA
E. Gianfelice, Fermilab, Batavia, IL, USA

Abstract

We present recent progress in simulations and studies for the EIC's Electron Storage RING (ESR) and the EIC's polarized injector the Rapid Cycling Synchrotron.

INTRODUCTION

The Electron Ion Collider (EIC) to be built will collide polarized electrons and ions up to 140 GeV center of mass with a time averaged polarization of 70% and luminosity up to 10^{34} cm^{-2} s^{-1} (see Fig. 1). The EIC's Rapid Cycling Synchrotron (RCS) will accelerate 2 polarized electrons bunches from 400 MeV to energies of 5, 10 and 18 GeV and inject them into the EIC's Electron Storage Ring (ESR).These bunches will be stored between 4-6 minutes at 18 GeV in bunches parallel and anti-parallel to the dipole guide field. The time in store is determined by the polarization lifetime and the requirement to maintain average polarization at 70%. In this paper we study the impact of misalignments on polarization lifetime and approaches to correct and counter act their effects on lifetime.
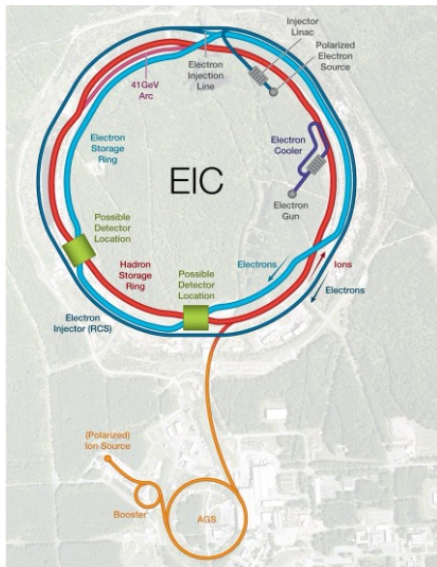

Figure 1: EIC Complex

The RCS injector is designed to accelerate polarized electrons maintaining 85% polarization. This is accomplished due to the special lattice design which avoids and minimizes the spin resonances in the acceleration range. We present progress on development of this lattice and studies of the impact of misalignments and approaches to correct for their effects on polarization.

---

* vranjbar@bnl.gov

POLARIZATION IN THE ESR

EIC experiments require an average polarization of at least 70% oriented in the longitudinal plane, using both helicities within the same store. The electrons will be stored in the ESR at energies of 5, 10 and 18 GeV. The radiative effects on polarization in an electron storage ring is given by the Sokolov-Ternov effect. In an ideal planar ring with out spin rotators, the periodic solution to the Thomas-BMT equation, $\hat{n}_0$, is vertical and electron polarization builds up anti-parallel wrt the dipole guide field. The asymptotic polarization is P_∞= 92.4%. The rate at which the polarization is built up is given by,

$$\tau_p^{-1} = \frac{5\sqrt{3}}{8} \frac{r_e \hbar \gamma^5}{m_0 C} \oint \frac{ds}{|\rho|^3} \,. \qquad (1)$$

Asymptotic Polarization in ESR

In an actual ring, $\hat{n}_0(s)$ is not vertical and the beam has a finite vertical size, thus photon emission leads to spin diffusion that lowers the asymptotic polarization. Because experiments require the simultaneous storage of electron bunches with both spin helicity, Sokolov-Ternov effect cannot be used to self-polarize the beam. Thus a full energy electron injector is needed and the EIC will use the RCS to inject with 85% polarization in the desired spin orientation. As well in the ESR since longitudinal polarization is required, the spin will be brought into the longitudinal direction at the interaction point (IP) using a combination of solenoids and dipoles to the left and right of the IP.

Depending on the actual equilibrium polarization, the Sokolov-Ternov effect can cause the rapid decay of a highly polarized beam. This decay is described using,

$$P(t) = P_\infty(1 - e^{t/\tau_P}) + P(0)e^{-t/\tau_P} \,. \qquad (2)$$

Here the polarization time constant can be estimated using,

$$\frac{1}{\tau_p} \approx \frac{1}{\tau_{BKS}} + \frac{1}{\tau_d}$$

$$P_\infty \approx \frac{\tau_p}{\tau_{BKS}} P_{BKS} \,. \qquad (3)$$

Here P_{BKS} and τ_{BKS} are the Baier-Katkov-Strakhovenko generalization of the Sokolov-Ternov quantities when $\hat{n}_0$ is not everywhere perpendicular to the velocity. These values can be calculated for a given lattice. Thus τ_d and P_∞ depends on the actual machine. While τ_d is the spin diffusion time for a given lattice, this is determined using direct spin-orbit tracking. We use MADX to manage the optics and misalignments together with the spin tracking codes: SITF

BEAM-BEAM INTERACTION IN SuperKEKB: SIMULATIONS AND EXPERIMENTAL RESULTS

D. Zhou*, K. Ohmi, Y. Funakoshi, Y. Ohnishi, KEK, Tsukuba, Japan
Y. Zhang, IHEP, Beijing, China

Abstract

The beam-beam interaction is one of the most critical factors determining the luminosity performance of SuperKEKB. Simulations and experimental results from SuperKEKB have shown that a complete understanding of the beam-beam effects demands reliable models of 1) the nonlinear beam-beam interaction at the interaction point, 2) the one-turn lattice transfer map with machine imperfections, and 3) other intensity-dependent collective effects. The interplay of these factors makes it difficult to predict the luminosity performance of SuperKEKB via simulations.

INTRODUCTION

This paper continues the authors' previous work to discuss the beam-beam effects on luminosity in SuperKEKB [1]. SuperKEKB commissioning had three phases: Phase-1 [2, 3] (February - June 2016, without installation of the final focusing superconducting QCS magnets and roll-in of Belle II detector), Phase-2 [4] (February - July 2018, with QCS and Belle II, but without the vertex detector), and Phase-3 [5] (from March 2019 until present with the full Belle II detector). Beam commissioning without collisions in Phase-1 achieved small vertical emittances of less than 10 pm for both beams, which is essential for high luminosity. Machine tuning with collisions in Phase-2 confirmed the nano-beam collision scheme [6], i.e., collision with a large crossing angle and vertical beta function β_y^* at the IP much smaller than bunch length σ_z. However, without the CW, the beam-beam (BB) driven vertical emittance blowup was severe, causing degradation of specific luminosity (L_{sp}) as bunch currents increased.

The uncontrollable blowup in vertical emittances sets a severe limit on the luminosity performance and motivated the installation of the CW in SuperKEKB [7]. Beam commissioning with the CW at SuperKEKB has been successful with β_y^* = 1 and 0.8 mm [7]. Experiments have shown that the CW effectively suppresses vertical blowup and allows larger beam currents to be stored in the rings [8]. On Jun. 22, 2022, a luminosity record of 4.71×10^{34} cm^{-2}s^{-1} was achieved at SuperKEKB with β_y^* = 1 mm and total beam currents I_+/I_- = 1.46/1.145 A [9].

LUMINOSITY PERFORMANCE WITH CRAB WAIST

Since April 2020, the crab waist (CW) has been implemented at SuperKEKB to suppress beam-beam resonances [10, 11]. Luminosity performance has been im-

proving with the following observations (see Refs. [7, 8] for reviews): 1) Luminosity performance became closer to the predictions of simulations; 2) Balanced collision (i.e., $\sigma_{y+}^* \approx \sigma_{y-}^*$, the vertical beam sizes at the IP are close to each other) was achieved with careful tuning knobs; 3) The fractional working point could be set around the design values (.53, .57); 4) The total beam currents were not limited by BB blowup, but by injection power and by machine failures of sudden beam losses (SBLs, their sources are unclear so far); 5) There still exists an unexpected degradation of L_sp vs. product of bunch currents (see Figs. 1 and 4). In particular, increasing the beam current does not give large increases in luminosity.

Figures 1, 2 and 3 compare the L_{sp} and transverse beam sizes at the IP from strong-strong BB simulations and measurements using X-ray monitors (XRMs). The machine parameters of 2022.04.05 in Table 1 are used for BB simulations. Optics functions at the IP and the XRMs calculated from a lattice model are used to estimate the beam sizes at the IP in measurements. In both simulations and experiments, the luminosity is sensitive to the vertical beam sizes at the IP. With the standard settings of 40% and 80% CW strengths in the experiments, respectively, for HER and LER (40% CW strength was set for HER due to a technical constraint), the decrease of L_{sp} in strong-strong BB simulation is mainly attributed to bunch lengthening due to the longitudinal wakefields and weak vertical blowup of HER beam due to insufficient CW strength. However, experimental results showed a much faster L_{sp} decrease as bunch currents increase. The sources of luminosity degradation are discussed in the next section. The plots also show simulations with the CW strengths varied. It is seen that the L_{sp} drop in simulations correlates with BB-driven blowup in the positron beam because its vertical fractional tune .589 is close to the 5th-order BB resonances.

Figures 4, 5 and 6 show a comparison of simulations and measurements with machine conditions of 2021. One can see that the machine operation after April of 2022 showed gradual beam-size blowup as the bunch currents were increased (see Figs. 2 and 3); while in 2021, the beam-size blowup was severe for both e+ and e- beams. At that time, it was difficult to achieve a balanced collision (i.e., $\sigma_{y+}^* \approx \sigma_{y-}^*$). A "flip-flop" blowup appeared when the bunch-current product $I_{b+}I_{b-} \gtrsim 0.4$ mA^2: When one beam was tuned to have a small vertical beam size at IP, another beam blew up severely. This severe blowup at high bunch currents was believed to be related to the "-1 mode instability" of the positron beam, which was driven by the interplay of vertical impedance (dominated by small-gap collimators) and the bunch-by-bunch (BxB) feedback (FB) system as discussed in detail in

---

* dmzhou@post.kek.jp

STUDY FOR -1 MODE INSTABILITY IN SuperKEKB LOW ENERGY RING

K. Ohmi, H. Fukuma, T. Ishibashi, S. Terui, M. Tobiyama, D. Zhou

KEK, Tsukuba, Ibaraki, Japan

Abstract

A beam size blow-up has been observed in increasing beam current in superKEKB Low Energy Ring (LER). The blow-up is a single bunch effect, which appears at high bunch current $I_b \approx 1$ mA. -1 mode ($\nu_y - \nu_s$) signal was detected in a beam position monitor at the appearance of the blow-up. The blow up is suppressed at vertical tune $\nu_y > 0.59$, while the beam injection is hard at the tune. The blow-up disappeared at turning off a bunch-by-bunch feedback. The luminosity performance of SuperKEKB is limited by the blowup, because it depends on the feedback tuning, operating point and collimator conditions Measurements and simulations for the blow-up are presented to explain the phenomenon.

INTRODUCTION

SuperKEKB consists of Low Energy Ring (LER) and High Energy Ring (HER), which store 4 GeV positron beam and 7 GeV electron beam, respectively. In physics operation, lower vertical tune in LER has tended to have lower luminosity and beam instability. We began to measure LER beam size without collision to make clear the reason. A beam size blow-up has been observed increasing beam current ~ 1 A in LER since 2021 spring.

Several times of measurements have been performed since 2021. The blow-up has been seen in single beam operation of LER. The blow-up was independent of the number of bunch stored: i.e. it was seen at I = 90 mA in 99 bunches storage, while at around 1 A in 1000-1500 bunches storage in physics run. The beam size depended only on the bunch current. Therefore this phenomenon was concluded as single beam and single bunch effect.

The blow-up also depended on the collimator aperture. In LER, a few number of collimators contributes dominantly as impedance sources. Narrower aperture of the collimators resulted in larger beam size blow-up. The phenomenon was concluded as an impedance related effect. -1 mode ($\nu_y - \nu_s$) signal was detected in a beam position monitor at the appearance of the blow-up. The separation of ν_y and $\nu_y - \nu_s$ signals was sufficient to exclude the possibility of TMCI.

The blow-up depends on bunch-by-bunch feedback system. The bunch-by-bunch feedback is essential for multi-bunch and high-current operation. The feedback could be turned off in accelerator experiments with a very small number of bunches (~ 30) and beam current I=30mA. The blow-up disappeared when turn off the feedback.

We call this beam-size blow-up -1 mode instability. This paper shows the experimental results and discussions for mechanism of the beam-size blow up or -1 mode instability.

MEASUREMENTS OF LER

The beam size blow-up is related to the vertical impedance. Amplitude of the vertical impedance is evaluated by measurement of current dependent tune shift, which is expressed by the well known formula,

$$\Delta\nu_y = \frac{Ne^2}{4\pi E} \sum_i \beta_{y,i} k_{y,i} \tag{1}$$

$$= 2 \times 10^{-19} \sum_i \beta_{y,i} k_{y,i} [V/C] I[mA]. \tag{2}$$

where LER parameters are substituted into Eq. (1) on Eq.(2). The vertical kick factor (k_y) is expresse by the vertical wake field and/or impedance

$$k_y = \iint_{-\infty}^{\infty} W_y(z - z')\rho(z)\rho(z')dzdz' \tag{3}$$

$$= -\frac{i}{2\pi} \int_{-\infty}^{\infty} d\omega Z_y(\omega)e^{-\omega^2 \sigma_z^2/c^2} \tag{4}$$

where Gaussian density distribution $\rho(z) = e^{-z^2/(2\sigma_z^2)}/(\sqrt{2\pi}\sigma_z)$ is assumed in Eq. (4).

Four vertical collimators D2V1,V2 (s =1800 m), D3V1 (s =2714 m) and D6V1 (s =1800 m) are installed to protect the physics detector Bell-II from beam background, where s is position from the Interaction Point. The collimators, especially D2V1 and D6V1, are dominant source of the vertical impedance.

Electro-magnetic filed simulations using GdFidl citeGDFDL and ECHO3D [2] gave $\sum \beta_y k_y = 3.3 \times 10^{16}$ V/C for collimators and 1.8×10^{16} V/C for the beam chamber in Interaction Region and others: i.e., 5.1×10^{16} V/C in total [3]. The impedance corresponds to a collimator aperture setting used in the measurements presented in this paper. The collimators are slightly opened in physics run: i.e., the collimator impedance is 2.9×10^{16} V/C.

The current dependent tune shift was measured in a single bunch operation. Figure 1 shows vertical tune shifts for $\nu_{y,0}$ =0.614 and 0.592 as functions of bunch current. Tune shift is linear for the bunch current. The linear coefficients are fitted as seen in the figure. The tune shift was determined as $\Delta\nu_y/I = 1.1$ mA^{-1}. Corresponding impedance/ kick factor is $\sum \beta_y k_y = 5.5 \times 10^{16}$ V/C. The difference between the measurement and simulations is within 10%.

Vertical beam size has been measured by Xray monitor using coded aperture mask [5] in SuperKEKB. Figure 2 shows the beam size as a function of the bunch current. Beam sizes for the two collimator apertures of D6V1 are plotted by blue and orange points. Corresponding collimator

CAVITY AND CRYOMODULE DEVELOPMENTS FOR EIC *

R. A. Rimmer†, E. Daly, J. Guo, J. Henry, J. Matalevich, H. Wang, JLab, Newport News, VA, USA

D. Holmes, K. Smith, W. Xu, A. Zaltsman, B. Xiao, BNL, Upton, NY, USA

S. De Silva, J. Delayen, Old Dominion University, Norfolk, VA, USA

Abstract

The EIC is a major new project under construction at BNL in partnership with JLab. It relies upon a number of new SRF cavities at 197 MHz, 394 MHz, 591 MHz and 1773 MHz to pre-bunch, accelerate, cool and crab the stored beams. R&D is focusing on the 591 MHz elliptical cavity and 197 MHz crab cavity first as these are the most challenging. Preliminary designs of these cavities are presented along with an R&D status report. To avoid developing multiple different cryostats a modular approach is adopted using a high degree of commonality of parts and systems. This approach may be easily adapted to other frequencies and applications.

OVERVIEW OF SRF SYSTEMS FOR EIC

The electron ion collider (EIC) [1], is a complex machine incorporating many of the challenges of e+e- factories, hadron-hadron colliders and even light sources. The complex consists of a hadron injector complex and storage ring based on upgrades to the RHIC facility, a new high-current electron storage ring and an RCS as a full energy injector. Most of the existing RF systems for RHIC will be retained or repurposed however new 591 MHz SRF bunching systems will be needed in both collider rings to attain the short bunches needed for high luminosity. In the high-current ESR these will be heavily HOM-damped single-cell cavities similar to those used in the B-factories, with high power beam line absorbers (BLAs). Table 1 lists the high level parameters for the ESR. Dual 400 kW fundamental power couplers will be used on each cavity. In the HSR the current is 0.75 A so multi-cell cavities can be used and the required voltage is about 20 MV. One or two 5-cell cavities can fulfil these requirements. Although HOM power will be lower than the ESR good damping is still required and the impedance of same-passband modes must be carefully managed. In the CDR a scaled version of a previous 5-cell cavity was assumed. Similar 5-cell cavities can be used in the RCS and in the ERL for strong hadron cooling (SHC). 1773 MHz harmonic cavities are needed to linearize the cooler linac and 197 MHz buncher cavities are needed in the injector. A low energy pre-cooler ERL is also proposed that would use 197 MHz accelerating cavities. The other major SRF system in EIC is the crabbing cavities for the interaction point (IP). Because of the large crossing angle a high crabbing voltage is needed. Due to the long bunch length in the hadron ring 197 MHz cavities are chosen with 394 MHz harmonic cavities to maintain a linear

crab kick along the bunch length. The shorter bunch length in the ESR allows single 394 MHz crabbing systems to be used. Given the large number of systems to be developed a modular cryostat approach with a high degree of commonality of components is being followed to minimize design effort and speed up development.

R&D PRIORITIES

Four items were chosen for early R&D based on risk; the 591 MHz ESR single cell, the 197 MHz crab cavity, the 400 kW FPC and the high power BLA. One prototype of each cavity will be built and tested and small batches of FPC's and BLA's will be built and evaluated. The other cavity types are assumed to be lower risk or can be developed by extrapolating from these designs, e.g. the 394 MHz crab cavity can be developed using lessons learned from the 197 MHz prototype and the 5-cell 591 MHz cavities can be developed from the single cell.

591 MHz ESR 1-CELL CAVITY

The CDR describes a symmetric 1-cell cavity using two large beam pipe absorbers, developed from an earlier 2-cell design in the pre-CDR. see Fig. 1. The number of cavities is determined by the peak voltage needed to maintain adequate bucket height at 18 GeV and the amount of coupler power needed to replace synchrotron radiation and other losses, see Table 1.

The high average current and naturally short bunch length lead to high HOM power of >40 kW per cavity. Up to 10 MW of beam power must be supplied and symmetric dual 400 kW FPC's will be fitted to each of the 17 single-cell cavities.
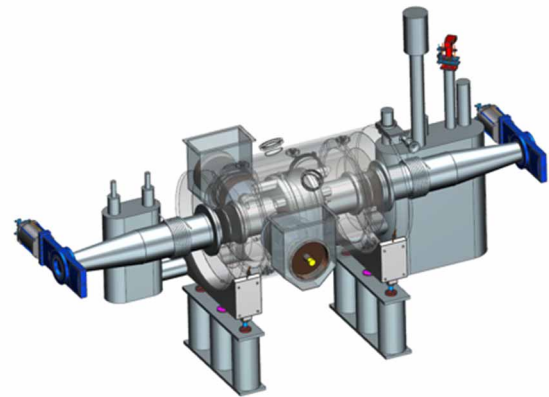

Figure 1: Symmetric single cell 591 MHz SRF cryomodule with two large warm BLA's and tapers in the CDR.

SuperKEKB OPERATING EXPERIENCE OF RF SYSTEM AT HIGH CURRENT

M. Nishiwaki*, T. Abe, K. Akai, S. Enomoto, T. Furuya, A. Kabe, T. Kageyama, T. Kobayashi,
K. Marutsuka, S. Mitsunobu, Y. Morita, K. Nakanishi, S. Ogasawara, T. Okada, M. Ono, H. Sakai,
Y. Takeuchi, K. Watanabe, M. Yoshida, S. Yoshimoto and K. Yoshino
High Energy Accelerator Research Organization (KEK), Tsukuba, Japan

Abstract

SuperKEKB aims for high luminosity on the order of 10^{35} /cm^2/s with high beam currents of 2.6 A for electron and 3.6 A for positron to search a new physics beyond the Standard Model in the B meson regime. In recent operations, we achieved new record of the luminosity of 4.7×10^{34} /cm^2/s with 1.1 A for electron and 1.3 A for positron. The RF system that is basically reused from KEKB is operating stably in the high current operation owing to the measures against to large beam power and HOM power. To cope with the large beam power, it has been increased the number of klystrons that drive only one normal conducting cavity (ARES) and reinforced the input couplers of ARES. As a measure against HOM power, the additional HOM dampers have been installed to superconducting cavities. One-third of LLRF control systems have been replaced with newly developed digital system to improve accuracy and flexibility. New damper system for coupled bunch instability expected in high current has been installed to new digital system. In this report, operation status of RF system under the high current operation will be presented.

INTRODUCTION

The SuperKEKB accelerator that is an electron-positron asymmetric energy collider is an upgrade machine from KEKB accelerator aiming for a significant increase of luminosity. SuperKEKB main ring consists of a 7 GeV electron ring (high energy ring, HER) and a 4 GeV positron ring (low energy ring, LER). To achieve high luminosity, the beam currents are designed as 2.6 A for HER and 3.6 A for LER [1]. The first commissioning beam operation without collision was performed in 2016 as Phase-1. After the Belle II detector rolled in, Phase-2 beam operation started and the first beam collision event was observed at Belle II in 2018. A full-scale collision experiment (Phase-3) has been continued since 2019. In recent operation, the achieved beam currents are 1.14 A for HER and 1.46 A for LER, and the peak luminosity of 4.65×10^{34} /cm^2/s was recorded [2, 3].

The RF-related operation parameters in KEKB (achieved) and SuperKEKB (design) are shown in Table 1. The design beam current is nearly twice as high as the KEKB achieved, and the beam power becomes large accordingly [4–6]. The RF system consisting both of normal-conducting cavities (ARES) [7–9] and superconducting cavities (SCC) [10, 11] has been reused from KEKB with reinforcement to handle the high beam current and the large beam power. The ARES stations have 1:2 configuration in which one klystron drives two ARESs, and 1:1 configuration in which one klystron drives one ARES. The SCC station has one cavity driven by one klystron.

The main upgrade items are as follows:
- Increasing the number of RF klystron stations of ARES 1:1 configuration.
- In ARES, changing input coupling factor β from 3 (1:2 configuration) to 5 (1:1 configuration).
- In SCC, installation of additional higher-order-mode (HOM) dampers.
- In High-Power RF (HPRF) system, replacement of deteriorated klystrons with higher gain and more stable ones.
- In Low-Level RF (LLRF) system, replacing with new digital LLRF system in a part of ARES 1:1 stations and development of new damper system for coupled instability.

The addition of klystron to upgrade from ARES 1:2 to 1:1 configuration and the increase of input coupling factor of ARES are essential to provide the large beam power. The HOM power excited in the SCC module at the design current is estimated to be more than double the power achieved in KEKB, and to exceed the allowable power of the existing ferrite dampers. Then, additional dampers are necessary to reduce the load of ferrite dampers. The replacement of the old HPRF and LLRF systems with new systems increases the stability and accuracy of beam operation.

The layout of RF stations in SuperKEKB at present is shown in Fig. 1. There are a total of 30 RF klystron stations consisting 16 ARES (22 cavities) stations in LER and 6 ARES (8 cavities) and 8 SCC stations in HER. To date, the number of ARES 1:1 station is partially increased to 10 (LER) and 4 (HER) stations. In addition, countermeasures against RF-related instabilities in LLRF are essential for the high beam current operation. These measures have been completed partially. Remaining update items will be performed in the future to achieve the target beam current and luminosity. The details of upgrade of each component are described in Refs. [9, 13–18]. In this report, the operation status of RF system and the high beam current-related issues in RF system are described.

OPERATION STATUS OF RF SYSTEM

In the recent beam operation, the RF system is operating stably without any troubles requiring long shutdown.

---

* michiru.nishiwaki@kek.jp

COLLECTIVE EFFECTS STUDIES FOR CEPC

Na Wang[1†], Yuan Zhang[1, 2], Haisheng Xu[1], Saike Tian[1], Yudong Liu[1], Chuntao Lin[3]
[1]Institute of High Energy Physics, CAS, Beijing, 100049, China
[2] University of Chinese Academy of Sciences, CAS, Beijing, 100049, China
[3]Institute of Advanced Science Facilities, Shenzhen, China

Abstract

The impedance model of the Circular Electron Positron Collider (CEPC) storage ring is updated according to the development of the vacuum components based on the circular beam pipe. With the impedance model, the single bunch and coupled bunch instabilities for different operation scenarios are investigated. Particularly, the key instability issues driven by the beam coupling impedance in the Z operation mode are discussed. The influence of the longitudinal impedance on the transverse mode coupling instability is analysed both numerically and analytically. In addition, trapped ions can induce bunch centroid oscillation and emittance growth. The possibility of ion trapping and fast beam ion instability in the CEPC storage ring are also investigated.

INTRODUCTION

The Circular Electron Positron Collider (CEPC) is a double ring lepton collider covers a wide beam energy range from 45 GeV (Z-pole) to 180 GeV (tt-bar) [1,2]. Since the Z mode has the lowest beam energy, as well as highest beam current and slowest synchrotron radiation damping, normally it shows the most critical requirements on the collective effects. In order to estimate the influence of these effects, the impedance model of the CEPC collider has been evolving since the start of the project [3-6]. Based on the impedance, systematic studies on the beam instability issues and their mitigations have been performed. In this paper, the resistive wall impedance and its induced coupled bunch instability are updated by considering more detailed vacuum chamber designs. In addition, macro particle simulations are performed for the single bunch effect and beam ion instabilities. The perturbation of longitudinal impedance on the transverse mode coupling instability is investigated analytically.

IMPEDANCE MODELING

The impedance model is developed considering both resistive wall and geometrical impedances. The main vacuum chamber has a circular cross section with radius of 28 mm, which is made of copper and has a layer of NEG coating on its inner surface to reduce the secondary electron yield as well as for the vacuum pumping. In order to evaluate the resistive wall impedance, multi-layer analytical formula from field matching is used [7].

Meanwhile, simplified formulas are derived for longitudinal and transverse resistive wall impedance of the coated metallic chambers:

---

† wangn@ihep.ac.cn

$$Z_\parallel^{\mathrm{RW}}(\omega) = \frac{Z_0 \delta_1 \mu_1 k_0 [\mathrm{sgn}(\omega) - i]}{4\pi b \mu_0} \times \frac{\alpha \tanh(x_1) + \tanh(x_2)}{\alpha + \tanh(x_1)\tanh(x_2)} \tag{1}$$

$$Z_\perp^{\mathrm{RW}}(\omega) = \frac{4 - k_r^2 b^2}{\sqrt{k_0^2 + k_r^2}} \frac{1 - i\mathrm{sgn}(\omega)}{4\pi b^3 \delta_1 \sigma_1} \times \frac{1 + \alpha \tanh(x_1)\tanh(x_2)}{\alpha \tanh(x_2) + \tanh(x_1)} \tag{2}$$

where b is the beam pipe aperture, $\alpha = \delta_1 \mu_1 / \delta_2 \mu_2$, $x_i = \lambda_i d_i$, $\lambda_i \simeq \sqrt{-2i}/\delta_i$, δ_i, d_i and μ_i are the skin depth, thickness and conductivity of the i'th layer, respectively. The numerical results are benchmarked with ImpedanceWake2D [8] and excellent agreements have been reached in the frequency range of interest.

Except the typical NEG coated vacuum chambers, the resistive wall impedance contributed by the MDI chambers, collimators in the interaction region and stainless steel chambers for flanges, bellows and BPMs are also considered. Since the Machine Detector Interface (MDI) and collimators may contribute large impedances, either due to the smaller beam pipe aperture or large local beta functions, the resistive wall impedance of the tapers are considered in more detail. Assuming the longitudinal and transverse resistive wall impedance is inverse proportional to the radius r or cubic of r, by integrating the impedance along the taper, we get the longitudinal and transverse resistive wall impedance of a taper is the impedance of a cylinder of unit length with the smaller aperture r_1 of the taper multiplied by the following factors

$$f_\parallel^{RW} = \frac{r_1}{\tan\theta} \log(1 + L/r_1\tan\theta), \tag{3}$$

$$f_T^{RW} = \frac{r_1}{2} \frac{2r_1/L + \tan\theta}{(r_1/L + \tan\theta)^2}, \tag{4}$$

where L and θ are the length and angle of the taper，respectively.

The longitudinal and transverse resistive wall impedance contributed from different vacuum components is summarized in Fig. 1 and Fig. 2, respectively. Here, the transverse impedance has been normalized by the local beta functions. In addition, geometrical form factors [9] are considered for the resistive wall impedance of the vacuum chambers with non-axial symmetry. We can see that the impedance contributed by the typical vacuum chamber dominates both the longitudinal and transverse resistive wall impedance. The contributions from the MDI and collimators are considerably small.

MITIGATION OF ELECTRON CLOUD EFFECT IN THE SuperKEKB POSITRON RING

Y. Suetsugu[1,†], H. Fukuma, K. Ohmi, M. Tobiyama[1], H. Ikeda[1], K. Shibata[1], T. Ishibashi[1], M. Shirai, S. Terui, K. Kanazawa, H. Hisamatsu, M. L. Yao[1], KEK, Tsukuba, Japan
[1]also at SOKENDAI, Hayama, Japan

Abstract

A critical issue for SuperKEKB is the electron cloud effect (ECE) in the positron ring. Various countermeasures, such as ante-chambers, TiN-film coatings, clearing electrodes, and grooved surfaces, were prepared before commencing commissioning. The ECE, however, was observed during Phase−1 commissioning (2016) caused by the electron cloud in Al-alloy bellows chambers and also in the beam pipes at drift spaces, although the beam pipes had antechambers and TiN-film coatings. The threshold of the current linear density for exciting the ECE was approximately 0.12 mA bunch⁻¹ RF-bucket⁻¹. Permanent magnets and solenoids were attached to them to generate magnetic fields in the beam direction as additional countermeasures. Consequently, the current linear density threshold increased up to over 0.53 mA bunch⁻¹ RF-bucket⁻¹ in Phase−3 commissioning (2019). Currently, there is no clear evidence of ECE during a normal operation. The effectiveness of the ante-chambers and TiN-film coatings of real beam pipes and groove structures used in bending magnets were experimentally re-evaluated. This report summarises the mitigation techniques used in SuperKEKB and the results thus far.

INTRODUCTION

The SuperKEKB is an electron-positron collider with asymmetric energies in KEK that aims for an extremely high luminosity utilising a "nano-beam" collision scheme (Fig. 1) [1, 2]. The main ring (MR) consists of two rings, that is, the high-energy ring (HER) for 7 GeV electrons and the low-energy ring (LER) for 4 GeV positrons. The beam pipes in the MR tunnel are shown in Fig. 2.

Figure 1: SuperKEKB at KEK Tsukuba campus.

† yusuke.suetsugu@kek.jp

Single-bunch instability caused by the electron cloud, that is, the electron cloud effect (ECE), is a severe problem for the SuperKEKB LER [3, 4]. Therefore, more effective countermeasures are required. From simulations, the average density of electrons in the ring should be less than ~3×10¹¹ m⁻³ to avoid excitation of the ECE [5]. Hence, various types of countermeasures against ECE were adopted in the SuperKEKB LER, which are summarized in Table 1, and typical views of each countermeasure are shown in Fig. 3 [6].
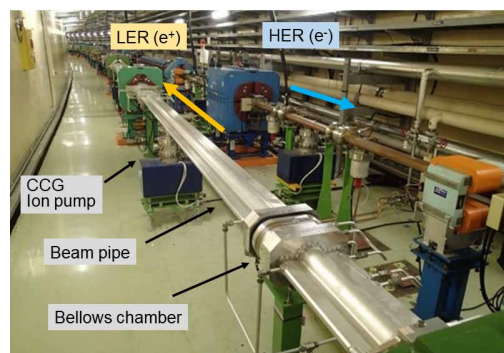

Figure 2: LER and HER in the MR tunnel.

COUNTERMEASURES IN SUPERKEKB

An antechamber helps to minimise the effects of photoelectrons because most of the synchrotron radiation (SR) is directly irradiated at its side wall (Fig. 3(a)). However, secondary electrons play a significant role in electron cloud formation in the high-bunch current regime. Most of the beam pipes for the LER were made of aluminium (Al)-alloy, and the beam channel was coated with a TiN film to reduce the secondary electron yield (SEY) (Fig. 3(b)). Clearing electrodes were installed in the beam pipes for wiggler magnets instead of TiN-film coating. A clearing electrode absorbs electrons around the beam orbit using a static electric field. These beam pipes also have antechambers and are made of copper (Fig. 3(c)). A grooved surface was adopted for the beam pipes in the bending magnets in the arc section. The grooved surface geometrically reduces the SEY. The TiN-film coating was subsequently applied to the grooved surface (Fig.3(d)). As a result, approximately 90% of the beam pipes in the ring had antechambers and TiN-film coating. A magnetic field in the beam direction (B_z) generated by solenoids or permanent magnets around the beam pipe is highly effective in suppressing the electron emissions from the inner wall. These are available only in the drift spaces (field-free regions) between electromagnets, such as quadrupole and sextupole magnets (Fig.3(e) and 3(f)). The circular dots in Table 1 indicate the

STUDIES AND POSSIBLE MITIGATION OF ELECTRON CLOUD EFFECTS IN FCC-ee

F. Yaman*,[1], İzmir Institute of Technology, İzmir, Türkiye

F. Zimmermann, CERN, Geneva, Switzerland

[1]also at STFC, Sci-Tech Daresbury, UK

Abstract

In this work, we present numerical results for the electron cloud build-up and mitigation studies considering Arc Dipole and Drift sections of the FCC-ee collider. We report the central electron density that could be reached by minimising secondary electron contributions and the photoelectron generation rates in order to achieve e^- densities lower than the single-bunch instability threshold, considering the baseline beam parameters. Additionally, simulation results revealing the behavior of electron-cloud formations for various SEY values, photoemission rates, vacuum chamber radii, and bunch spacings are included. In the last section, we discuss initial investigations to clean residual electrons after the beam pass.

INTRODUCTION

The FCC-ee, which is designed for performing precision measurements at each of several different collision energies between 88 and 365 GeV, is the first stage of the FCC project hosted by CERN [1, 2]. The design achieves a high luminosity with an e^+e^- circular collider of circumference ≈ 90 km, for the arcs of which we shall analyze electron cloud build-up scenarios. The exponential generation of electrons which may occur when the primary e^- hit the pipe walls, could cause beam loss, emittance growth, trajectory change, and wakefields [3,4]. The primary sources of the electrons in the accelerators and storage rings are photoemission, ionization of residual gases, and strikes of strayed beam particles to the beam pipes. For detailed investigations of the electron cloud mechanism, we employ PyECLOUD [5] to perform two-dimensional electrostatic particle in cell simulations. In the computations, the Furman-Pivi secondary electron yield model for copper, see Refs. [6,7] and ECLOUD model based on laboratory measurements at CERN for the copper surface of the LHC [8,9] are used.

MACHINE & SIMULATION PARAMETERS

We consider the machine and beam parameters which are given in Table 1 for the build-up simulations. Additionally, also the drift region, circular beam pipe radius 30 mm and 35 mm, bunch spacings 25 ns, 30 ns and 32 ns, total secondary emission parameter SEY = {1.1, 1.2, 1.3, 1.4}, the number of primary electrons generated by a single positively-charged particle per unit length n'_γ = {$10^{-3}, 10^{-4}, 10^{-5}, 10^{-6}$} m^{-1} are scanned

---

* fatihyaman@iyte.edu.tr

for the FCC-ee collider arcs. As a result, we obtain electron densities at the center of the vacuum chamber during 150 bunch passes where an average of all minimum density values is calculated to compare with the single-bunch instability threshold. The latter can be estimated as [12, 13]

$$\rho_{thr} = \frac{2\gamma Q_s \omega_e \sigma_z/c}{\sqrt{3}KQr_e\beta_y C},\tag{1}$$

where

$$\omega_e = \left(\frac{N_b r_e c^2}{\sqrt{2\pi}\sigma_z\sigma_y(\sigma_x+\sigma_y)}\right)^{1/2},\tag{2}$$

$K = \omega_e\sigma_z/c$, $Q = \min(\omega_e\sigma_z/c, 7)$, see Ref. [11].

Table 1: Simulation parameters for the simulations of electron-cloud evolution in an arc dipole, corresponding to collisions at 4 interaction points [10, 11].

Parameter	FCC-ee Collider Arc Dipole
beam energy [GeV]	45.6
bunches per train	150
trains per beam	1
r.m.s. bunch length [mm]	4.32
hor. r.m.s. beam size [µm]	207
vert. r.m.s. beam size [µm]	12.1
external magnetic field [T]	0.01415
bunch population N_b [10^{11}]	2.76
circumference C [km]	91.2
chamber radius r_0 [mm]	35
momentum compaction factor α_C [10^{-4}]	0.285
synchrotron tune Q_s	0.037
average beta function β_y [m]	50
threshold density ρ_{thr} [10^{12} m^{-3}]	0.043

NUMERICAL RESULTS

Firstly, Figure 1 displays minimum electron densities for a case without any secondary emission (SEY ≈ 0) and for a more realistic scenario (SEY = 1.1), considering a photoelectron rate of $n'_\gamma = 10^{-6}$ m^{-1}/e$^+$ and 32 ns bunch spacing. The former results for the arc dipoles reported in Ref. [11], even though the longitudinal rms bunch length, bunch population, and transverse beam sizes) had different

THIN FILMS ACTIVITIES IN THE IFAST PROGRAM

C.Z. Antoine†, S. Berry, Y. Kalboussi, T. Proslier, Université Paris-Saclay, CEA, Département des Accélérateurs, de la Cryogénie et du Magnétisme, Gif-sur-Yvette, France

O. Hryhorenko, D. Longuevergne, Thierry Pépin-Donat, Université Paris-Saclay, CNRS/IN2P3, IJCLab, Paris, France

R. Ries, E. Seiler, Institute of Electrical Engineering, SAS, Bratislava, Slovakia

S. Keckert, J. Knobloch[1], O. Kugeler, D. Tikhonov, Helmholtz-Zentrum Berlin für Materialien und Energie GmbH, Berlin, Germany

S. Prucnal, S. Zhou, Helmholtz-Zentrum Dresden-Rossendorf (HZDR), Institute of Ion Beam Physics and Materials Research, Dresden, Germany

O. Azzolini, E. Chyhyrynets, D. Ford, V. Garcia, G. Keppel, C. Pira, A. Salmaso, F. Stivanello, INFN Laboratori Nazionali di Legnaro, Legnaro (PD), Italy

M. Bertucci, R. Paparella, INFN LASA, Segrate (MI), Italy

G. Burt[2], D. Turner[2], D. Seal[2], H. Marks[2], Lancaster University, Lancaster, UK

J. W. Bradley[2], F. Walk[2], F. Lockwood-Estrin[2], Liverpool University, Liverpool UK

R. Berton, D. Piccoli, F. Piccoli, G. Squizzato, F. Telatin
PICCOLI s.r.l., Noale (VE), Italy

A. Medvids, A. Mychko, Laboratory of Semiconductor Physics, Riga Technical University, Riga, Latvia

O. Malyshev[2], R. Valizadeh[2], A. Hannah[2], J. Conlon[2], T. Sian[2], L. Smith[2], A. Vick[2]
STFC Daresbury Laboratory, Warrington, UK

Ö. Sezgin, M. Vogel, A. Zubtsovskii, X. Jiang, Institute of Materials Engineering, University of Siegen, Siegen, Germany

[1] also at Universität Siegen, 57072 Siegen
[2] also at Cockcroft Institute, Warrington, UK

Abstract

Now that bulk Nb technology has reached it full maturity, improving SRF technology demands that new materials need to be developed. For reasons explained in the talk, all next generation SRF materials will be in the form of thin films. The IFAST project has the ambition to coordinate European activities on that topic, not only throughout its own program (that will be presented here), but also by keeping in touch with all actors worldwide, with the hope of developing a more efficient collaborative actions in a limited funding context. In this paper, we will present the challenges presented by the development of new thin films materials, each developed for tailored applications and the main research direction proposed by the thin film community.

TAILORED MATERIAL FOR SRF

The SRF technology is mostly based on ultra pure bulk niobium, which is not optimized to maximize its superconducting properties (surface resistance), but rather to maximize thermal stabilization of dissipating defects. By separating each functions (mechanical structure, thermal transfer, surface resistance, surface protection…), one can achieve superconducting cavities with enhanced performance (Fig. 1). One can even hope to tune their performances for specific applications.

This process is already "en marche". For instance, the "doping procedure" proposed by FNAL [1] consist in diffusing interstitial atoms in a shallow part of the surface.

TOWARDS BEAM-BEAM SIMULATIONS FOR FCC-ee*

P. Kicsiny[†,1,2], X. Buffat[1], G. Iadarola[1], T. Pieloni[2], D. Schulte[1], M. Seidel[2,3]
[1]CERN, Geneva, Switzerland
[2]École Polytechnique Fédérale de Lausanne (EPFL), Lausanne, Switzerland
[3]Paul Scherrer Institut, 5232 Villigen PSI, Switzerland

Abstract

The FCC-ee (Future Circular Collider) lepton collider is currently the most favored next generation research infrastructure project at CERN, aimed at studying properties of standard model particles with the highest precision ever. The chosen parameters of the machine yield unprecedented conditions which give rise to previously unseen dynamical effects during collisions. The exploration and understanding of these beam-beam effects is of crucial importance for the success of the FCC-ee feasibility study. To address this challenge, a new general purpose software framework for beam dynamics simulations is currently under development at CERN. This presentation will discuss the contributions to the software development related to beam-beam effects with benchmark studies and applications.

INTRODUCTION

The FCC-ee feasibility study [1] aims at verifying the possibility to build a near 100 km long circular collider in the Geneva area. The study would be the first stage towards a 100 TeV hadron collider, termed FCC-hh. These colliders aim notably to search for new physics beyond the standard model. During beam-beam collisions the particles in the two colliding beams experience an electromagnetic (EM) force by the presence of the opposite beam. This nonlinear beam-beam "kick" perturbs the particle trajectories resulting in long term changes in the dynamical behavior of the beams, collectively referred to as beam-beam effects [2]. Due to the nonlinear nature of the interaction, a purely analytical treatment of these effects is excluded. Instead, numerical multiparticle simulations are commonly used where the dynamical variables of the particles are tracked. The difficulty in simulating this dynamics lies in the complexity of the FCC-ee machine and the interplay of the different dynamical effects.

The collider infrastructure is designed to maximize achievable luminosity. To this end, a setup called the crab-waist scheme [3] has been proposed, which mitigates the nonlinear effect of beam-beam collisions and achieves extremely small, nanometer sized beams at the interaction points (IPs) by colliding beams with a crossing angle of 30 mrad and by using special purpose, so called crab-sextupoles. Another setup, commonly used in synchrotron light sources, is the top-up injection scheme [4], which means that new, low intensity

beam bunches are injected with a high frequency to maintain high bunch intensities in the beams. This helps to maintain high luminosity, which decreases due to the reduced beam lifetime caused mainly by the emission of radiation during the collision.

Beamstrahlung

Arguably one of the most important beam-beam effects in the FCC-ee is beamstrahlung, i.e., the emission of high energy (up to GeV order) photons relative to the particle energy during collision. The photon emission happens due to the local bending of the particle trajectories in the collective EM field of the opposite bunch. Beamstrahlung has deteriorating impact on the bunch quality. The quantum nature of photon emission increases the energy spread of the beam, which is converted to an increase of the bunch length [5]. It also reduces the luminosity and leads to an increased loss rate of particles due to the reduction of the dynamic aperture [6].

SIMULATION OF FCC-ee BEAM-BEAM EFFECTS

The FCC-ee is a highly complex machine, where many dynamical effects interplay with each other. Therefore a simulation that aims to model the beam dynamics has to be self-consistent, i.e., not relying on any other external input or modification of intermediate variables during the simulation. Currently there exist several toolkits to model beam dynamics in high energy colliders. Some of the most well known codes are `MAD-X` [7], `SixTrack` [8], `PyHEADTAIL` [9] and `COMBIp` [10]. Each of these codes have been developed aiming for different studies, each having different features. There are other codes which were developed specifically for studying beam-beam effects in colliders. Some of the most well known are `BBWS` [11] and `BBSS` [12], `LIFETRAC` [13] and `GUINEA-PIG` [14]. Each of these codes uses different approximations to boost performance or numerical precision for certain types of studies. The main challenge that limits simulation capabilities is to interface such codes when we want to study the interplay of different mechanisms, crucial for the FCC-ee feasibility study. Hence the need for a single, self-consistent and open source simulation tool following mainstream computing paradigms, i.e., modern programming languages and compatibility with multiple platforms such as CPU or GPU from different vendors and which incorporates all elements of a complex accelerator, necessary for studying FCC-ee beam dynamics. A new simulation tool, called `xsuite` [15], targets the above outlined demanding

OVERVIEW AND PROSPECTS OF THE SuperKEKB COMMISSIONING

Y. Funakoshi* on behalf of the SuperKEKB commissioning group

KEK, Tsukuba, Ibaraki 305-0801, Japan

Abstract

The Phase 3 beam commissioning of SuperKEKB is summarized. As for the prospects of SuperKEKB commissioning, we focus on critical issues toward the next mile stone of the luminosity of $1 \times 10^{35} \mathrm{cm}^{-2}\mathrm{s}^{-1}$.

INTRODUCTION

The purpose of SuperKEKB is to search for a new physics beyond the standard model of the particle physics in the B meson regime. SuperKEKB consists of the injector linac, a damping ring for the positron beam, two main rings; *i.e.* the low energy ring (LER) for positrons and the high energy ring (HER) for electrons and the physics detector named Belle II. The beam energies of LER and HER are 4 GeV and 7 GeV, respectively. The design beam currents of LER and HER are 3.6 A and 2.6 A, respectively. The design luminosity is $8 \times 10^{35} \mathrm{cm}^{-2}\mathrm{s}^{-1}$. More detailed design parameters of SuperKEKB is described elsewhere [1]. The Phase 1 beam commissioning was done from Feb. 2016 to June 2016. In this phase, the machine operation was done without the IR (Interaction Region) devises nor the Belle II detector. The purposes of the operation in Phase 1 were vacuum scrubbing, low emittance tuning and beam background study using specially designed background detectors. The Phase 2 beam commissioning was done from March 2018 to July 2018. In this phase, a pilot run of SuperKEKB and the Belle II detector was performed. Although most of the Belle II detector was installed, the most sensitive detectors to the beam background, *i.e.* the pixel vertex detectors and the silicon vertex detectors were not installed in this phase. The purposes of the operation in Phase 2 were demonstration of "nano-beam collision scheme" and the study on beam background with much lower beta functions at the IP than those in KEKB. The achieved luminosity in Phase 2 was $5.6 \times 10^{33} \mathrm{cm}^{-2}\mathrm{s}^{-1}$ with $^*_y$ of 3 mm. The Phase 3 beam operation started in March 2019 and has continued until now. An initial report on the Phase 3 operation is shown elsewhere [2]. In this report, we summarize the progress of SuperKEKB in Phase 3. The machine operation of SuperKEKB was halted on June 22nd 2022 for a long shutdown (LS1: Long Shutdown 1). During LS1, we will do several upgrade works as is shown below. After LS1, the machine operation will be resumed in autumn 2023 or later. Also discussed in this report are critical issues on luminosity improvement after LS1. We focus on the most critical issues and more comprehensive discussions are given elsewhere [3, 4].

OVERVIEW OF PHASE 3 OPERATION

The history of machine operation in Phase 3 is shown in Fig. 1. In the figure shown are the history of the HER

---

* email: yoshihiro.funakoshi@kek.jp

beam current, the LER beam current, the peak luminosity and the total integrated luminosity (delivered and recorded values) from the top to the bottom, respectively. Both in the beam currents and the luminosity, there has been a great progress since IPAC2020 held in May 2020. Table 1 shows a comparison of machine parameters in 4 cases. The highest peak luminosity so far achieved is $4.65 \times 10^{34} \mathrm{cm}^{-2}\mathrm{s}^{-1}$ as is shown in Fig. 1. This is the official record on the peak luminosity at SuperKEKB. A higher value of $4.71 \times 10^{34} \mathrm{cm}^{-2}\mathrm{s}^{-1}$ was achieved in a test run with the Belle II detector HV off. The recorded and delivered total integrated luminosity so far are 424 and 491 fb^{-1}, respectively. In comparison between the parameters at present with those achieved by KEKB, the peak luminosity at present is more than twice higher than the achieved value at KEKB. But comparing the present beam performance with the design of SuperKEKB, we are still at an early stage of the project. In the following, we summarized progress in Phase 3 on the three parameters related to the luminosity; *i.e.* vertical beta function at the IP (β_y^*), the beam currents and the vertical beam-beam parameter (ξ_y).

Squeezing β_y^*

In Phase 2, we successfully squeezed β_y^* down to 3 mm. This value was already a half of the value achieved at KEKB and demonstrated effectiveness of the nano-beam scheme. Progress in squeezing β_y^* in Phase 3 is also shown in Fig. 1. The physics run in Phase 3 started with β_y^* of 3 mm in 2019. At the end of 2019, we successfully reached β_y^* of 1 mm. In the process of squeezing β_y^*, we found that minimising the x–y coupling parameters at the IP is essentially important to get a high luminosity. Roughly speaking, the achieved luminosity has been inversely proportional to β_y^* with the x–y coupling tuning in the range of β_y^* from 3 mm to 1 mm. In 2020 and 2022, we tried to squeeze β_y^* down to 0.8 mm as is seen in Fig. 1. The operations with β_y^* of 0.8 mm were short time trials. In both trials, we could not store the same beam currents as the case of β_y^* of 1 mm mainly due to poor injection efficiency. As a result, an achieved luminosity with β_y^* of 0.8 mm so far is much lower than that with β_y^*
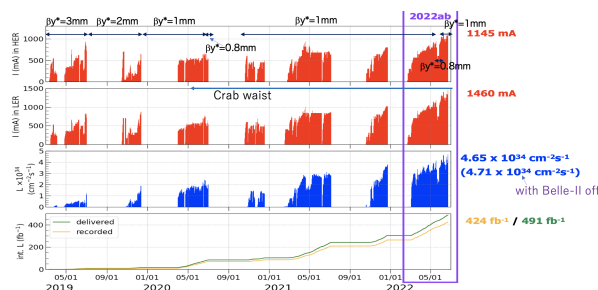

Figure 1: Operation history in Phase 3.

FCC-ee CIVIL ENGINEERING AND INFRASTRUCTURE STUDIES

L. Bromiley, J. Osborne, CERN, Geneva, Switzerland

Abstract

The European Organisation for Nuclear Research (CERN) is planning a Future Circular Collider (FCC), to be the successor of the current Large Hadron Collider (LHC). Significant civil engineering is required to accommodate the physics experiments and associated infrastructure. The 91.2 km, 5.5 m diameter tunnel will be situated in the Geneva region, straddling the Swiss-French border. Civil engineering studies are to incorporate the needs of both the FCC lepton collider (FCC-ee) and the FCC hadron collider (FCC-hh), as the tunnel will host both machines consecutively.

INTRODUCTION

At completion, the FCC tunnel will house the world's largest particle accelerator. The study, currently in the feasibility stage, officially commenced in 2013 following recommendations made by the European Strategy for Particle Physics Update (ESPPU). To support the physics requirements, the CERN civil engineering team has been studying the feasibility of constructing a 91.2 km circumference tunnel project beneath the Geneva region.
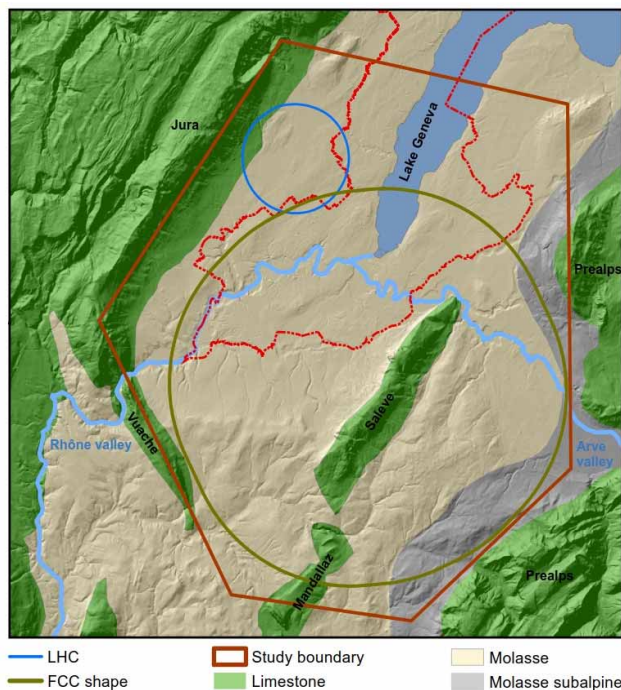

Figure 1: FCC study area (CERN).

CERN has a history of completing large civil engineering works to facilitate physics research. When CERN completed construction of the LEP (Large Electron-Positron) in 1989 [1], it was the largest physics facility ever built. This made Europe a worldwide leader in science and technology [2].

To validate the physics case of FCC, the tunnelling studies must satisfy requirements for both a lepton (ee) and a hadron (hh) machine, as well as reuse the existing LEP/LHC infrastructure.

Like the LHC before it, the FCC will extend into the territories of both France and Switzerland. As a result, the main challenges encountered by the civil engineers will be the geological features, local stakeholders, environmental constraints, and project costs.

Geological site investigations are therefore required to validate the geological assumptions made at the conceptual design stage. An initial site investigation campaign is planned to start in 2023 in the areas of highest geological uncertainty.

This paper describes the present state of the civil engineering feasibility studies for the FCC tunnel.

FEASIBILITY STUDY

Project Description

Following studies of various locations and geometries of the accelerator machine, the conceptual design of the FCC considers a quasi-circular tunnel, with a circumference of 91.2 km situated in the Geneva basin. The tunnel will be buried underground at an average elevation of 300 m ASL.

In addition to the main tunnel, approximately 10 km of transfer tunnels, 4 km of beam dump tunnels, 6 km of by-pass tunnels, 14 shafts, 12 large caverns and 8 surface sites are required.

The primary objective of the civil engineering studies so far has been to locate the tunnel within the topographical and geological boundaries of the Geneva basin. While also ensuring adequate connection to existing LHC infrastructure.

The locations of the surface sites have been selected to match the machine's layout, for example the predefined experimental points, but also considering surface access and local environment factors.

Approximately 9 million cubic metres of spoil will result from the excavations of FCC tunnels and structures [3]. Around 95% of this will be molasse, the reuse potential of which – although it has proved to be a good rock for tunnelling – is not obvious. Research is currently being undertaken to investigate opportunities to reuse or recycle tunnel spoil rather than resorting to typical landfill disposal.

Summary of Main Structures

- 1 machine tunnel of 91.2 km length, 5.5 m diameter
- 14 vertical shafts of 12 – 18 m diameter, 140 – 400 m depth
- 8 service caverns, 100 to 150 m length, 15 m high, 25 m wide

METHODS AND EXPERIENCES OF AUTOMATED TUNING OF ACCELERATORS*

Xiaobiao Huang†, SLAC National Accelerator Laboratory, Menlo Park, CA, USA

Abstract

Automated tuning, or beam-based optimization, is a general approach to improve accelerator performances. The approach is different from the other common approach of beam-based correction. The differences between these two approaches and the advantages of the optimization approach are discussed. Two online optimization methods, the robust conjugate direction search (RCDS) and the multi-generation Gaussian process optimizer (MG-GPO), are described. Experiences of apply the methods to storage ring nonlinear dynamics optimization at SPEAR3 and APS storage rings, as well as application to other machines, are presented.

INTRODUCTION

An accelerator typically has many error sources that cause its behavior to differ from the ideal design. The performance of the machine can be substantially degraded due to the errors. The machine also has many control parameters (i.e., knobs) that can be used to change its behavior, which could compensate the effects of the errors and restore the machine performance. Accelerator physicists use beam-based measurements to determine the desired knob adjustments. The methods employed to find the accelerator setting based on beam-based measurements could be classified into two categories: beam-based correction and beam-based optimization [1].

In this paper, we will first discuss the characteristics of these two approaches. This is followed by discussions on the methods and application of beam-based optimization. The methods to be focused on are the robust conjugate direction search (RCDS) method [2] and the multi-generation Gaussian process optimizer (MG-GPO) [3]. Considerations on application of the methods to real-life accelerator tuning problems are discussed. Some important applications, such as minimization of the vertical emittance in storage rings, tuning of linac front end, and optimization of nonlinear beam dynamics of storage rings, are described.

BEAM-BASED CORRECTION AND OPTIMIZATION

The performance of an accelerator can be characterized by various metrics, such as beam intensity, beam size, beam lifetime, beam loss, transmission efficiency, injection efficiency, and beam stability. These metrics could be constantly monitored, or in some cases, are measured on demand. Depending on the purpose of the machine, each accelerator may have a different set of performance metrics of importance.

In many cases, a set of knobs can target one performance metric without affecting the others. However, in some cases, the same set of knobs that are used to tune one metric can simultaneously impact the other metrics.

The diagnostic system of the accelerator measure and monitor many signals that represent the state of the machine or the beam. For example, the orbit of the beam throughout the accelerator is typically monitored with beam position monitors (BPMs). The transverse beam profile and in turn the transverse beam size can be measured at some locations. In circular accelerators, the betatron tunes can be constantly monitored. Some machine state variables can be derived from the monitor signals. In some cases, the beam or the machine are intentionally perturbed in order to perform an observation of the machine state. For example, the betatron phase advances can be measured from turn-by-turn BPM data when the beam is kicked. The closed orbit response, measured by making a small change to an orbit corrector, is another example.

The machine state as characterized by the diagnostic system could be directly correlated with the performance metrics, such that restoring the machine state automatically also restores the performance. In other cases, the correlation is not as strong; yet, it is still generally preferred to operate under certain machine states. In those cases, a "golden" machine state can be defined as the target configuration. For example, a golden beam orbit is usually defined for a storage ring. Desired values of betatron tunes and chromaticities are also specified. In a linac or transport line, the desired orbit and beam distribution is often specified at some strategically important locations, for example, at the end of the transport line for injection to another accelerator or at the entrance of the undulators in a free electron laser.

Often times, a known set of knobs can be used to change a certain aspect of the machine state. If there are enough effective knobs, it may be possible to move the machine into any reasonable state with those knobs. Because usually each knob has a definitive and predictable effect to the machine state, given the current machine state, the current knob setting, and the target machine state, one could work out the required adjustment to the knobs in a deterministic fashion. As not everything is perfectly known, it may take several iterations to reach the target state. The process of of bringing the machine state as measured by the beam diagnostic system to a target state with control knobs via a deterministic procedure is called beam-based correction.

Beam-based correction requires beam diagnostics that can sufficiently characterize the machine states, a known target machine state, knobs that can effectively change the machine state, and a deterministic procedure to determine the required knob changes toward the target. Reaching the

LESSONS LEARNED FROM OPERATIONAL EXPERIENCE OF SuperKEKB IR MAGNETS AND UPGRADE PLANS FOR THE FUTURE

Y. Arimoto*, K. Aoki, M. Kawai, T. Kawamoto, M. Maszawa, S. Nakamura, Y. Ohsawa,
N. Ohuichi, T. Oki, R. Ueki, X. Wang, H. Yamaoka, Z. Zong, KEK, Tsukuba, Japan

Abstract

SuperKEKB is an upgraded accelerator from KEKB, aiming at a luminosity of 6×10^{35} cm⁻² s⁻¹. It is currently in operation, setting new luminosity records. We have completely redesigned the final-focus-magnet system to achieve the target luminosity by upgrading from KEKB to SuperKEKB. After the completion of the system, it started its practical operation in 2018 after measuring the magnetic field in IR. The operation is generally stable, but some troubles have occurred. One of them is a quench. Radiation related to stored beam deposit energy on the superconducting coil. And then, we experienced the tune variations in LER, which suggested fluctuations in the main quadrupole magnetic field, and measurements using the R & D magnet demonstrated this phenomenon. In addition, we are seeking a plan to upgrade the QCS for the long shutdown around 2027.

INTRODUCTION

KEKB is a B-Factory and is an e^+/e^- collider operated from 1998 to 2010 [1]. It achieved a peak luminosity of 2.11×10^{34} cm⁻² s⁻¹ and an integrated luminosity of 1040 fb⁻¹. The Belle experiment using KEKB has achieved many physics results. To make precise measurements of weak interaction parameters and find new physics beyond the Standard Model, the KEKB has been upgraded to the SuperKEKB [2]. It aims at a peak luminosity of 6×10^{35} cm⁻² s⁻¹ and the integrated luminosity of 50 ab⁻¹. The operation of the SuperKEKB started from 2018 and achieved the peak luminosity of 4.7×10^{34} cm⁻² s⁻¹ up to 2022 [3].

FINAL FOCUS SYSTEM OF KEKB AND SUPERKEKB

One of the critical components for the accelerator upgrade from KEKB to SuperKEKB is a final focus system with superconducting (SC) magnets called QCS. At an interaction point (IP), a design vertical-beam size, σ_y^* of SuperKEKB is 50 nm and is 20 times smaller than KEKB.

To achieve this, the QCS system designed for SuperKEKB has independent quadrupole doublets for each ring. For the KEKB-QCS (in this section, we denote this as K-QCS), the electron and positron beam went through the same quadrupole magnets of the QCS. So, the SuperKEKB-QCS (in this section, we denote this as SK-QCS) consists of eight quadrupole doublets; on the other hand, the K-QCS has two quadrupole magnets [4, 5]. Figures 1 and 2 show schematic layouts of the QCS of KEKB and SuperKEKB, respectively.

_____
* yasushi.arimoto@kek.jp

The SK-QCS also has the leak field cancel magnets; they cancel the leak field from QC1LP and QC1RP to HER. The four solenoids of the SK-QCS compensate for the integral solenoid field of Belle II detector , while the K-QCS has two compensation solenoids.

Table 1: KEKB and SuperKEKB Main Parameters

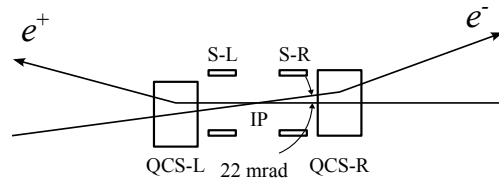|	KEKB		SuperKEKB	
	LER	HER	LER	HER
E [GeV]	3.5	8.0	4.0	7.0
θ_{cross} [mrad]	22		83	
β_y^* [mm]	5.9	5.9	0.27	0.30
σ_y^* [nm]	900	900	48	62

Figure 1: The schematic layout of the KEKB-QCS. S-L and S-R are the compensation solenoids, and the QCS-L and QCS-R are the SC quarupole magnets.
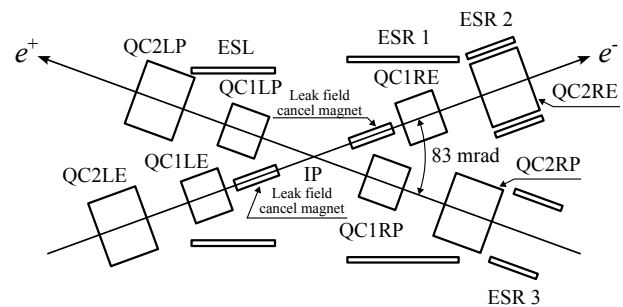

Figure 2: Schematic layout of SuperKEKB-QCS. The magnets representing with "QC" at beginning are the superconducting quadrupole magnets. The leak field cancel magnets are canceling the leak field from QC1RP and QC1LP quads. ESL, ESR1, ESR2, and ESR3 are the compensation solenoids.

Tables 2 and 3 show the main parameters for the quadrupole magnets of KEK and SuperKEKB, respectively. The letter "L" or "R" in all magnet names indicates the magnet on the left or right side of the IP, viewing the IP from the center of the accelerator ring, respectively. The QCS-L and QCS-R magnets are the vertical-focusing quadrupole magnets for KEKB in Table 2. The vertical-focusing quadrupole

STATUS OF INTERACTION REGION MAGNETS FOR CEPC*

Chuang Shen[1,2], Yingshun Zhu[†,1,2], Xiangchen Yang[1], Ran Liang[1], Fusan Chen[1,2], Wei Zou[3],
Yi Wan[3], Xinlian Wu[3]

[1] Key Laboratory of Particle Acceleration Physics and Technology,
Institute of High Energy Physics, Chinese Academy of Science, Beijing, China
[2] University of Chinese Academy of Sciences, Beijing, China
[3] Hefei Keye Electrical Physical Equipment Manufacturing Co., Ltd, Hefei, China

Abstract

High gradient quadrupole magnets are required on both sides of the interaction points in the proposed Circular Electron Positron Collider (CEPC). There are three double aperture superconducting quadrupoles with a crossing angle between two aperture centerlines of 33 mrad. It is challenging to meet stringent design requirements, including limited space, magnetic field crosstalk between two apertures, magnetic field gradients up to 142 T/m, etc. In this paper, status of superconducting magnets in CEPC interaction region in the technical design stage is described. Magnetic design of superconducting quadrupole magnet with three kinds of quadrupole coil structures, including $\cos 2\theta$ coil, CCT coil, and Serpentine coil is presented and compared. In addition, the development status of a single aperture short model quadrupole magnet with a magnetic length of 0.5 m is presented.

INTRODUCTION

To further study Higgs particles, Chinese physicists put forward a plan to build a Circular Electron Positron Collider (CEPC). Since the publication of CEPC conceptual design report (CDR) in 2018 [1], related research is going on. To pursue higher collision luminosity, accelerator physicists proposed a CEPC technical design report (TDR) based on the CEPC CDR study [2]. The superconducting quadrupole magnet QD0 is divided into two superconducting quadrupole magnets Q1a and Q1b. As shown in Fig. 1, compact high gradient quadrupole Q1a, Q1b and Q2 are required on both sides of the collision points. Q1a, Q1b and Q2 are double aperture quadrupoles and are operated fully inside the solenoid field of the detector magnet which has a central field of 3.0 T. To minimize the effect of the longitudinal solenoid field on the accelerator beam, anti-solenoids before Q1a and compensating solenoid outside Q1a, Q1b and Q2 are needed [3]. Their magnetic field direction is opposite to the detector solenoid, and the total integral longitudinal field generated by the detector solenoid and anti-solenoid coils is zero. It is also required that the total solenoid field inside the Q1a, Q1b and Q2 magnet aperture be close to zero.
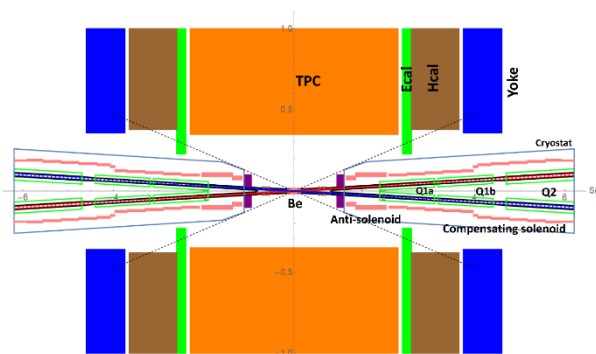
Figure 1: Layout of CEPC TDR interaction region (TPC = Time Projection Chamber, Ecal = Electromagnetic Calorimeter, Hcal = Hadronic Calorimeter, Be = beam tube near the IP. The dotted line refers to the included angle of the outer contour of cryostat).

SUPERCONDUCTING MAGNET ELECTROMAGNETIC DESIGN

Quadrupole Magnet Q1a Design

The first double-aperture quadrupole magnet Q1a was moved forward to a position 1.9 m from the interaction point (IP). The minimum distance between two aperture centerlines is only 62.71 mm, so a very limited radial space is available. The gradient of superconducting magnet Q1a is required to be 142 T/m, and the magnetic length is 1.21 m. The magnetic field harmonics in the good field region are required to be less than 5×10^{-4}. The field crosstalk of the two apertures in Q1a with such a small aperture separation distance is serious, and the dipole field at the center of each aperture is required to be less than 3 mT. The design requirements of the double aperture superconducting quadrupole magnet Q1a are listed in Table 1.

Table 1: Design requirements of the double aperture superconducting quadrupole magnet Q1a.

Item	Value	Unit
Field gradient	142.3	T/m
Magnetic length	1210	mm
Reference radius	7.46	mm
Minimum distance between two aperture centerlines	62.71	mm
High order field harmonics	$\leq 5 \times 10^{-4}$	
Dipole field at the center of each aperture	≤ 3	mT

SuperKEKB BEAM INSTABILITIES CHALLENGES AND EXPERIENCE

H. Ikeda[*,1,2], H. Fukuma[1], T. Kobayashi[1,2], T. Mimashi[1,2], T. Mitsuhashi[1], G. Mitsuka[1,2], S. Sasaki[1], M. Tobiyama[1,2]

[1] High Energy Accelerator Research Organization (KEK), Tsukuba, Japan

[2] SOKENDAI, Tsukuba, Japan

Abstract

KEKB was upgraded from 2011 over 5 years in order to increase the luminosity and started SuperKEKB commissioning in 2018 after the test operation. In order to cope with large beam currents and small beam sizes, various updates have been applied to the beam instrumentation system. This talk summarizes the performance of beam instrumentation in SuperKEKB Phase-III and challenges to it.

INTRODUCTION

SuperKEKB is a collider with 7 GeV electrons (HER) and 4 GeV positrons (LER). The circumference of the ring is 3 km and many beam instrumentation system are installed as shown in Table 1 [1]. Aiming at the world's highest luminosity, we adopted the nanobeam method. Therefore, as design values, we adopted a squeeze of βy* by 20 and a beam current by 2 relative to KEKB ones, and recorded a peak luminosity two times larger than KEKB [2]. Among various improvements related to beam monitors to get higher luminosity, we will focus on improvements related to synchrotron radiation monitors (SRM) and beam loss monitors (LM) in this paper.

SYNCHROTRON RADIATION MONITOR

We use emission-light from the bending magnet that located last part of the arc section of electron and positron rings. An extraction chamber is set at 23 m downstream of the source bending magnet. A diamond mirror is inserted in the chamber as shown in Fig.1. The emission-light is sent through an optical window and several transfer mirrors to an optical hut for various measurements.

We replaced the extraction mirrors for better measurements, and introduced a coronagraph for beam halo measurements and an injection beam measurement system using the same optics system as the coronagraph.

Diamond Mirror

An extraction mirror of visible light is made of diamond to suppress the thermal deformation. We developed a single crystal diamond mirror and made efforts to suppress the current dependence of thermal deformation, but the mirror had not only the current dependence of the deformation at high currents, but also some deformations made during manufacturing process at the beginning of SuperKEKB [3]. We made a new thick polycrystalline diamond mirror that is not easily deformed by heat, then installed it in 2020 [4].

Resistance to thermal deformation of the new mirror is similar to single crystal and its reflectance is high because the coating is changed from gold to platinum. As the result, we succeeded to obtain a sufficient amount of light for beam profile measurement of each bunch, and it became possible to measure the beam halo and injection beam for each turn.

Table 1: SuperKEKB Beam Instrumentation System

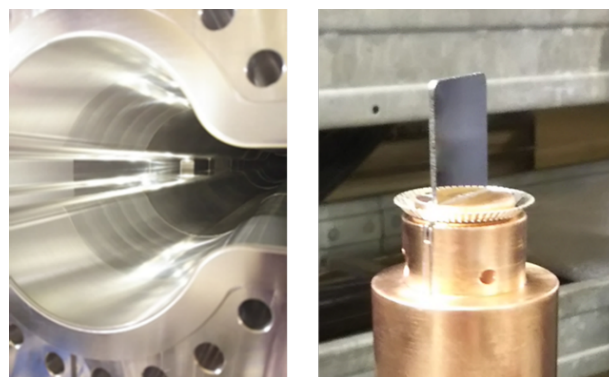| System	Quantity		
	HER	**LER**	**DR**
Beam position monitor (BPM)	466	444	83
Displacement sensor	110	108	0
Transverse bunch feedback system	2	2	1
Longitudinal bunch feedback system	0	1	0
Visible SR size monitor	1	1	1
X-ray size monitor	1	1	0
Beamstrahlung monitor	1	1	0
Betatron tune monitor	2	2	1
Beam loss monitor		207	34
DCCT	1	1	1
CT	1	1	0
Bunch current monitor	1	1	1

Figure 1: Extraction chamber (left) and Diamond mirror (right).

Coronagraph

Beam halo may cause unexpected beam loss or long-term irradiation leading to luminosity degradation and damage to accelerator components. Understanding and hopefully lowering beam halos have been attempted in

_____
* hitomi.ikeda@kek.jp

BEAM INSTRUMENTATION CHALLENGES FOR FCC-ee

E. Carideo, T. Lefevre, S. Mazzoni, A. Schlögelhofer, M. Wendt*, CERN, Geneva, Switzerland

B. Härer, G. Niehues, M. Reißig, A.-S. Müller, KIT, Kalrsruhe, Germany

U. Iriso, ALBA-CELLS, Bellaterra, Spain

T. Mitsuhashi, KEK, Tsukuba, Japan

M. Siano, University of Milano, Milano, Italy

Abstract

For the accelerator-based future of high energy physics at the energy frontier, CERN started to investigate a 92 km circumference Future Circular Collider (FCC), as e+/e− collider the FCC-ee will operate at beam energies up to 182.5 GeV. Beside the machine operational aspects, beam instrumentation will play a key role in verifying and optimizing the machine to achieve the ambitious beam parameters and quality. This paper gives a brief overview of the various challenges to develop the required beam instruments, with focus on beam position, beam size and bunch length measurements, and well as an outline of the planned R&D activities.
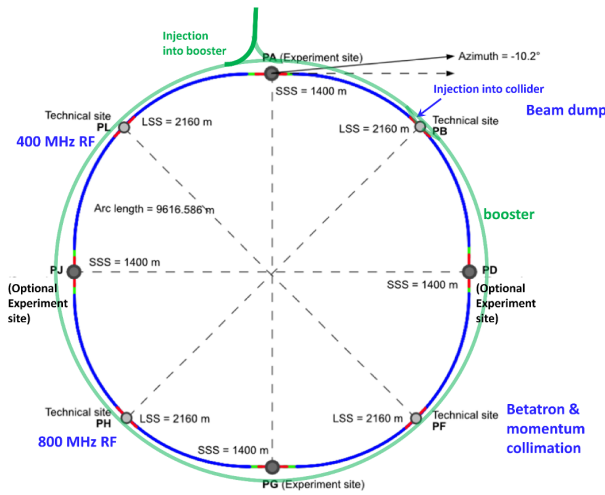
INTRODUCTION

Figure 1: Layout of the main rings of FCC-ee.

The FCC-ee project [1] consists of two main rings and a booster ring in a tunnel of approximately 92 km circumference, plus the injectors and a positron source. For this discussion on the challenges and requirements of the FCC-ee beam instrumentation we focus on the main rings, see Fig. 1, which – with except of the large circumference – has many aspects in common with 4th-generation synchrotron light sources.

Table 1 lists those FCC-ee beam parameters which are particular relevant for the beam instrumentation, with the red highlighted values presenting the biggest challenges.

Table 1: FCC-ee beam parameters relevant to beam instrumentation.

Parameter (4 IPs, $t_{rev} = 304\,\mu s$)	Value
circumference [km]	91.18
max. beam energy [GeV]	182.5
max. beam current [mA]	1280
max. # of bunches/beam	10000
min. bunch spacing [ns]	25 (15)
max. bunch intensity [10^{11}]	2.43
min. H geometric emittance [nm]	0.71
min. V geometric emittance [pm]	1.42
min. H rms IP spot size [μm]	8
min. V rms IP spot size [nm]	34
min. rms bunch length SR/BS [mm]	1.95 / 2.75

BEAM POSITION MEASUREMENT

The two main rings and the booster ring together will need a total of approximately 7000 beam position monitors (BPM), distributed along the ~90 km FCC-ee tunnel. In the arcs, the preferred location of the button-style BPM pick-ups is next to the quadrupole, with the BPM body rigidly fixed to the pole shoes at one end of the magnet. An study currently investigates the integration of the BPM pickup with the quadrupole in a way that no extra space is required. While many details of the four, symmetrically arranged BPM pickup electrodes still need to be developed, a study to optimize new manufacturing processes of the the BPM body with the vacuum chamber made out of copper, together with the button RF UHV feedthrough have been initiated, see also Fig. 2.
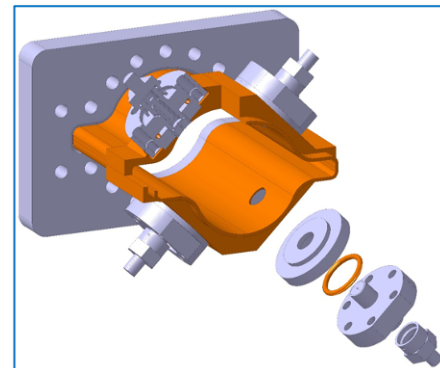

Figure 2: Manufacturing R&D for FCC-ee BPM pickups.

---

* manfred.wendt@cern.ch

P³: A POSITRON SOURCE DEMONSTRATOR FOR FCC-ee

N. Vallis[1,*], B. Auchmann[2], P. Craievich, M. Duda, H. Garcia-Rodrigues, J. Kosse, M. Schaer,
R. Zennaro, Paul Scherrer Institut, 5232 Villigen PSI, Switzerland
[1]also at EPFL, Lausanne, Switzerland
[2]also at CERN, Geneva, Switzerland

Abstract

The PSI Positron Production project (P³ or P-cubed) is a demonstrator for a novel positron source for FCC-ee. The high current requirements of future colliders can be compromised by the extremely high positron emittance at the production target and consequent poor capture and transport to the damping ring. However, recent advances in high-temperature superconductors allow for a highly efficient matching of such an emittance through the use a solenoid around the target delivering a field over 10 T on-axis. Moreover, the emittance of the matched positron beam can be contained through large aperture RF cavities surrounded by a multi-Tesla field generated by conventional superconducting solenoids, where simulations estimate a yield higher by one order of magnitude with respect to the state-of-the-art. The goal of P³ is to demonstrate this basic principle by implementing the aforementioned solenoids into a prototype positron source based on a 6 GeV electron beam from the SwissFEL linac, including two RF capture cavities and a beam diagnostics section.

INTRODUCTION

The Future Circular Collider (FCC) study group published in 2019 a Conceptual Design Report for an electron-positron collider (FCC-ee) with a centre-of-mass energy from 90 to 365 GeV and a beam current up to 1.4 A [1]. This high current requirement depends largely upon an injector complex (see Fig. 1) consisting of two separate sources and linacs for electrons and positrons up to 1.54 GeV, a damping ring (DR) to cool the positron emittance and a common linac up to 6 GeV [2].
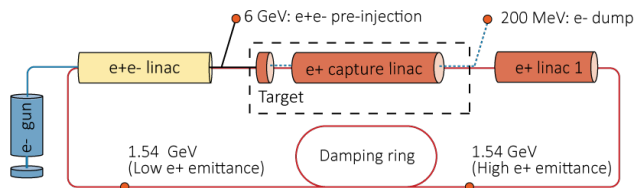

Figure 1: Latest proposal for the FCC-ee Injector Complex.

The principle method for positron production at FCC-ee is based on a 6 GeV electron beam impinging a 17.5 mm-thick (or $5X_0$) amorphous W target, which generates a positron yield around 13 N_{e+}/N_{e-} at the target exit [3]. However, the extremely high emittance and energy spread of the secondary distribution can lead to poor capture rates, compromising the

yield of positrons accepted at the DR. The state-of-the art for a similar positron source is that of the SuperKEKB factory, allowing for 0.5 N_{e+}/N_{e-}, based on a 3.2 GeV electron drive beam with a bunch charge of 10 nC [4]. By contrast, the FCC-ee injection requires yield of 1 N_{e+}/N_{e-} at the DR, plus a safety factor of 2 in the design [5].

The PSI Positron Production project (P³ or P-cubed) was proposed as a demonstrator for a novel solution for the FCC-ee positron source and capture linac. The baseline design of P³ (see Fig. 2) consists of an adiabatic matching device (AMD) based on high-temperature superconducting (HTS) solenoids surrounding the target with a max. field on-axis of 12.7 T and two standing-wave (SW) capture RF cavities in S-band with a large iris aperture of 20 mm radius surrounded by conventional superconducting solenoids with a max. 1.5 T field on-axis. A beam diagnostics section will provide the first exprerimental estimations of the positron yield, which according to simulations is expected to improve the SuperKEKB record by one order of magnitude.

P³ will use a 6 GeV drive electron beam generated at the SwissFEL linac. On the one hand, SwissFEL can provide the desired beam energy and transverse size with extreme precision. On the other hand, due to the radioprotection limitations at SwissFEL, the drive beams of P³ and FCC-ee show substantial differences regarding bunch charge and time structure (see Table 1). This results in a significantly lower radiation load in the P³ target, excluding any thermo-mechanical studies from the scope of the experiment.

Table 1: Main Drive Linac Parameters

	FCC-ee	P³ (SwissFEL)
Energy [GeV]	6	
$\sigma_{x,RMS}$ [mm]	0.5 - 1.0	
Q_{bunch} [nC]	0.88 - 1.17[1]	0.20
Repetition rate [Hz]	200	1
Bunches per pulse	2	1

[1]Based on 5.0 - 5.5 nC requirements at booster ring and preliminary yield estimations of 4.7 - 5.7 N_{e+}/N_{e-}.

KEY TECHNOLOGY

HTS Adiabatic Matching Device

HTS solenoids will be used to deliver a peak on-axis field of 12.7 T around the target in order to match the extremely high positron emittance. This technology can lead to significantly higher yields with respect a conventional, normal-conducting flux concentrator (FC) [6]. The solenoids will be

* nicolas.vallis@psi.ch

ISSUES RELATED TO CEPC e+/e- INJECTION*

Cai Meng[†], Jie Gao, Xiaoping Li, Guoxi Pei, Dou Wang, Jingru Zhang
Key Laboratory of Particle Acceleration Physics and Technology,
Institute of High Energy Physics, Beijing, China

Abstract

Circular Electron-Positron Collider (CEPC) is a 100 km ring collider as a Higgs factory. It consists of a double ring collider, a full energy booster, a Linac and several transport lines. The Linac is a normal conducting S-band and C-band linear accelerator and provide electron and positron beam at an energy up to 30 GeV with repetition frequency of 100 Hz. After a conventional positron source, there is a 1.1 GeV damping ring to reduce the emittance of positron beam. C-band accelerating structures are adopted to accelerate electron and positron beam from 1.1 GeV to 30 GeV. For Z mode, in order to obtain higher injection speed, the Linac operates in double-bunch acceleration mode. The physics design and dynamic simulation results of the Linac will be detailed presented in this paper.

INTRODUCTION

The Higgs boson was discovery at the ATLAS and CMS experiments of the Large Hadron Collider at CERN in July 2012 [1, 2]. In Autumn 2012, Chinese scientists proposed a Circular Electron Positron Collider (CEPC) at 240 GeV centre of mass for Higgs studies [3]. The CEPC is a 100 km ring collider as a Higgs factory and it could later be used to host a Super Proton Proton Collider (SppC) as a machine for new physics and discovery. The CEPC accelerator comprises a double ring collider, a booster, a Linac and several transport lines. The booster and the collider ring are placed in the same tunnel and have the same circumference, which is about 100 m underground. In addition to the Higgs mode (120 GeV), CEPC will also run in W (80 GeV), Z (45.5 GeV), and ttbar mode (180 GeV).

From the pre-CDR stage to TDR stage, the CEPC Linac has undergone several iterations [4, 5] and evolution of parameters is shown in Fig. 1. For the 100 km booster with maximum extraction energy of 180 GeV, the dipole magnetic field is low at the injection energy and high at the maximum extraction energy. So, the design of booster dipole magnet and power supply is very difficult. In order to solve the problem, we choose the injection energy as 20 GeV and used iron-corn magnet which material is oriented silicon steel sheet. However, non-oriented silicon steel sheet is very expensive. If the Linac energy is increased from 20 GeV to 30 GeV, booster dipole magnet material can use non-oriented silicon steel sheet instead of oriented silicon steel sheet. Comprehensively considering the cost of the injector, the Linac energy was determined to be 30 GeV. Currently, for the latest scheme of Linac, the energy is 30 GeV, emittance is 6.5 nm and the bunch charge is 1.5 nC. Considering maintaining the potential to meet high requirements and future upgrades, the maximum bunch charge is 3 nC. At the Z mode with large bunch number in collider ring, the Linac run in double-bunch acceleration mode to speed up the injection speed.

Stage			PreCDR	CDR													TDR		
Parameter		Unit	V1	V2			V3										V4		
				V2.1	V2.2	V2.3	V3.1	V3.2	V3.3	V3.4	V3.5	V3.6	V3.7	V3.8		V4.1	V4.2	V4.3
Beam energy (e+/e-)	E_{e-}/E_{e+}	GeV	6	10			4	10					20	10/20		20		30
Repetition rate	f_{rep}	Hz	50				100											
Bunch number per pulse			1														1&2		
Bunch population (e+/e-)	N_{e-}/N_{e+}	×10⁹	20				6.25		6.25(18.8)				9.4 (18.8)					
		nC	3.2				1		1(3)				1.5 (3)					
Energy spread (e+/e-)	σ_E	×10⁻³	1				2									1.5		
e- bunch charge at target		nC	10															
e- beam energy at target		GeV	4						2				4					
Emittance	ε	nm	300							120	60	40				10		6.5
Damping Ring	E_{e+}	GeV	Yes			No					Yes	Yes			Yes			
			1.1								1.1	1.1			1.1			
	C	m	58.5								58.5	75.4			147			
	ε_0	mm-mrad	287								287	377			94			
Bunch compressor			No					Yes		No					Yes			
Accelerating strucutre			S-band											S-band+C-band			
RF frequency	f_{RF}	MHz	2856.75									2860		2860/5720			
Accelerating gradient		MV/m	15/27	18/27 or. 18/21			21							22 & 27/45			
Klystron-to-ACC.Struc.			1-t-2	1-t-2 or. 1-t-4			1-t-4							1-t-4 & 1-t-2(S)/1-t-2(C)			
Shared Linac Energy range		MeV	200-1100	No													
Linac tunnel length		km	600	1200			500	1200						1400			1800
Collider circumference		km	54 & 61	61			100										
Layout			shared Linac	3 layout schemes			TGB or EBTL	Pre-BST		EBTL							
Date			Apr-16	Nov-16			Dec-16	Apr-17	Aug-17	Oct-17	Dec-17	Jul-18	Mar-19	Sep-19		May-21	Mar-22	Jun-22

Figure 1: Evolution of the CEPC Linac parameters.

FCC-ee e+e− INJECTION AND BOOSTER RING

R. Ramjiawan*, M. Barnes, W. Bartmann, J. Borburgh, Y. Dutheil, M. Hofer, E. Howling
CERN, Geneva, Switzerland
A. Chance, B. Dalena, CEA, Paris, France
P. J. Hunchak, University of Saskatchewan, Saskatoon, Canada

Abstract

The Future Circular electron-positron Collider (FCC-ee) is a proposal for a 91.17 km collider, which would operate in four modes with energies ranging from 45.6 GeV (Z-pole) to 182.5 GeV (t$\bar{\text{t}}$-production). At high energies the beam lifetime could be as low as 6 minutes, requiring the beam to be continuously topped up to reach a high integrated luminosity. This top-up injection would use a separate booster ring in the same tunnel as the collider, which would accelerate the beams to the collider energy. The booster ring should achieve a lower equilibrium emittance than the collider, despite challenges such as a long damping time and no magnet-strength tapering to compensate for the impact of synchrotron radiation. For top-up injection into the collider, we consider two strategies: conventional bump injection, employing a closed orbit bump, and injection using a multipole kicker magnet. On-axis and off-axis sub-schemes will be studied for both. We compare these injection strategies on aspects including spatial constraints, machine protection, perturbation to the stored beam and hardware parameters.

INTRODUCTION

The FCC-ee

The FCC-ee [1] is a proposed, high-luminosity, circular lepton collider offering the opportunity for precision study of the Higgs and electroweak sectors. To maximise the sensitivity to new physics, it would operate in four modes, from the lowest energy Z-mode to the highest energy t$\bar{\text{t}}$-production threshold. The lowest and highest energy machine parameters are given in Table 1. The beam lifetime would be less than an hour for the highest energies because of radiative Bhabha scattering and beamstrahlung. Therefore, to achieve a high integrated luminosity there will need to be continuous full-energy, top-up injection into the collider. During injection, the disturbance to collisions and any stoppage to data-taking in the detectors should be minimised.

Top-up injection is planned via a booster ring in the same tunnel as the collider ring. The booster would be the final stage of the FCC-ee injector chain. The beam is first accelerated within a pre-injector complex, after which it will be transferred to either a pre-booster ring, such as the CERN SPS, or a 20 GeV linac. Following this, the beam will be injected into the booster ring, where the required number of bunches will be accumulated. The booster will only hold up to 10% of the charge of the collider, so that the initial filling of the collider will need 10 injections from the booster.

* rebecca.louise.ramjiawan@cern.ch

Once the bunches are accumulated in the booster, they will be accelerated from 20 GeV to the collider energy. Operating across this energy range presents challenges for the booster, for example, achieving the necessary field quality and reproducibility between cycles at the lowest energies.

The booster ring could either be stacked vertically above the collider ring or side-by-side. Regardless of the positioning of the booster ring, injection into the collider ring must be in the horizontal plane because of the much smaller vertical emittance.

To prevent longitudinal instability of the colliding beams, the charge balance between the electron and positron beams should be kept within 3-5% of each other. This would require alternating electron and positron top-up and an injector chain which could provide bunch-to-bunch charge variations from 0-100% of the nominal value.

Table 1: FCC-ee parameters (CDR [1]) for Z- and t$\bar{\text{t}}$-operations. The beam lifetime is given as that from Bhabha scattering/beamstrahlung.

Parameter	Unit	Z	t$\bar{\text{t}}$
Beam energy	GeV	45.6	182.5
Beam lifetime	min	68/>200	39/18
Beam current	mA	1390	5.4
# bunches/beam		16 640	48
Magnetic rigidity	Tm	152.1	608.7
Emittance (x/y)	nm/pm	0.27/1.0	1.46/2.9
Energy spread	%	0.132	0.192

Injection into the Collider

The collider injection system is proposed to be located in the Long Straight Section (LSS) B. In these proceedings we consider two methods of top-up injection: conventional bump injection and multipole kicker injection (MKI), with off-axis and on-axis sub-schemes for each. A previous study of several top-up injection methods for lepton colliders established these as the most suitable [2]. Here, we present a comparison of the schemes with the goal of converging towards one.

By Liouville's theorem [3], the density of particles in phase-space stays constant while under conservative forces, meaning that you cannot inject particles into the phase-space of the stored bunches. Beams are instead injected with a separation from the stored beams and merge via synchrotron radiation damping. For *off-axis* injection, the bunches are injected with a transverse separation from the stored beam

STATUS AND EXPERIENCES OF THE VACUUM SYSTEM IN THE SuperKEKB MAIN RING

T. Ishibashi[1,2] †, Y. Suetsugu[1,2], K. Shibata[1,2], M. Shirai[1], S. Terui[1], K. Kanazawa[1,2], H. Hisamatsu[1], M. L. Yao[2]

[1]KEK Accelerator Laboratory, Tsukuba, Ibaraki, Japan
[2]SOKENDAI, Hayama, Kanagawa, Japan

Abstract

Since the SuperKEKB began operation in 2016, the stored beam currents in the main ring have been gradually increased. When the system was commissioned in the Spring of 2022, the maximum beam currents were ~1460 mA in the low-energy ring for positrons (LER) and ~1145 mA in the high-energy ring for electrons (HER). The beam doses are ~7312 Ah in the LER and ~6199 Ah in the HER, and vacuum scrubbing of the beam pipes is proceeding well. However, during these operations, problems such as abnormal pressure rises, vacuum leaks, and collimator damage have occurred. Here, we report on our experiences and the status of the vacuum system after its commissioning in the spring of 2019, known as Phase 3.

INTRODUCTION

The SuperKEKB accelerator is an electron–positron collider with storage rings [1]. The main ring consists of a low-energy ring (LER) for positrons (beam energy: 4 GeV; designed beam current: 3.6 A) and high-energy ring (HER) for electrons (beam energy: 7 GeV; designed beam current: 2.6 A), both with a circumference of about 3 km. Cessation of the operation of the KEKB accelerator ceased in 2010 was followed by about six years of construction of upgrades. During this period, approximately 93% of the vacuum components in the LER and approximately 20% of those in the HER were newly developed and installed [2]. Fig. 1 show the layout of the SuperKEKB main ring. Names of vertical and horizontal collimators are indicated by the letters V and H, respectively. The ring has four arc sections and four straight sections. IR: interaction region; SC: superconducting cavity region; ARES: normal-conducting RF cavity region. The ring is divided in to 12 sections, D01 to D12. Figure 2 shows a photograph of an arc-section of the ring, where: IP is ion pump; NEG is nonevaporable getter pump. Rectifiers are installed in the heater of the NEG pumps and in bending magnets in the LER, and are used to activate these while the magnets are excited

The SuperKEKB main ring began operating in 2016, and this first commissioning stage from February to June of that year was named Phase 1 [3, 4]. The second commissioning stage from March to July of 2018 was named Phase 2, and a positron-damping ring (DR) was introduced after this stage [5, 6]. In 2019, a full-scale physics experiment with the Belle II detector started; this was named Phase 3, which continues to the present.
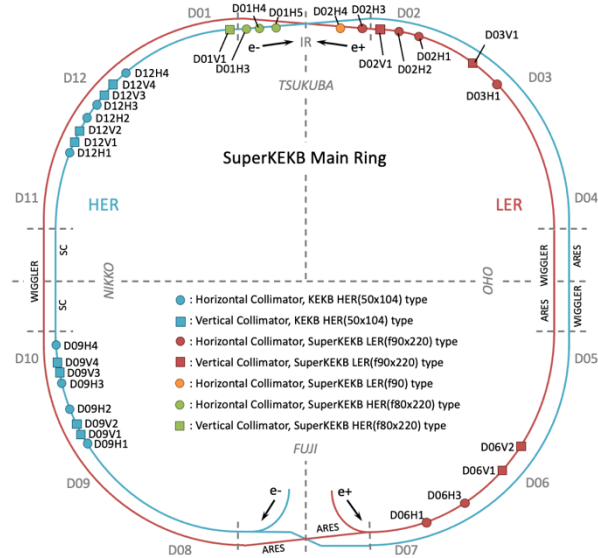
† takuya.ishibashi@kek.jp
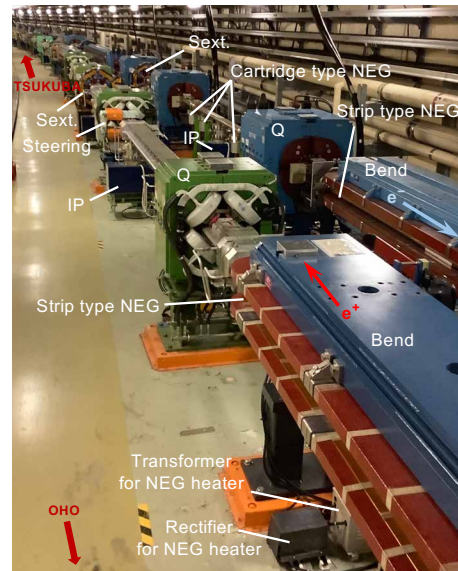
Figure 1: Layout of the SuperKEKB main ring.

Figure 2: Photograph of an arc-section of the SuperKEKB main ring.

After breaking the world record for luminosity in 2020 [7], SuperKEKB has continued to set new records. The record peak luminosity was ~4.7 × 10³⁴ cm⁻² s⁻¹ with 1.4 A in the LER and 1.1 A in the HER when the stored bunch number was 2249 during the spring run of 2022 [8].

VACUUM SYSTEM OF THE FCC-ee*

R. Kersevan†, CERN, Geneva, Switzerland

Abstract

The analysis and design of the vacuum system for the FCC-ee e- and e+ rings is outlined. The main vacuum-relevant parameters are recalled, with particular emphasis on the copious emission of synchrotron radiation (SR) along the rings, and its direct and indirect effects on vacuum, namely surface heating, SR-induced molecular desorption, generation of photoelectrons. A status report of the present design, analysis, and prototyping phase of several key vacuum components is also given.

VACUUM-RELEVANT MACHINE PARAMETERS

This paper refers to the version of the machine described in the Conceptual Design Report [1], i.e. the 97.756 km circumference rings. Out of the 5 beam energies foreseen for the experimental runs, see table on inset of Fig 1, we have analysed only the lowest-energy, highest beam current Z and the highest-energy, lowest beam current ttbar, as they represent all cases vacuum-wise.

All machines are bound to generate 50 MW of SR, therefore their beam currents scale as $1/E^4$, with E being the beam energy. There is therefore a large change of stored current, which makes the design challenging for vacuum, especially for the 45.6 GeV, 1390 mA, Z energy.

Synchrotron Radiation Spectra

The SR spectrum for e⁻/e⁺ circular accelerators is strongly dependent on beam energy. Its characteristic parameter is the critical energy ε_c of its spectrum, which varies as the third power of the beam energy E. Figure 1 shows the spectra of the five machines. The table on the figure also shows some vacuum-relevant parameter, such as the linear photon-stimulated desorption (PSD) yield, in units of mbar·l/s/m, computed assuming a molecular yield of
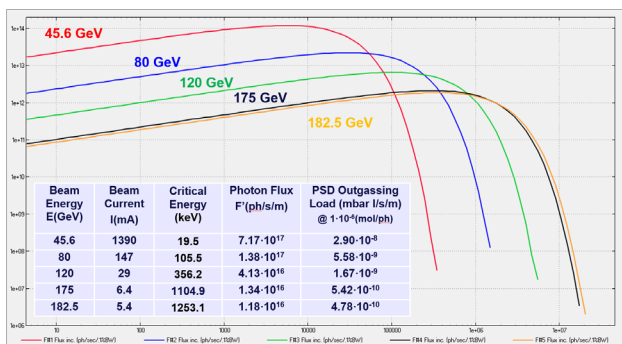

Figure 1: SR spectra: Units: Vertical: ph/s/m/(0.1% Bandwidth); Horizontal: eV; Intervals: Vertical: [106; 2·1014]; Horizontal : [4; 5·106]; Inset table: linear photon flux, and linear PSD rate at each energy.

$1 \cdot 10^{-6}$ molecule/photon (mol/ph). The "per meter" unit refers to length along the arc dipole orbits, with bending radius $\rho = 10.760$ km.

It can be seen on Fig. 1 that the spectrum for the Z machine is almost entirely generated below the Compton threshold for aluminium or copper (~100 and 200 keV, respectively), while for all other higher energy machines there is going to be a substantial fraction of the total photon flux generated above the Compton threshold. Operation with LEP-2 at high energies has shown that this Compton-generated photons interact with the vacuum chamber material and can created a rather isotropic background of X and gamma rays, which can then re-enter the vacuum system and generate additional outgassing [2, 3]. We have therefore devised a way to contain locally this high-energy isotropic source of radiation which could otherwise activate and damage machine and tunnel components [4].

VACUUM HARDWARE

Synchrotron Radiation Absorbers

The operation timeline adopted for the FCC-ee physics program, see Fig. 3 of Ref. [1], calls for an initial 4-year time span during which the machine starts at the Z energy and then in a matter of 2 years it gets to nominal luminosity. This is a very challenging specification, as the Z machine corresponds to a very high beam current, B-factory-level, at unprecedented high energy: we need to design a very performing vacuum system, with high linear pumping speed, low dynamic desorption, and quick conditioning. To cope with this requirement and reduce the Compton-scattered background (see previous section), we have explored via numerical simulations the possibility to implement a number of short, lumped SR ures which collect and concentrate the SR that would otherwise impinge along the external wall of the vacuum chamber, like done at most modern light sources. For all machines, the linear SR power density, if the SR fan hits the external wall, is around 620 W/m (including a dipole packing factor of 0.85). Using 150 mm-long lumped absorbers we can collect the SR fan which would otherwise on average hit 5.6 m of external wall, therefore speeding up the conditioning time by a factor between 4 and 7, depending on the exponent of the power-law conditioning curve [5]. Some details and calculations are shown in Fig. 2. Correspondingly, the SR power density on the SR absorbers' surface goes up from 1.4 W/mm² to 32 W/mm² (flat wall vs inclined surface of the SR absorber) for the Z machine, and from 4 W/mm² to 115 W/mm² for the ttbar at 182.5 GeV. The material chosen for the SR absorbers is CuCrZr, and the manufacturing technology is additive manufacturing, 3D printing. The absorbers will be connected to the chamber either via brazing or using other techniques. First prototypes will be available at the beginning of 2023.

POSITRON AND DAMPING RING REQUIREMENTS FOR FUTURE e+e- COLLIDERS*

John T. Seeman†, SLAC National Accelerator Laboratory, Menlo Park, California, USA

Abstract

Future e+e- colliders will need positron sources that stretch present technical capabilities. The project teams for these proposed colliders are working to extend these capabilities. A positron source encompasses many elements: an electron driver, production target, lattice optics, capture section, damping ring(s), injection/extraction short-pulse kickers, an emittance preserving complex delivery system, specific injection specifications, and (perhaps) polarization. The required technical parameters need to accommodate many beam aspects including bunch intensities, final emittances, spacings, train lengths, and desired damping times. For this note, the technical requirements for positrons related to bunch charges, number of bunches, damping ring (DR) lengths and damping times for the various positron sources for the presently proposed colliders are compared, concentrating on their DR specifications.

INTRODUCTION

An Implementation Task Force (ITF) [1] was started as a part of the Snowmass-2022 exercise that looked at the proposed future colliders. As a part of the ITF studies, positron production, accumulation, storage, and damping were briefly investigated as an important aspect of the design of the various colliders. Although positrons were not a specific part of the charge of the ITF, positron production issues entered many of the designs in a major manner. In this note some positron aspects and parameters are discussed for producing and delivering trains of positron bunches for future colliders relative to the damping rings.

ELECTRON-POSITRON COLLIDERS

The positron damping rings (DR) for fifteen e+e- colliders are reviewed. Four of these for past or present colliders are discussed first and, then, eleven are discussed from proposed future colliders ranging from rings to linear colliders. A brief description is given for each collider and then the technical parameters of their positron DR systems are discussed.

Over the course of the two-year Snowmass-2022 process, many of the proposed colliders changed parameters such as repetition rates, bunch charges, number of bunches, and machine lengths. The well-established proposed colliders changed only a little (e.g. ILC, FCCee, and CEPC) but some of the lesser developed changed greatly (e.g. plasma wakes, structure wakes, energy recovery proposals). Below are brief collider descriptions

The SLC [2] was a collider at SLAC operating at the Z using the SLAC copper "two mile" linac colliding single e+ and e- bunches.

The LEP ring collider [3] at CERN operated at the Z and higher while colliding 4 to 8 bunches.

The PEP-II ring collider [4] at SLAC operated with two rings of different energies at the Upsilon energy colliding 1732 bunches in each ring.

The present SuperKEKB collider [5] at KEK operates with two rings of different energies at the Upsilon energy colliding 2151 bunches in each ring.

The proposed FCCee ring collider [6] would use a new tunnel near CERN with two rings with energies up to ttbar colliding about 10,000 bunches in each ring.

The proposed CEPC ring collider [7] would use a new tunnel in China with two rings with energies upgradable to ttbar colliding up to 12,000 bunches in each ring.

The proposed ILC collider [8] would be a pulsed SC linac in Japan that would collide trains up to 1312 bunches per pulse initially at the Higgs energy.

The proposed CLIC collider [9] would be a pulsed, two-beam copper linac near CERN colliding trains of up to 352 bunches per pulse.

The proposed cold copper collider C3 [10] would be a pulsed cold copper linac colliding bunch trains up to 133 bunches per pulse.

The proposed circular energy recovery collider CERC [11] would use a 100 km circular tunnel to ramp up and down the two beams in energy over several turns recovering the beam energy in SC RF linacs and collision particles in damping rings with top-up injection.

The proposed energy recovery linear collider ERLC [12] would be two CW SC linacs with energy and particle recovery while operating with continuous bunches with top-up injection.

The proposed recycling linear collider ReLiC [13] would be a CW SC linac energy recovery linac operating with nearly continuous bunch trains with beam energy recovery in the linacs and particles recovery in damping rings.

The proposed plasma wake PWFA-LC [14] would be a pulsed beam-driven plasma linac, colliding single e+ and e- bunches up to 10,000 Hz.

The proposed laser-driven plasma wake LWFA-LC [15] would be a pulsed linac, colliding single e+ and e- bunches up to 50,000 Hz.

The proposed structure wake SWFA-LC [16] would be a pulsed two-beam-driven linac colliding trains of e+ and e- bunches.

POSITRON DAMPING RINGS

The colliders described above all need damping rings to reduce the emittances of the positron bunches either generated from scratch or being recycled after collisions and to accommodate the needed bunch spacing and trains. In Table 1 are listed the colliders, the respective DR energies, and required modes of operation. The DR energies were

THYAT0101

KEK e+/e- INJECTOR LINAC

T. Natsui[†], M. Akemoto, D. Arakawa, H. Ego, Y. Enomoto, K. Furukawa, T. Higo, N. Iida,
K. Kakihara, T. Kamitani, H. Katagiri, M. Kawamura, S. Matsumoto, T. Matsumoto,
H. Matsushita, T. Miura, F. Miyahara, H. Nakajima, Y. Okayasu, I. Satake, M. Satoh, Y. Seimiya,
T. Shidara, A. Shirakawa, T. Suwada, M. Tanaka, D. Wang, Y. Yano, K. Yokoyama,
M. Yoshida, T. Yoshimoto, R. Zhang, X. Zhou, KEK, Ibaraki, Japan

Abstract

The KEK injector linac feeds the beams into four rings. It is called J-Linac. The SuperKEKB main rings are high-energy rings (HER) and low-energy rings (LER). The linac injects a 7 GeV electron beam to the HER and a 4 GeV positron beam to the LER. It also injects electron beams into the two light source rings. We successfully performed this simultaneous four-ring injection. We achieved this complex simultaneous injection using two electron guns, a positron source with a flux concentrator, and pulsed magnets. In SuperKEKB phase 3 operation, 2 nC electron and 3 nC positron beam injections were achieved.

INTRODUCTION

The KEK electron/positron injector linac was designed to inject different types of beams into four different rings. This injector achieved simultaneous four-ring injection at 50 pps. SuperKEKB has two rings: the HER and LER [1]. The other rings are the light source rings of the PF and PF-AR rings. An electron beam with an energy of 7 GeV and a positron beam with an energy of 4 GeV are required for the HER and LER, respectively. The energies of the PF ring and PF-AR are 2.5 GeV and 6.5 GeV, respectively.

The injector linac consists of eight sectors (sector A-C and 1-5) and a bending sector (J-arc) with a total length of 600 m. This shape resembled that of J, as shown in Fig. 1. One sector has eight klystrons, and one klystron drives four 2-m accelerating structures. The energy is adjusted from pulse to pulse by switching the accelerating or standby mode of each accelerating structure.

We used two types of electron gun: a photocathode RF gun and a thermionic cathode DC gun. An RF gun with a high-power laser was used to generate a low-emittance electron beam for the HER injection [2]. The RF gun charge and emittance design values were 5 nC and 6 mm-mrad, respectively. Positrons were generated by hitting a primary electron beam onto a tungsten target. These positrons were focused with flux concentrator (FC) [3] and accelerated with large aperture S-band (LAS) [4] accelerating structures. We obtained a 4 nC positron beam with a 10 nC primary electron beam. The generated and accelerated 1.1 GeV positron beam was injected into a damping ring to reduce the emittance. A pulse-bend magnet merged these two electron gun lines, and these beams were injected into a common acceleration beamline. A thermionic gun was used as the electron source for the light source rings.

Sector A to 2 has common optics that use DC magnets. However, sector 3 to 5 has independent optics using pulse magnets. These pulse quadrupole and steering magnet systems were developed for the SuperKEKB project and can change the optics at 50 pps.

We achieved this complex four-ring simultaneous injection using two types of electron guns: a positron source and pulsed magnet system [5].

LINAC BEAM STATUS FOR SUPERKEKB

The SuperKEKB phase 3 operation began in 2019. The linac beam quality was gradually improved. Table 1 lists the current beam status and final goal. The energy was set to the required value, and a sufficient energy margin was maintained by providing standby units. The amounts of bunch charges in operation didn't reach the target values. However, these were almost sufficient for 2022b. The emittance was improved in a step-by-step manner. Simultaneous injection to four rings and damping ring was completed.
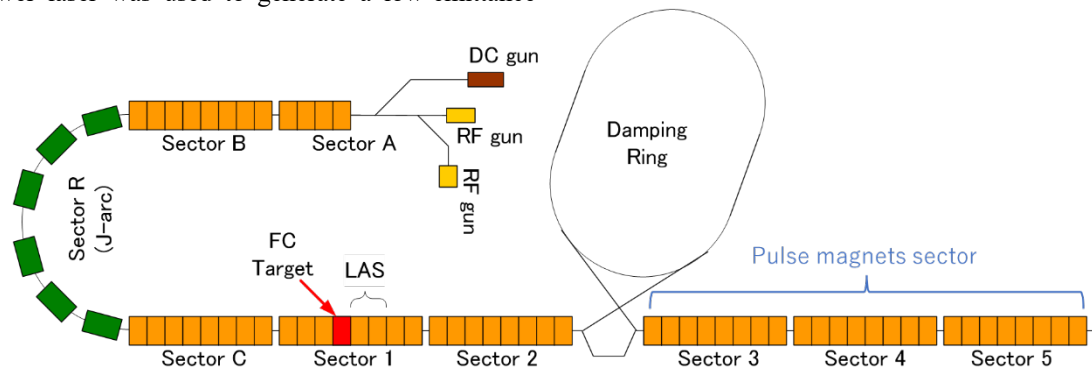

Figure 1: KEK injector linac.

† takuya.natsui@kek.jp

POWER BUDGETS AND PERFORMANCE CONSIDERATIONS FOR FUTURE HIGGS FACTORIES*

F. Zimmermann[†], CERN, Geneva, Switzerland
B. List, DESY, Hamburg, Germany
S. Belomestnykh, V. Shiltsev, FNAL, Batavia, USA
J. Gao, IHEP, Beijing, China
A. Faus-Golfe, IJCLab, Orsay, France
M. Biagini, M. Boscolo, INFN-LNF, Italy
R. Rimmer, T. Satogata, JLAB, Newport News, USA
M. Koratzinos, PSI, Villigen, Switzerland
E. Nanni, P. Raimondi, T. O. Raubenheimer, J. Seeman, SLAC, Menlo Park, USA
V.N. Litvinenko, Stony Brook Univ., Stony Brook, USA
K. Oide, Univ. Geneva, Geneva, Switzerland

Abstract

A special session at eeFACT'22 reviewed the electrical power budgets and luminosity risks for eight proposed future Higgs and electroweak factories (C^3, CEPC, CERC, CLIC, FCC-ee, HELEN, ILC, and RELIC) and, in comparison, for a lepton-hadron collider (EIC) presently under construction. We report highlights of presentations and discussions.

INTRODUCTION

During the Snowmass Community Summer Study in Seattle [1], questions arose on the feasibility of power and luminosity numbers communicated for various collider proposals. The Accelerator Frontier Implementation Task Force (ITF) had received many inputs on various collider concepts and just released their evaluation report [2]. While many comparative evaluations were extremely helpful and welcome, the ITF specifically mentioned that they had not reviewed luminosity and power consumption projections (i.e., they used proponents' numbers of luminosity and power).

The following ICFA Workshop eeFACT'22, organized at Frascati in September 2022, was charged with helping the broader accelerator and HEP community by taking a look at the luminosity and power consumption projections for various e⁺e⁻ Higgs factories and providing an "expert comparative evaluation" for them [3]. Given the strength of the cohort of anticipated participants, such "independent" evaluation was expected to be very helpful.

For this purpose, a special session was set up during eeFACT'22 [4], where representatives from all major proposals were invited to present and discuss their respective numbers and the underlying assumptions [3].

POWER CONSUMPTION

The power consumption estimates, including the underlying assumptions and level of completeness and maturity, differ significantly between proposals. The special session at eeFACT'22 [4], addressed this theme, with pertinent brief presentations from all e⁺e⁻ Higgs and Electroweak Factory proposals. The eeFACT'22 discussions and presentations [3, 5–12], resulted in the power budgets compiled in Table 2.

For CEPC, the 260 MW power required for the Higgs factory operation is significantly lower than the value of 340 MW, which had been submitted to the ITF.

The annual power consumption in TWh numbers does not look fully consistent across various machines. As an example, for the FCC-ee, the annual power consumption is higher than the product of instantaneous power and effective physics time, since power needs during annual hardware commissioning, beam commissioning, operational downtimes, technical stops, machine development periods and shutdowns are also taken into account [13], as sketched in Table 1.

Table 1: Electrical power consumption for FCC-ee at 240 GeV c.m. energy [13] (slightly adapted), yielding a total of 1.52 TWh per year.

Mode	# days	Power [MW]
beam operation	143	301
downtime operation	42	109
h.w. & beam commissioning	30	139
machine development	20	177
technical stop	10	87
shutdown	120	61

We note that this was the first attempt to get a detailed comparative accounting of the power consumption needs, that several numbers are still missing for CERC, C^3, RELIC, etc., and that some of the numbers have not been fully critically assessed. Hence, this comparative analysis will need to be continued.

CEPC ACCELERATOR TDR STATUS AND AC POWER CONSUMPTIONS*

J. Gao [†], Institute of High Energy Physics, Chinese Academy of Science, Beijing, China

Abstract

The discovery of the Higgs boson at Large Hadron Collider (LHC) of CERN in July 2012 raised new opportunities for a large-scale accelerator. The Higgs boson is the heart of the Standard Model (SM) and is at the center of many mysteries of universe. In Sept. 2012, Chinese scientists proposed a 240 GeV Circular Electron Positron Collider (CEPC), having two large detectors for Higgs studies as a Higgs Factory and other topical researches. The 100 km tunnel of CEPC could also host a Super proton proton Collider (SppC) to reach energies above 100 TeV. CEPC Conceptual Design Report (CDR) has been released in Nov. 2018, and CEPC Technical Design Report (TDR) will be completed at the end of 2022. in this paper, CEPC Technical Design Report (TDR) status, upgrade possibilities and AC power consumption have been reported.

INTRODUCTION

The discovery of the Higgs boson at CERN's Large Hadron Collider (LHC) in July 2012 raised new opportunities for large-scale accelerators. The Higgs boson is the heart of the Standard Model (SM), and is at the center of our understanding the mysteries of universe. Precise measurements of the properties of the Higgs boson serve as probes of the underlying fundamental physics principles of the SM and beyond. Due to the modest Higgs boson mass of 125 GeV, it is possible to produce it in the relatively clean environment of a circular electron–positron collider with high luminosity and multi detectors. In Sept. 2012, Chinese scientists proposed a 240 GeV Circular Electron Positron Collider (CEPC), serving two large detectors for Higgs studies and other topics as shown in Fig. 1. The 100 km tunnel for such a machine could also host a Super Proton Proton Collider (SPPC) to reach energies above 100 TeV.

CEPC is a Higgs factory composed of a linac injector (10 Gev for CDR, 30 GeV for TDR), 100 km circumference full energy booster and collider ring equipped with 2 detectors. In addition to operate at center of mass energy for Higgs of 240 GeV, CEPC could operate also at different energies, such as Z-pole of 45.5 GeV, W of 80 GeV, and as last phase upgrade possibility, ttbar of 180 GeV. The Conceptual Design Report (CEPC Accelerator CDR) [1] has been released in Nov. 2018. CEPC as a Chinese proposed international large science project, it participates the international high energy strategic planning and collaborations. In May 2019, CEPC accelerator document was submitted to European High Energy Physics Strategy workshop for worldwide discussions [2]. In 2022, CEPC accelerator document was submitted to the Particle Physics Community Planning Exercise (Snowmass'21) of USA [3].

CEPC TRD PARAMETERS

According to the CEPC TDR baseline physics goals at the Higgs and Z-pole energies, the CEPC should provide e+e- collisions at the center-of-mass energy of 240 GeV and deliver a peak luminosity of $5 \times 10^{34} cm^{-2} s^{-1}$ at each interaction point. The CEPC has two IPs (two detecors) for e+e- collisions and is compatible with four energy modes (Higgs, Z-pole, W, and ttbar). At the Z-pole energy the luminosity is required to be larger than $1 \times 10^{36} cm^{-2} s^{-1}$ per IP. The experiments at ttbar energy is an energy upgrade option at the last stage of CEPC.

The CEPC TDR baseline design is a 100 km double ring scheme based on crab waist collision and 30 MW radiation power per beam at four energy modes, with the shared RF system for Higgs/ttbar energies and independent RF system for W/ Z energies. The CEPC main parameters for TDR are listed in Table 2. The luminosity at Higgs energy is $5 \times 10^{34} cm^{-2} s^{-1}$. At the Z-pole, the luminosity is $1.15 \times 10^{36} cm^{-2} s^{-1}$ for 2T detector solenoid.

The CEPC TDR power upgrade parameters of 50 MW SR power/beam at Higgs, W, Z and ttbar energy operations and the luminosities are shown in Table 3. The luminosities at Higgs and the Z-pole energies are $8.3 \times 10^{34} cm^{-2} s^{-1}$ and $1.91 \times 10^{36} cm^{-2} s^{-1}$, respectively.

CEPC TDR DESIGN STATUS

Collider Ring

For CEPC collider design, the crab-waist scheme increases the luminosity by suppressing vertical blow up, which is a must to reach high luminosity. Beamstrahlung is synchrotron radiation excited by the beam-beam force, which is a new phenomenon in a storage ring based collider especially at high energy region. It will increase the energy spread, lengthen the bunch and may reduce the beam lifetime due to the long tail of the photon spectrum. The beam-beam limit at the W/Z is mainly determined by the coherent x-z instability instead of the beamstrahlung lifetime as in the tt/Higgs mode. A smaller phase advance of the FODO cell (60/60) for the collider ring optics is chosen at the W/Z mode to suppress the beam-beam instability when we consider the beam-beam effect and longitudinal impedance consistently. The CEPC TDR design goals have been evaluated and checked from the point view of beam-beam interaction, which are feasible and achievable.

MDI

The CEPC machine detector interface (MDI) is about 14 m (±7m from the IP) in length in the Interaction Region